TWO-PHASE PUMP PERFORMANCE PROGRAM
PRELIMINARY TEST PLAN

NP-128
(Research Project 301)

Key Phase Report

September 1975

Prepared by

C-E Power Systems
Combustion Engineering, Inc.
Windsor, Connecticut

Authors
W. G. Kennedy
M. C. Jacob
J. R. Shuckerow

Program Manager
Donn L. Dixson

Prepared for

Electric Power Research Institute
3412 Hillview Avenue
Palo Alto, California 94304

Project Manager
Kjell A. Nilsson

NOTICE

PREFACE

A major concern in the design of power reactors is that sufficient cooling capability be provided to keep fuel element clad temperatures below specified values, even for a postulated break in principal coolant loop components such as the main recirculation loop pipe. Therefore, it is necessary to be able to predict reactor system performance in such a loss-of-coolant accident (LOCA) and to evaluate accident preventing and/or mitigating steps in the design of the system. As a part of the continuing effort for improving and advancing safety technology, the C-E/EPRI Two-Phase Pump Performance Project is designed to provide basic data on the reactor coolant recirculation pump performance under two-phase flow LOCA conditions.

Calculational analysis of a postulated LOCA includes predicted core flow and broken loop pump overspeed, both of which are dependent on the assumed performance characteristics of the reactor coolant pumps. The pump in the broken pipe leg directly affects the rate of system depressurization by retarding blowdown flow, and the remaining pumps affect the flow rates and distribution throughout the system. Present pump analytical models generally in use for LOCA calculations employ homologous flow relationships to derive head and torque behavior in the two-phase flow regimes, and an empirical head degradation factor based on limited experimental information is generally used.

This project is aimed at providing sufficient steady-state and transient two-phase empirical data to improve the presently used analytical modeling. Pump overspeed characteristics will also be examined.

This preliminary test plan report was originally to be an informal document. However, the background and logic which went into it is considered valuable in the overall understanding of the project, and the report is therefore being printed. The reader is asked to have the understanding that the figures and graphs were originally not intended for publication and may thus not be of the best quality. The tests described in this report will be performed at the C-E Kreisinger Development Laboratories (KDL) in Windsor, Connecticut.

The C-E/EPRI Two-Phase Pump Performance Project is one part of EPRI's work in the program area of Light Water Reactor Safety. Previous reports issued as part of this project are listed in Appendix A and are available from the EPRI Library. This Preface and Section 1.1 below was written by EPRI to put the report in perspective. For further information regarding this project, please contact Kjell A. Nilsson, EPRI Project Manager, telephone: 415-493-4800.

TABLE OF CONTENTS

LIST OF FIGURES

LIST OF TABLES

1. INTRODUCTION

1.1 Project Background

During 1973 joint meetings were held between the former U.S. Atomic Energy Commission (AEC) and the four light water reactor (LWR) nuclear steam supply system (NSSS) vendors on the effect of two-phase flow loss-of-coolant accident (LOCA) conditions on reactor coolant pump performance. These meetings resulted in a request from the AEC to each vendor to submit a program and schedule for obtaining experimental information on which to base more refined analytical modeling for determining pump speed during LOCA conditions. The present pump project, jointly funded by EPRI and C-E, is a result of those AEC meetings.

1.2 Project Objectives

Pressurized water reactor LOCA calculations of core flow and broken leg pump overspeed are dependent on the assumed performance characteristics of the reactor coolant pumps. Current pump calculational models generally use homologous flow relationships to derive two-phase flow head and torque with an empirical head degradation factor based on limited experimental information.

The basic objectives of this model pump test program are to:

(a) Obtain sufficient steady-state and transient two-phase empirical data to substantiate, and ultimately improve, the mathematical model of the reactor recirculation pump presently used for LOCA analysis.

(b) Obtain sufficient data on pump overspeed characteristics under transient two-phase blowdown conditions to verify the pump flywheel integrity to satisfy the requirements of AEC Regulatory Guide No. 1.14.

1.3 Project Summary

In order to determine the appropriate range of model pump test conditions, typical ranges of power plant pump operating conditions as calculated in LOCA analyses were compiled. The compilation covers, for two nuclear power plant designs, a variety of break sizes for pump discharge and suction line breaks. The calculated conditions are displayed for pumps in both the broken and intact legs of the broken loop, and also for pumps in the intact legs of the intact loop.

Pump performance is generally described in terms of head and hydraulic torque for a given speed, volume flow rate and fluid density. For two-phase flow, additional important parameters are pressure level, void fraction and flow regime. For two-phase flow transients, also the rates-of-change of hydraulic parameters, particularly void fraction, are important.

To predict the performance from a model pump to a full-sized pump or from one flow condition to another requires geometric similarity of the pumps and flow patterns. The primary criterion used for indicating hydraulic flow similarity is the homologous ratio ν/α_N which is the ratio of volume flow to pump speed normalized to rated conditions and in turn proportional to fluid velocity/rotor velocity. Additional criteria judged to be useful for indicating similarity in two-phase flow are the pump average void fraction α_F and the flow regime.

A one-fifth scale model reactor coolant pump will be tested in steady-state runs with two-phase mixtures of water and steam in a range of operating conditions representative of postulated LOCA's. Reversible drive and flow booster facilities allow steady-state testing with any desired combination of rotation and flow directions. The test model pump has a specific speed of 4200 and a cold water rating of 252 ft head, 3500 gpm and 308 ft-lb torque at 4500 rpm. The test system also models typical NSSS suction and discharge lines adjacent to the pump. The steady-state test data will be incorporated into the existing dynamic calculational pump model as appropriate to update the input pump characteristics. Transient two-phase performance of the test pump will be predicted for selected cases using the calculational model, and transient (blowdown) tests will be run to verify the applicability of the calculational model to transient conditions. The blowdown tests

start from steady-state circulation and the test facility can be set up for blowdown through either the pump discharge or suction line (forward or reverse blowdowns). Blowdown calculations with the CEFLASH-4A code for forward blowdowns indicate that transients can be achieved which show a rate-of-change of void fraction $d\alpha/dt$ up to 1/2 of large break LOCA values. These transients appear to be severe enough to determine the applicability of the pump calculational model to transient blowdown conditions.

After completion of test loop modification and shakedown, the pump test program will begin with several spot checks of the manufacturer's single phase performance data. Subsequent testing will be divided into three phases with intermissions of at least 4 weeks each for data evaluation and further test planning. The test program is considered to be a dynamic or "live" program with allowance for filling in or modifying the test matrices in accordance with results obtained from tests up to that point. Phase I will provide a broad sampling of test conditions to reveal overall performance trends and comprises: (1) sampling the effects of changing void fraction (other conditions constant), (2) one full steady-state performance map, (3) additional steady flow points near predicted conditions for initial transient tests, and (4) initial forward and reverse blowdown rungs. Phase II will emphasize steady-state mapping and moderate blowdowns. Phase III will primarily fill in with needed supplemental tests and larger break blowdowns.

A steady-state matrix of 300 test settings is indicated to span the combinations of pump average void fraction α_F and inlet pressure P_{in} predicted for LOCA's. Complete performance maps will be run at three combinations of void fraction and inlet pressure, and partial maps elsewhere will enable interpolation and separation of the effects of the different variables. A complete map will involve approximately 55 points distributed over the range of speeds and flows provided by the test facility. For extrapolating beyond the available speeds and flows, some test settings will be selected at values of homologous ratios suitable for calculational model scaling through the use of similarity "laws."

The transient test matrix indicates the steady-state operating conditions from which blowdowns will start and the effective break sizes and flow routing to be used. Twenty-five points are planned and 17 more reserved for

later fill-ins. The tests cover various initial pressures and speeds, forward and reverse flow through various break sizes, with motor power left on or shut off.

Basic test measurements cover: (1) pump suction and discharge pressure, temperature, density, speed and velocity head, (2) water and steam orifice flow measurements, (3) pump shaft speed and torque, (4) steam drum initial inventory, (5) time after initiation of blowdowns, and (6) pump seal injection flow quantities and temperatures in and out.

Data acquisition will be accomplished by an accurate high speed digital recorder supplemented by optical or magnetic tape recording if necessary for transient testing. Computerized conversion of raw test data will account for instrumentation corrections and time intervals between readings. Current plans for data processing are to develop a computerized regression analysis (least squares) curve fit for pump head or torque as a function of volume flow at constant speed. This would lead to H vs. Q and T_H vs. Q performance maps. By replotting, the alternate form of map with contours of constant H and T_H on a speed vs. flow coordinate grid can be drawn. Also by further normalization to rated conditions the first maps above can be converted to homologous ratio maps of h/α_N^2 and β/α_N^2 vs. ν/α_N, etc.

The applicability of the pump calculational model to transient conditions will be determined by checking how well the pump performance measured in the transient test compares with the pump performance predicted by the analytical model.

2. BACKGROUND AND OBJECTIVES

Calculational analyses of postulated Loss-of-Coolant Accidents (LOCA's) include predicted core flow and broken loop pump overspeed, both of which are dependent on the assumed performance characteristics of the reactor coolant pumps. The pump in the broken pipe leg directly affects the rate of system depressurization by retarding blowdown flow, and the remaining pumps affect the flow rates and distribution throughout the system. Present pump analytical models generally in use for LOCA calculations employ homologous flow relationships to derive head and torque behavior in the two-phase flow regimes. An empirical head degradation factor based on limited experimental information is also generally used.

The basic objectives of this program are to:

(a) Obtain sufficient steady-state and transient two-phase empirical data to substantiate, and ultimately improve, the mathematical model of the reactor recirculation pump presently used for LOCA analysis.

(b) Obtain sufficient data on pump overspeed characteristics under transient two-phase blowdown conditions to verify the pump flywheel integrity to satisfy the requirements of the AEC Regulatory Guide No. 1.14.

3. OVERALL APPROACH

A one-fifth scale model PWR primary system coolant pump will be tested in steady-state runs with mixtures of hot water and steam over a range of operating conditions typical of those encountered in a PWR NSSS during postulated LOCA events. These steady-state data will then be employed in existing pump calculational models to predict pump performance in test loop blowdown runs designed to generate representative transient conditions with either forward or reverse flow through the test pump.

3.1 Basic Test Configurations

The basic arrangement and functions of the test system are presented briefly here. A more detailed description can be found in the Preliminary Test Facility Description (Reference 3.1). The basic elements of the test system are shown schematically in Figure 3.1. The test pump rotor can be locked or be driven in either direction by the reversible electric motor, which can also act as a braking generator. Various hot water/steam mixtures can be supplied either passively or forcibly (by booster pumps) to either the test pump normal inlet or outlet. These features allow steady-state testing of the pump with all desired combinations of rotation and flow directions, as indicated in Figure 3.2.

Blowdown tests will be accomplished by locking the rotors of the booster pumps, establishing recirculating flow in the test loop by running the test pump, and then opening the blowdown line suddenly by means of rupture diaphragms. The reversible piping connections allow blowdown from either the pump discharge or suction line. Bypass blowdown flow through the return line can be interrupted by closing the throttle valve. The basic pump blowdown modes are indicated in Figure 3.3.

The test pump is a 1/5 scale model of the Byron-Jackson main reactor coolant pumps used in the Palisades power plant. These are mixed-flow (centrifugal/radial) pumps with a specific speed of approximately 4200 rpm. The model has rated (normal peak efficiency) values of performance parameters from cold water tests (Reference 3.1) as follows:

Figure 3.1

BASIC ELEMENTS OF TEST SYSTEM (SCHEMATIC PLAN VIEW)

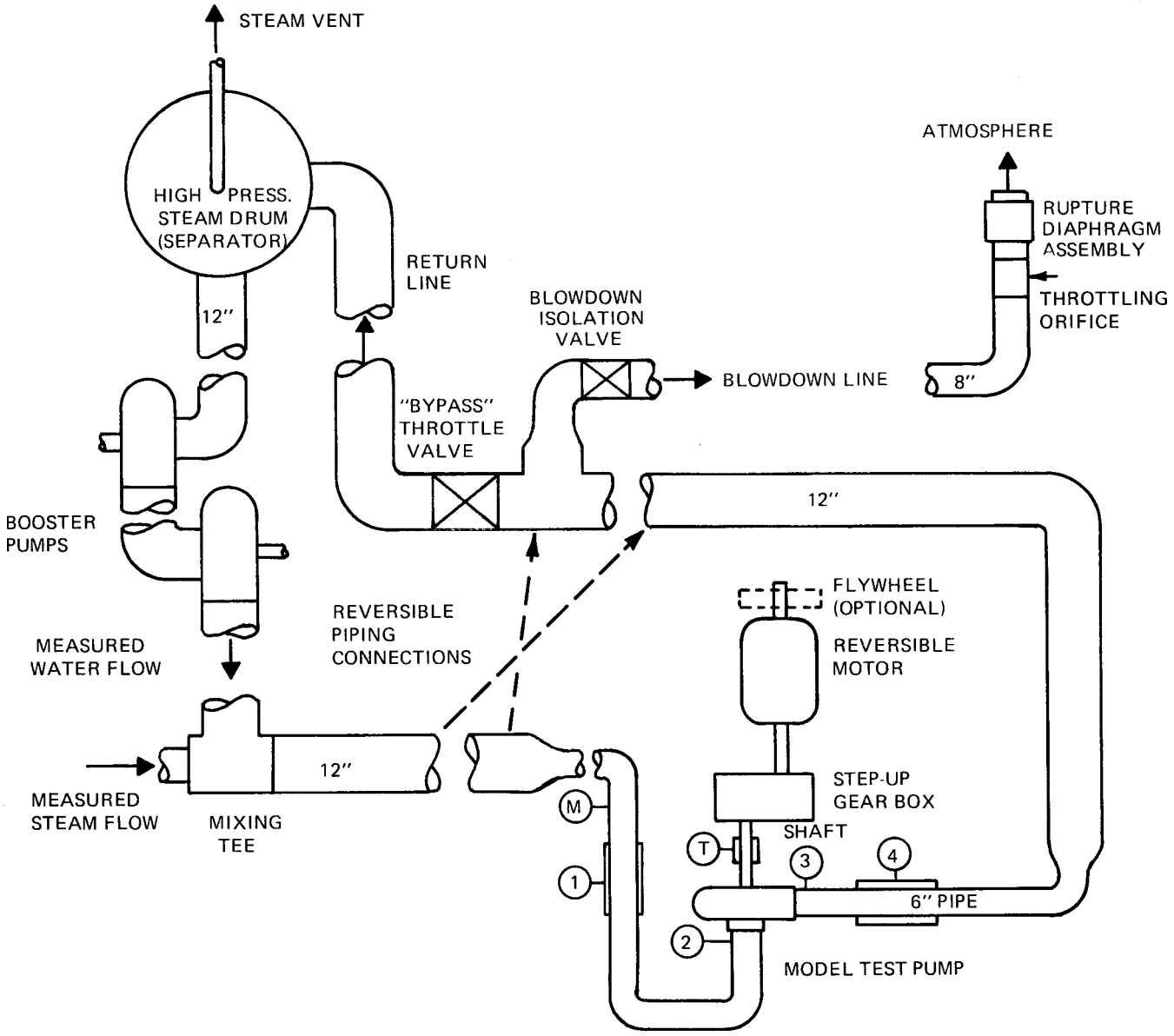

Figure 3.2

STEADY STATE TEST CONFIGURATIONS
SINGLE AND TWO PHASE

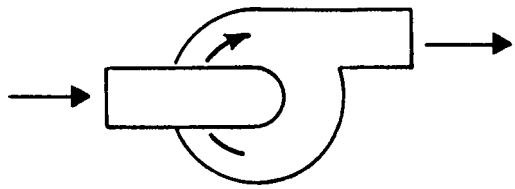

POSITIVE (NORMAL) FLOW
NORMAL ROTATION

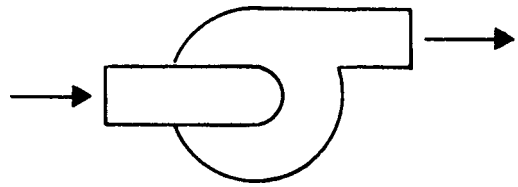

POSITIVE FLOW
LOCKED ROTOR

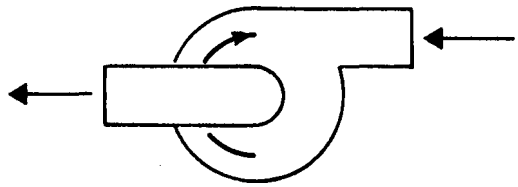

REVERSE FLOW
POSITIVE ROTATION

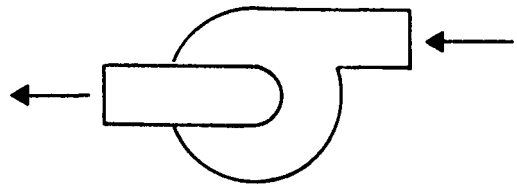

REVERSE FLOW
LOCKED ROTOR

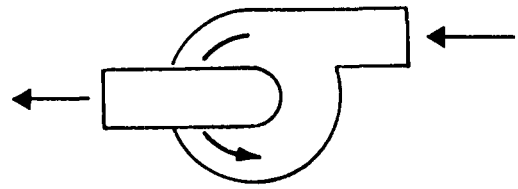

REVERSE FLOW
REVERSE ROTATION

Figure 3.3

TRANSIENT (BLOWDOWN) TEST CONFIGURATIONS

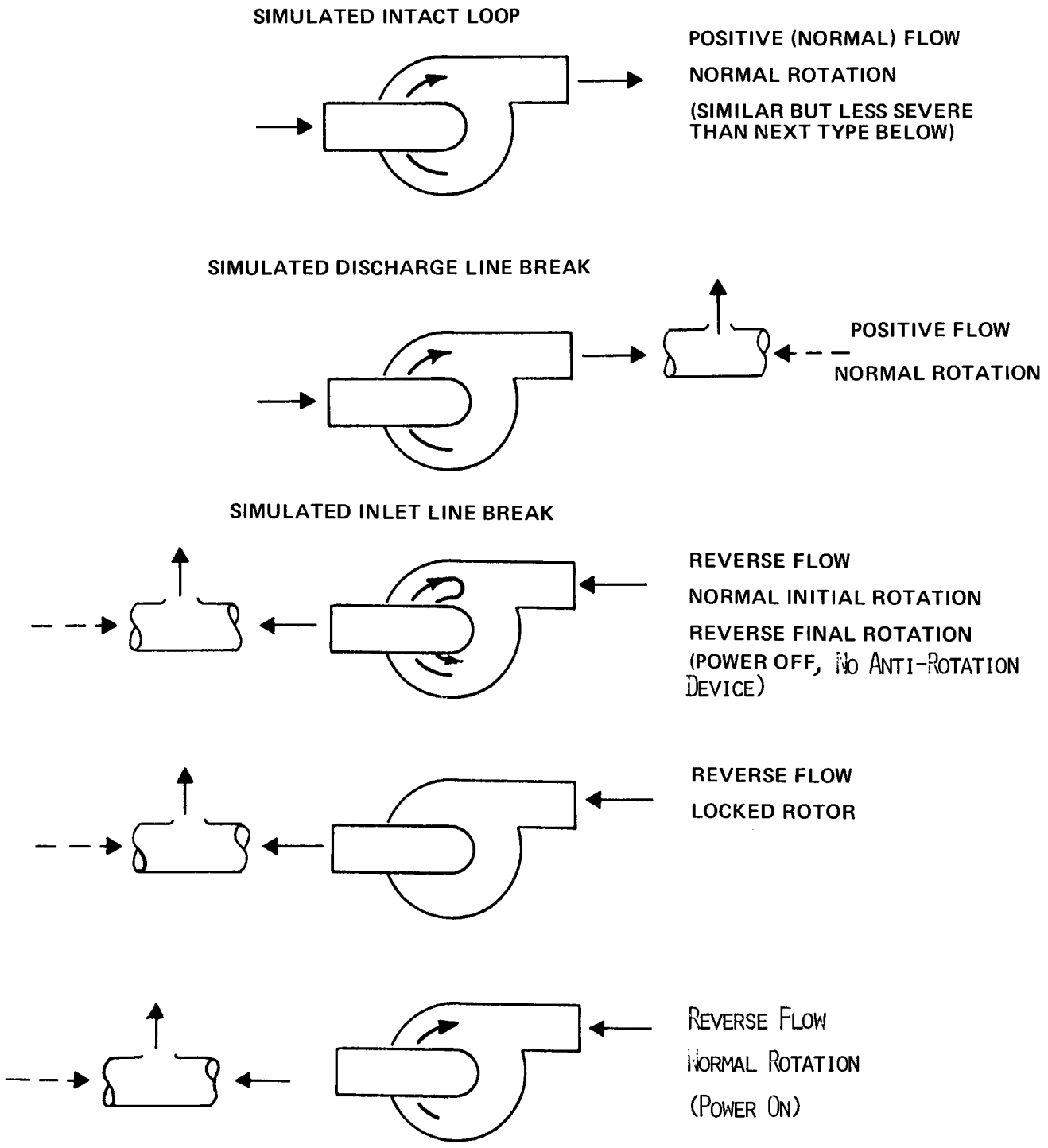

Head	252 ft
Flow	3500 gpm
Speed	4500 rpm (5 times full-size synchronous speed)
Torque	308 ft-lb at 62.4 lb ft^{-3} density

Because there is a possibility of interaction between the pump and the adjoining sections of suction and discharge piping, the test system also models on a 1/5 scale (6 inch ID) the suction line with two 90° elbows and the straight discharge line similar to NSSS installations (Reference 3.1).

3.2 Test Parameters

Pump performance is generally measured and described in terms of head and torque for a given speed, volume flow rate and fluid density. This is illustrated in Figure 3.4 below showing two common types of performance curves.

Torque curves would be drawn in similar fashion. The torque basic to the hydraulic behavior, including two-phase effects, is the hydraulic torque which results from the interaction of the fluid and impeller vanes. To derive this from total shaft torque requires determination of friction and windage torques, and if acceleration is involved, requires moment of inertia and angular acceleration also.

For two-phase flow the fluid density and phase behavior are related not only to pressure and/or temperature but also to void fraction and degree of homogeneity (flow "regime").

Performance measured on a scale model may be properly applied to a full sized pump if dynamic similarity is achieved in the fluid flow. This requires that the pumps be geometrically similar and have matching flow patterns (flow paths relative to pump passages), velocity ratios, relative friction losses (if important), and choking effects (if any). It is also possible to interpolate or extrapolate pump performance from one condition to another, including conditions outside the tested range if dynamic similarity exists between the measured and projected points. More detail on dynamic similarity and scaling appears in Section 5 below.

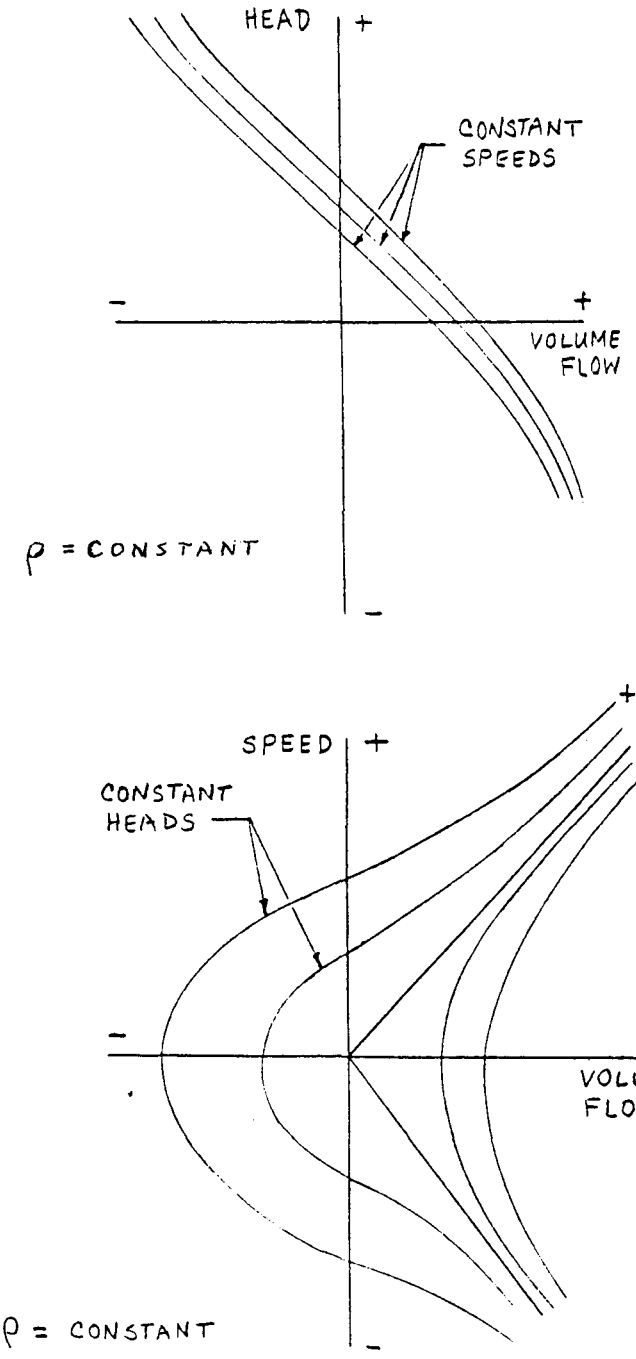

FIGURE 3.4

Typical Pump Performance Curves

For transient (blowdown) tests there is the additional aspect of indicating how severe (rapid) the changes are. This can be described in terms of how any important hydraulic parameter varies with time, but as discussed in Section 5, the main index to severity of blowdown transient operating conditions chosen here is considered to be the rate of change in two-phase mixture as expressed by average pump path void fraction versus time.

3.3 Basic Data Requirements

In order for the test program to provide confirmation of dynamic pump calculational models currently in use for NSSS LOCA analyses, the test data must:

(a) Describe pump performance in terms compatible with the calculational model.

(b) Span most of the anticipated range of operating conditions of interest to NSSS LOCA analyses and provide the basis for deriving performance at conditions not measured directly.

(c) Provide enough values with sufficient accuracy to specify and justify the calculational model inputs to the certainty required for NSSS LOCA analyses.

Overall comments on these items are given here and more detail in later sections as indicated.

(a) Regarding Item (a), the existing calculational pump models and any anticipated refinements can utilize performance information in the form of the basic parameters stated in Section 3.2, namely, head, torques, speed, volume flow rate, density, and possibly pressure for single phase flows, plus void fraction and some indication of phase distribution (e.g., gross phase velocities as possible indices to flow regime) for two-phase flows. The manner in which these parameters may be used either directly or to form dimensionless groupings based on dynamic similarity is described in more detail in Sections 5, 7 and 8 below.

(b) The anticipated ranges of operating conditions for pumps in NSSS accident analyses are derived from results of representative analyses as described in Section 4 below. The methods and data requirements for interpolation and extrapolation of measured performance to accident conditions is discussed further in Sections 4, 5, 7 and 8.

(c) More details on quantity and accuracy of data are given in Sections 6 and 7.

4. TEST CONFIGURATIONS

4.1 Modeled Accident Conditions

The pump test configurations and modes of operation are being selected to cover a range of conditions typical of those anticipated for postulated NSSS LOCA incidents. Therefore, the results of LOCA analyses of various kinds for representative NSSS power plants have been examined and typical pump conditions compiled. This means primarily the blowdown phase of LOCA's with break sizes at least 0.5 ft^2, in which pump influence on flows and the potential for pump overspeed are of some significance.

The larger-break LOCA analyses must usually be made for a range of break sizes, break geometries, and locations. The sizes range from 0.5 to nearly 10 ft^2, twice the cross-sectional area of the broken pipe. The break geometry ranges from (1) a "slot" in the side of the pipe with flow still communicating past the break to (2) a "guillotine" (or double-offset shear) break across the pipe with no communication. Break locations include (see Figure 4.1) pump discharge leg, suction leg, the hot leg between reactor vessel and steam generator, and the surge line. The survey of operating conditions presented here has been confined to the pump discharge and suction leg breaks since analysis has indicated that they are the ones most critical to maximum fuel clad temperature and/or potential pump overspeed.

Since there are pumps at four locations in the usual C-E NSSS (see Figure 4.1), any one pipe break generates different pumping conditions for the various pumps, i.e., for (1) the broken leg pump, (2) the intact leg pump in the broken loop, and (3) the two pumps in the intact loop.

The LOCA calculation results which have been compiled to show a variety of typical NSSS pump operating conditions during various postulated accidents are summarized in the next section (4.2). These include NSSS's with somewhat different operating temperatures and therefore saturation pressures. Also for some cases examined, the pumps are of somewhat different design, with specific speeds near 5000. Thus, the compiled results represent not only a range of conditions in a single NSSS installation due to various accidental blowdowns, but also cover additional conditions due to variations in design and/or normal operating conditions. This seems appropriate when it is

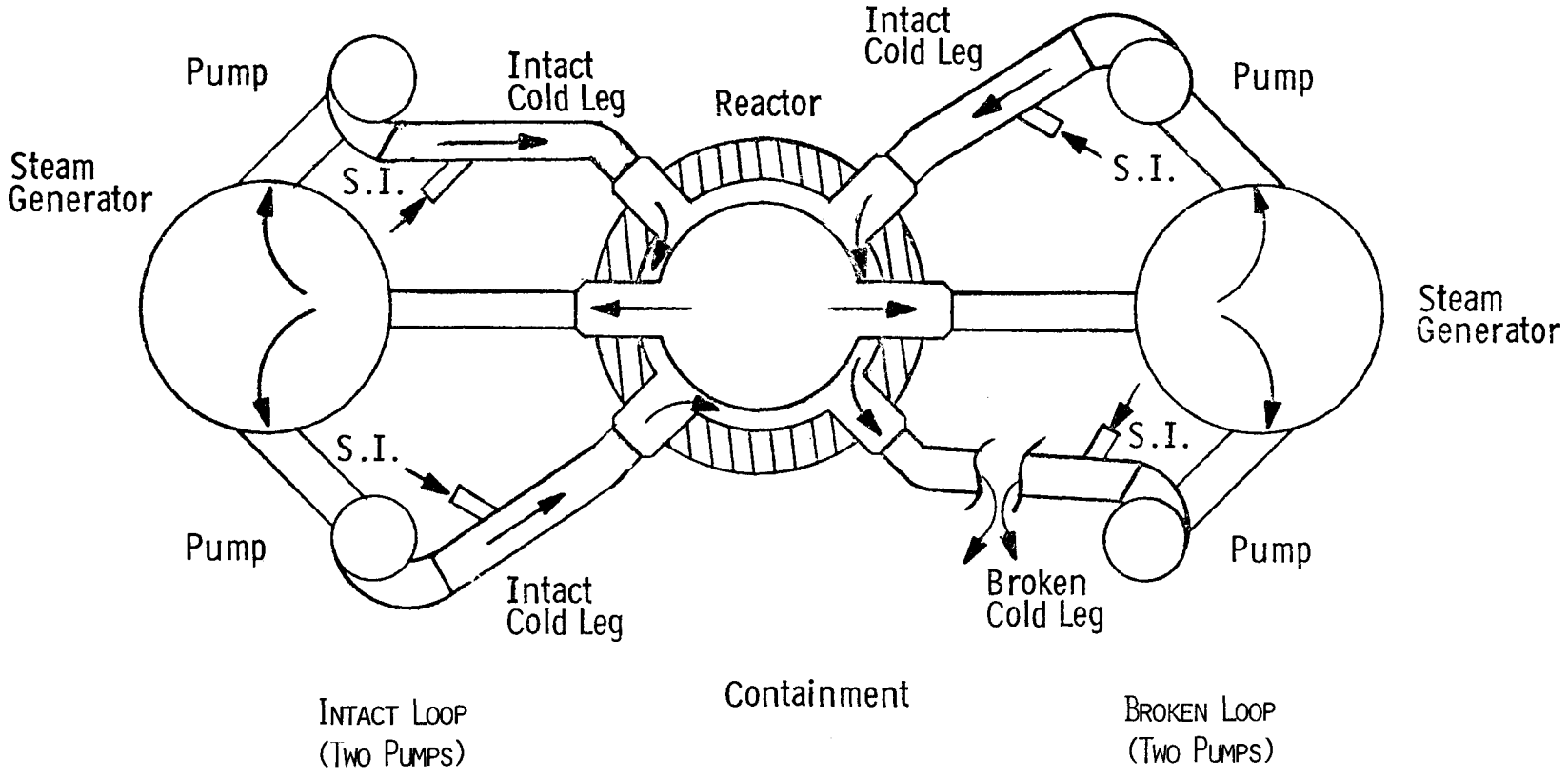

FIGURE 4.1 PLAN VIEW OF REACTOR AND PRIMARY LOOPS

recognized that the pump test results are hoped to be indicative of performance for a class of NSSS pumps and installations as well as for the particular model design.

4.2 Pump Performance During LOCA's

The pump performance predictions compiled here are taken from calculations using the computerized CEFLASH-4A code developed to predict thermal-hydraulic response of PWR's to LOCA's.

For a pump in the broken pipe leg, typical calculated operating conditions during LOCA's resulting from pump discharge leg breaks of various types and sizes are shown in Figures 4.2 to 4.11. The initial subcooled decompression involves, of course, only single phase conditions, and is of such short duration (of the order of 0.1 second) that pump speed does not change significantly. Thus, direct testing of subcooled decompression will not be a feature of the model pump test program.

Vaporization and two-phase conditions begin at each point in the system when the pressure falls to the saturation level for the prevailing temperature, reaching the pump a couple of seconds or more after the break occurs as shown by the plots of quality (x) and void fraction (α_F) in Figures 4.2 to 4.6. After vaporization starts, the pressure dropoff is slower. The mass flow rate ($\dot{M}$) continues to fall rapidly but the increase in specific volume with vaporization results in volume flow rates (Q) rising again, quite markedly for the larger breaks. Note that flow rates $\dot{M}$ and Q in the plots have been scaled down by a factor of 25 in order to make the flow per unit suction and discharge pipe area directly comparable with flows in the 1/5 scale test model.

The increasingly higher volume flow rates tend to produce an accelerating hydraulic torque on the pump impeller (so that impeller torque is negative, or opposite from torque normally driving the fluid) as shown in the plots of torque ratio T/To in Figures 4.7 to 4.11. Even after subtracting out windage and friction drag, the pump speed increases for the larger breaks as shown by the plots of speed ratio N/No. Electrical torque is assumed to be lost coincident with the pipe break in all of these LOCA's. It should be noted that the speeds plotted here were calculated on the basis of no two-phase

FIGURE 4.2

Typical NSSS Large Break Blowdown, Flow Through Pump in Broken Leg, (0.8 DE Slot, Discharge Leg)

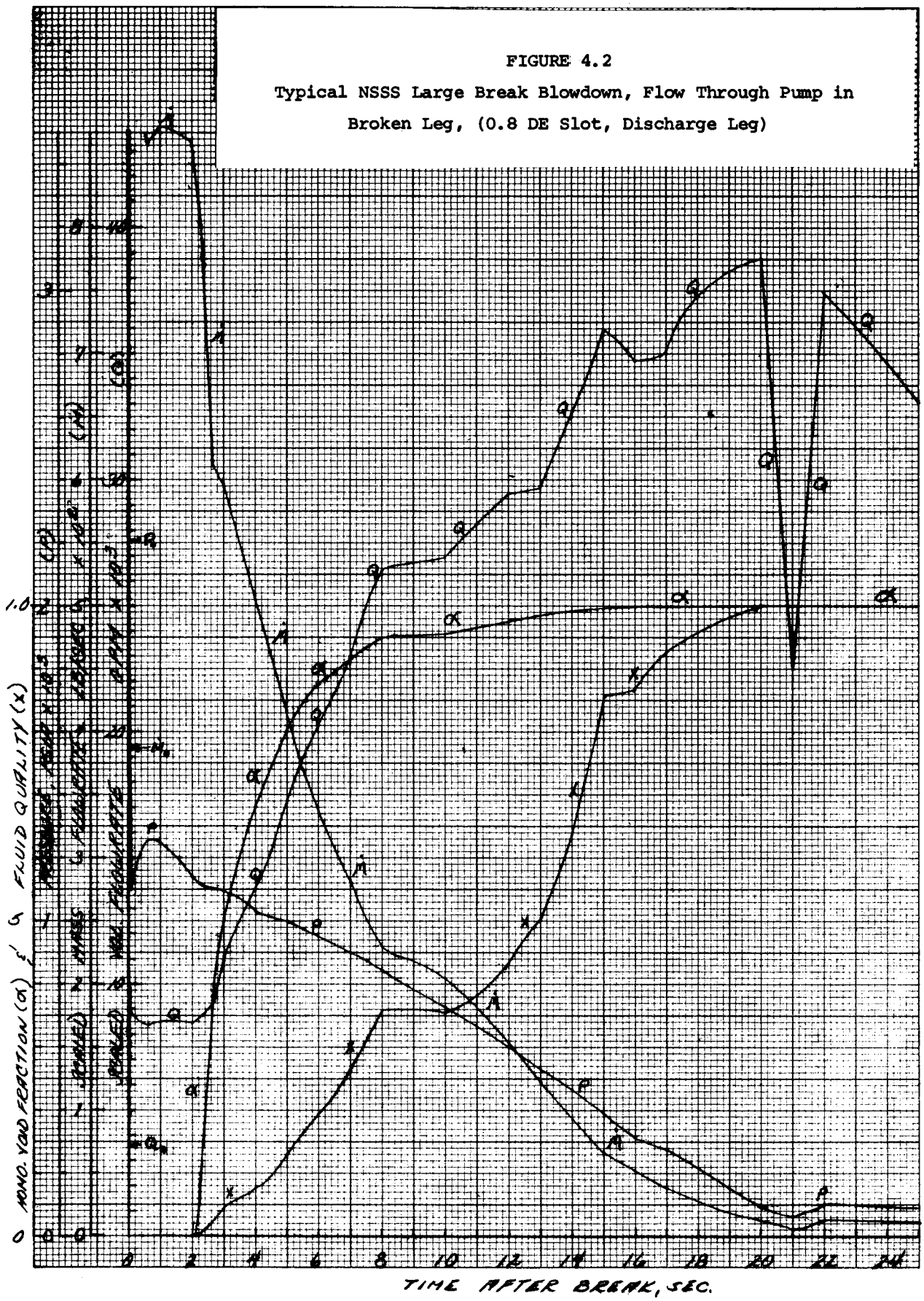

CLW 4/10/85

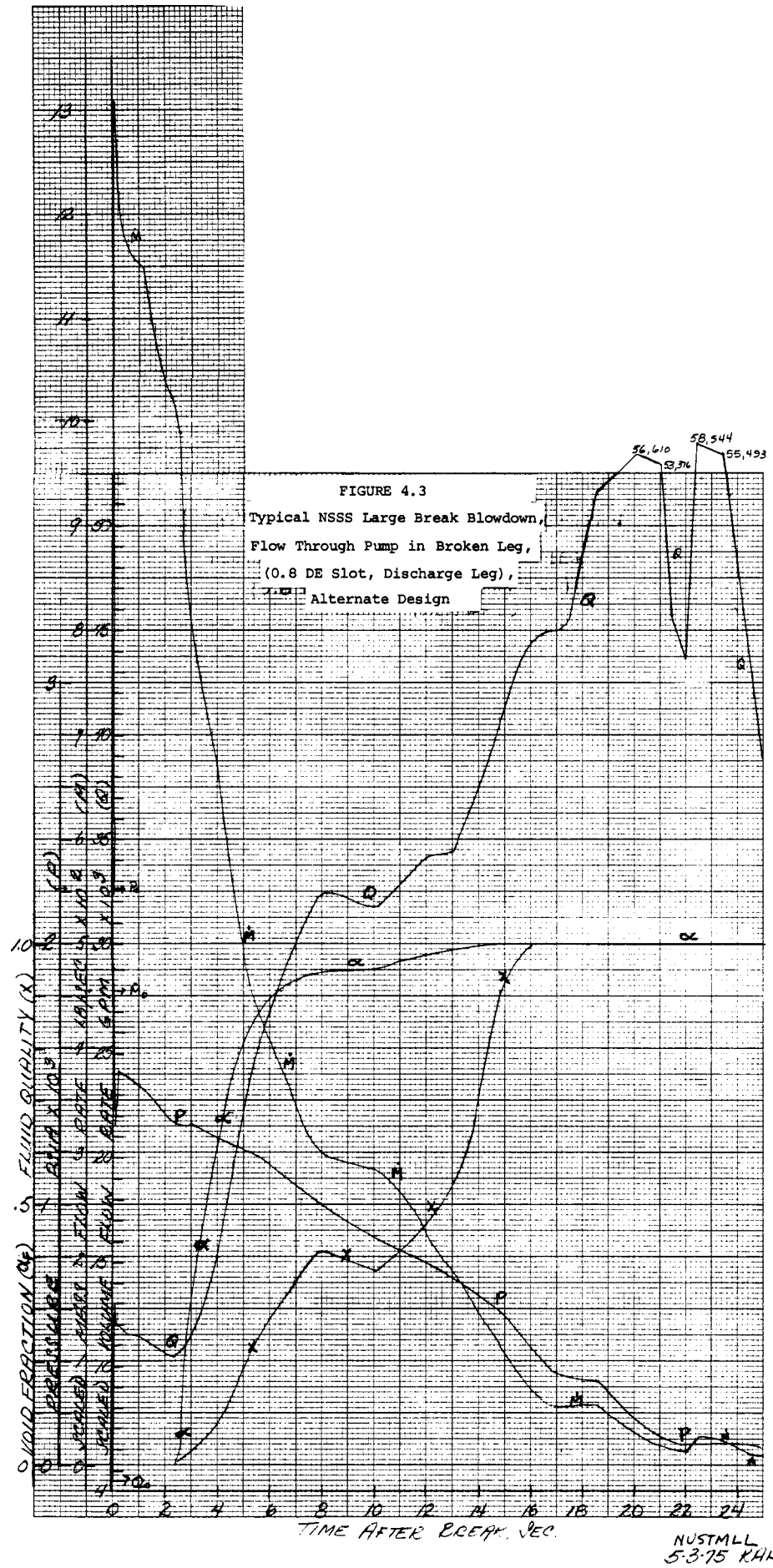

FIGURE 4.3
Typical NSSS Large Break Blowdown, Flow Through Pump in Broken Leg, (0.8 DE Slot, Discharge Leg), Alternate Design

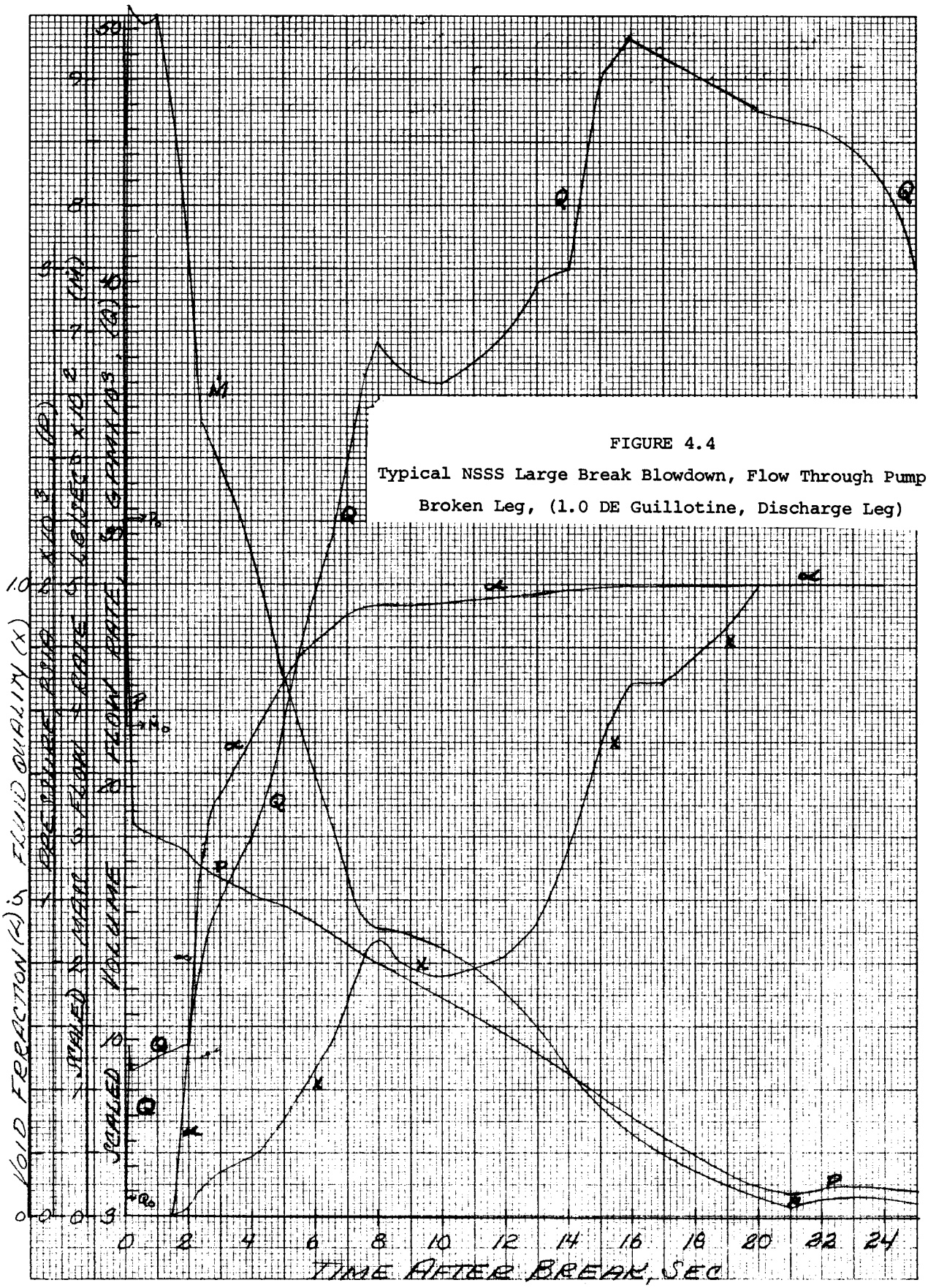

FIGURE 4.4

Typical NSSS Large Break Blowdown, Flow Through Pump in Broken Leg, (1.0 DE Guillotine, Discharge Leg)

KAHL 4-28-75

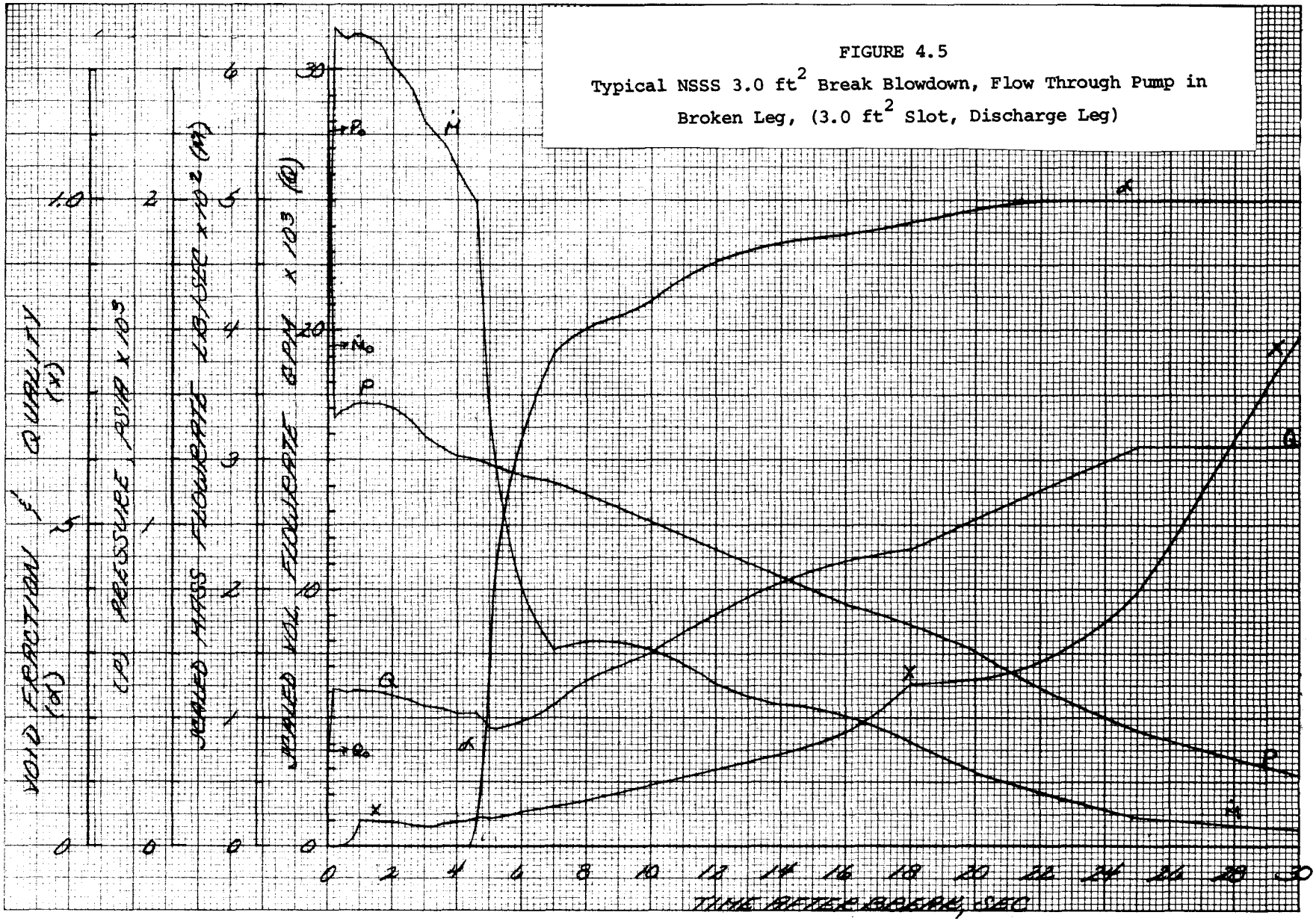

FIGURE 4.5

Typical NSSS 3.0 ft^2 Break Blowdown, Flow Through Pump in Broken Leg, (3.0 ft^2 Slot, Discharge Leg)

W 9-11-75

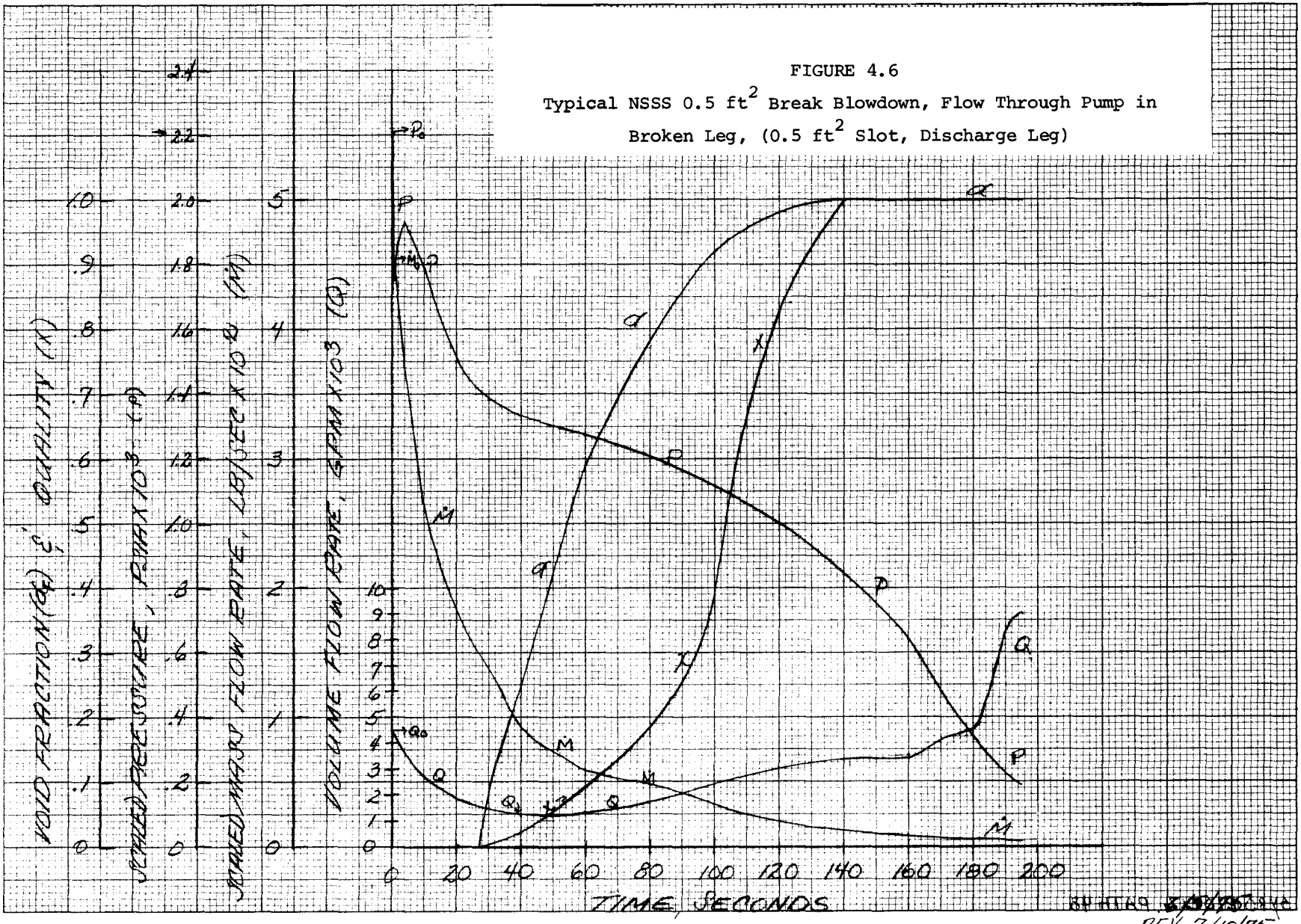

FIGURE 4.6

Typical NSSS 0.5 ft^2 Break Blowdown, Flow Through Pump in Broken Leg, (0.5 ft^2 Slot, Discharge Leg)

FIGURE 4.7

Typical NSSS Large Break Blowdown, Speed and Torque of Pump in Broken Leg, (0.8 DE Slot, Discharge Leg)

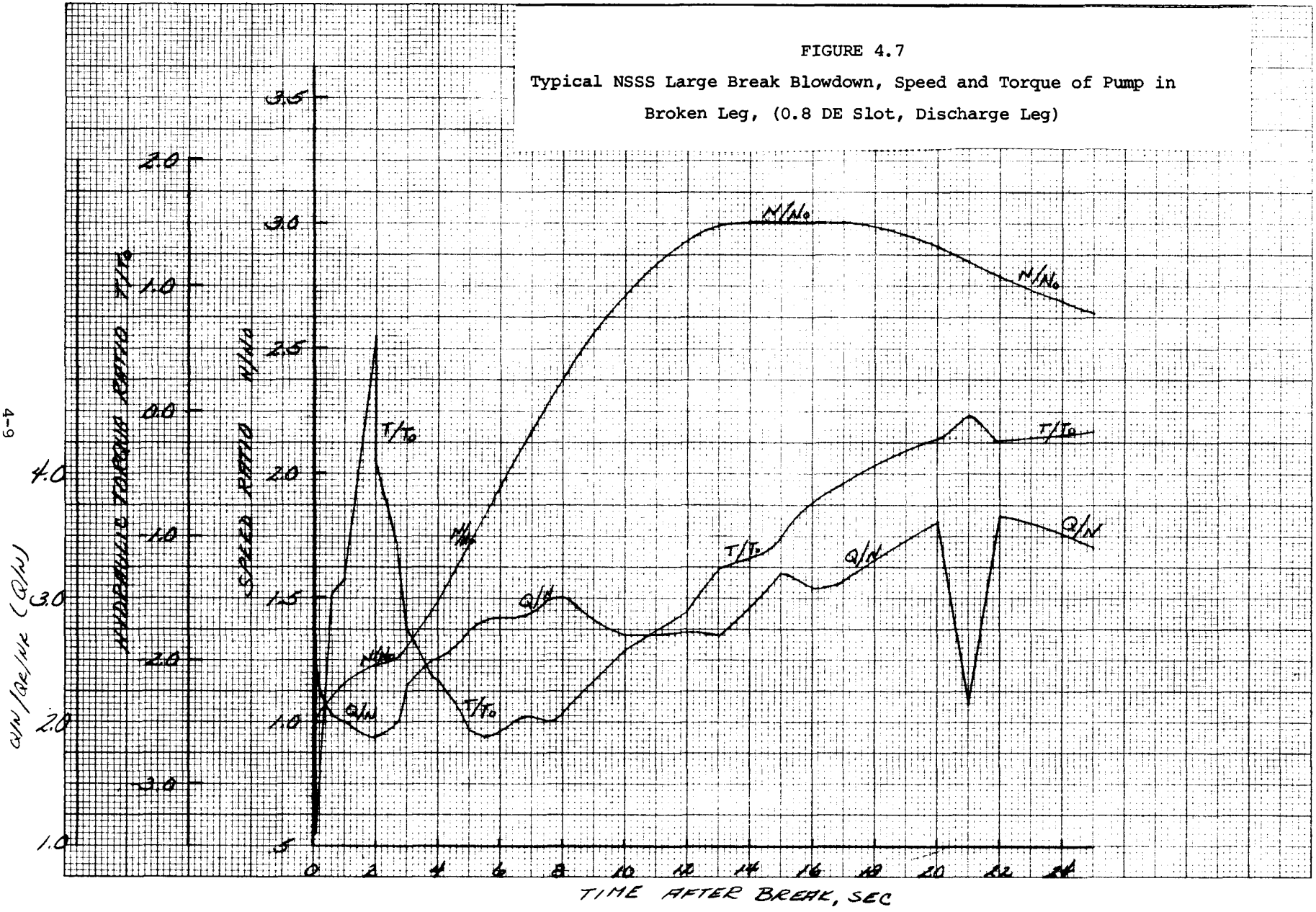

CLW 4/10/85

FIGURE 4.8

Typical NSSS Large Break Blowdown, Speed and Torque of Pump in Broken Leg, (0.8 DE Slot, Discharge Leg), Alternate Design

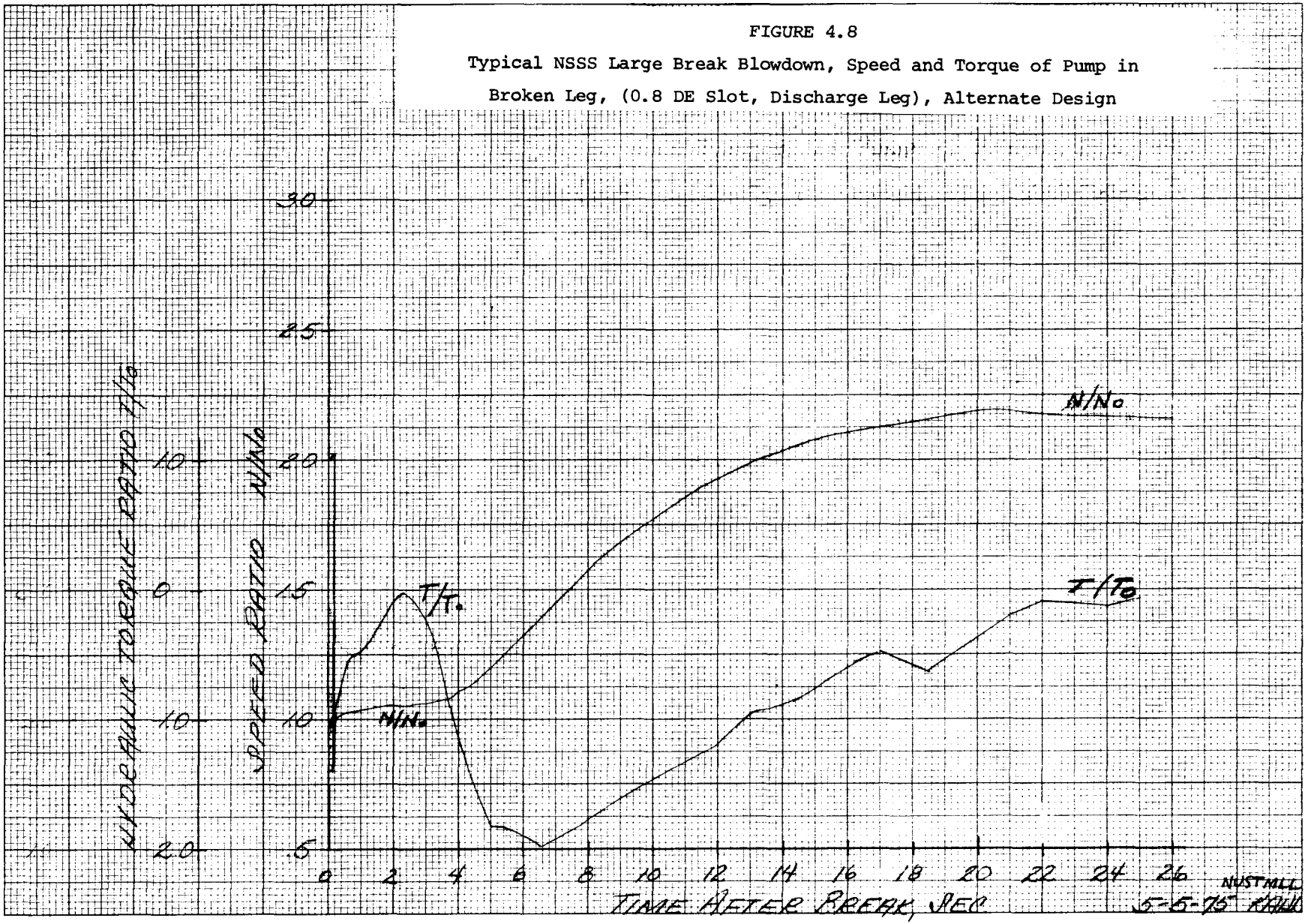

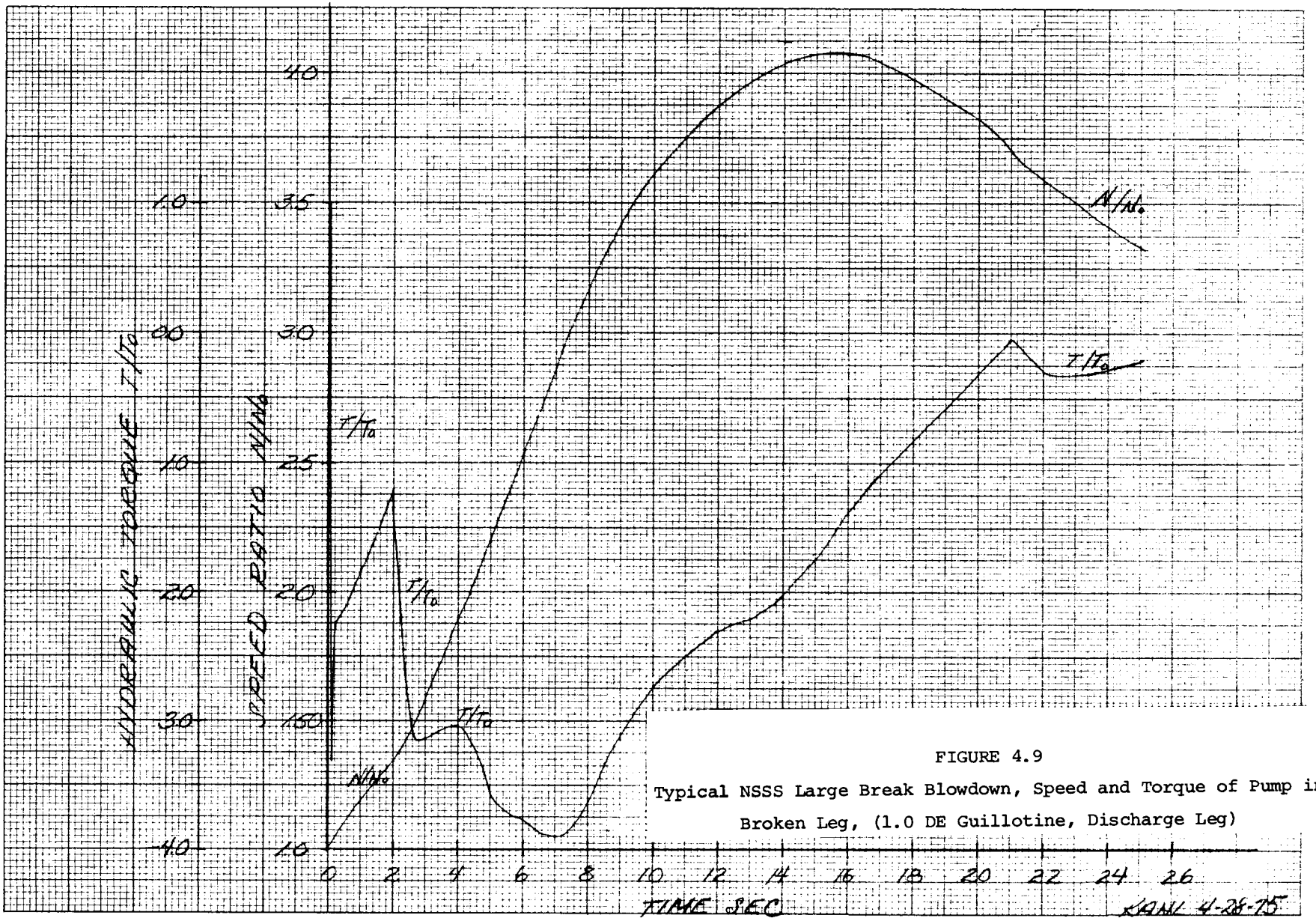

FIGURE 4.9

Typical NSSS Large Break Blowdown, Speed and Torque of Pump in Broken Leg, (1.0 DE Guillotine, Discharge Leg)

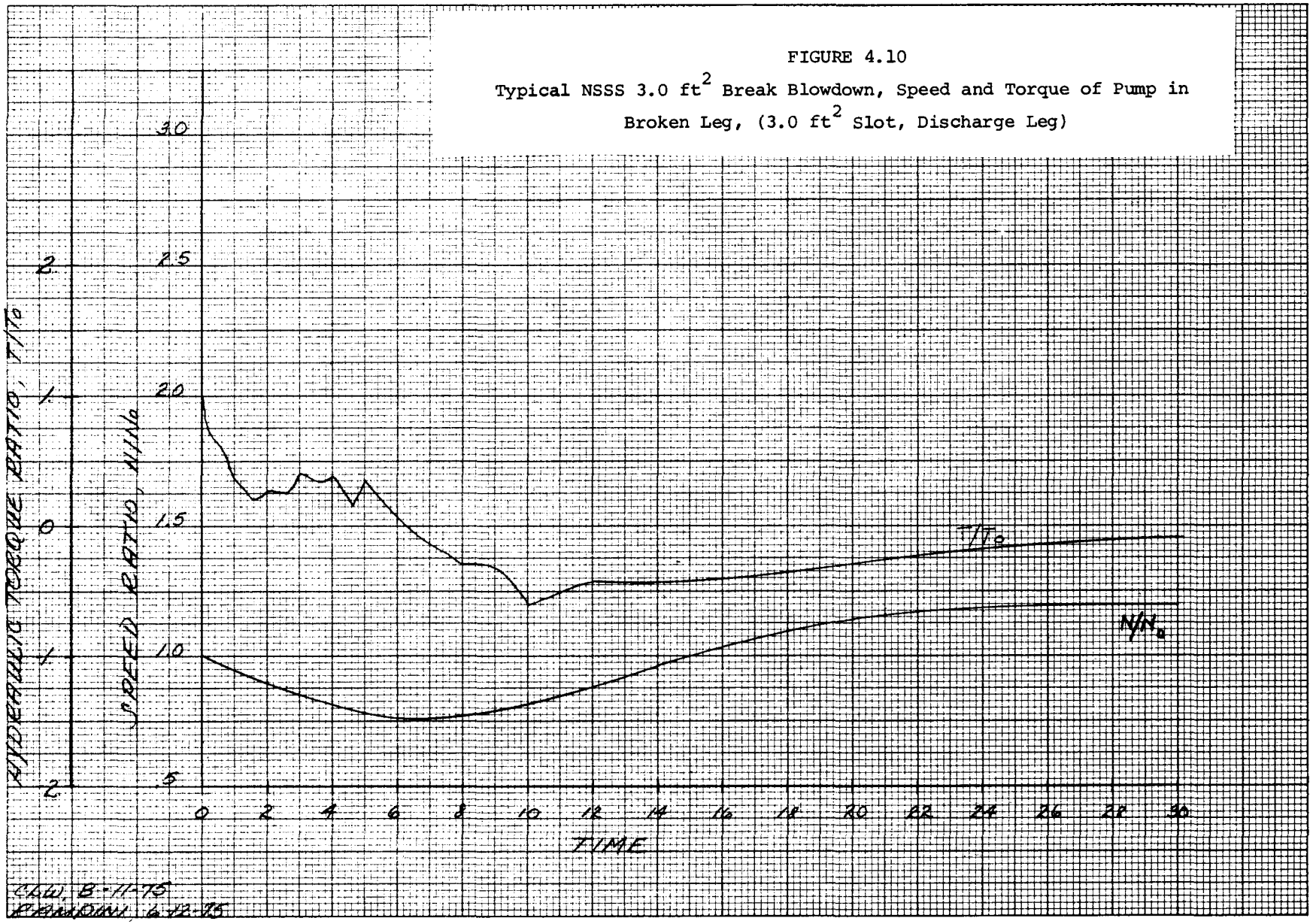

FIGURE 4.10

Typical NSSS 3.0 ft^2 Break Blowdown, Speed and Torque of Pump in Broken Leg, (3.0 ft^2 Slot, Discharge Leg)

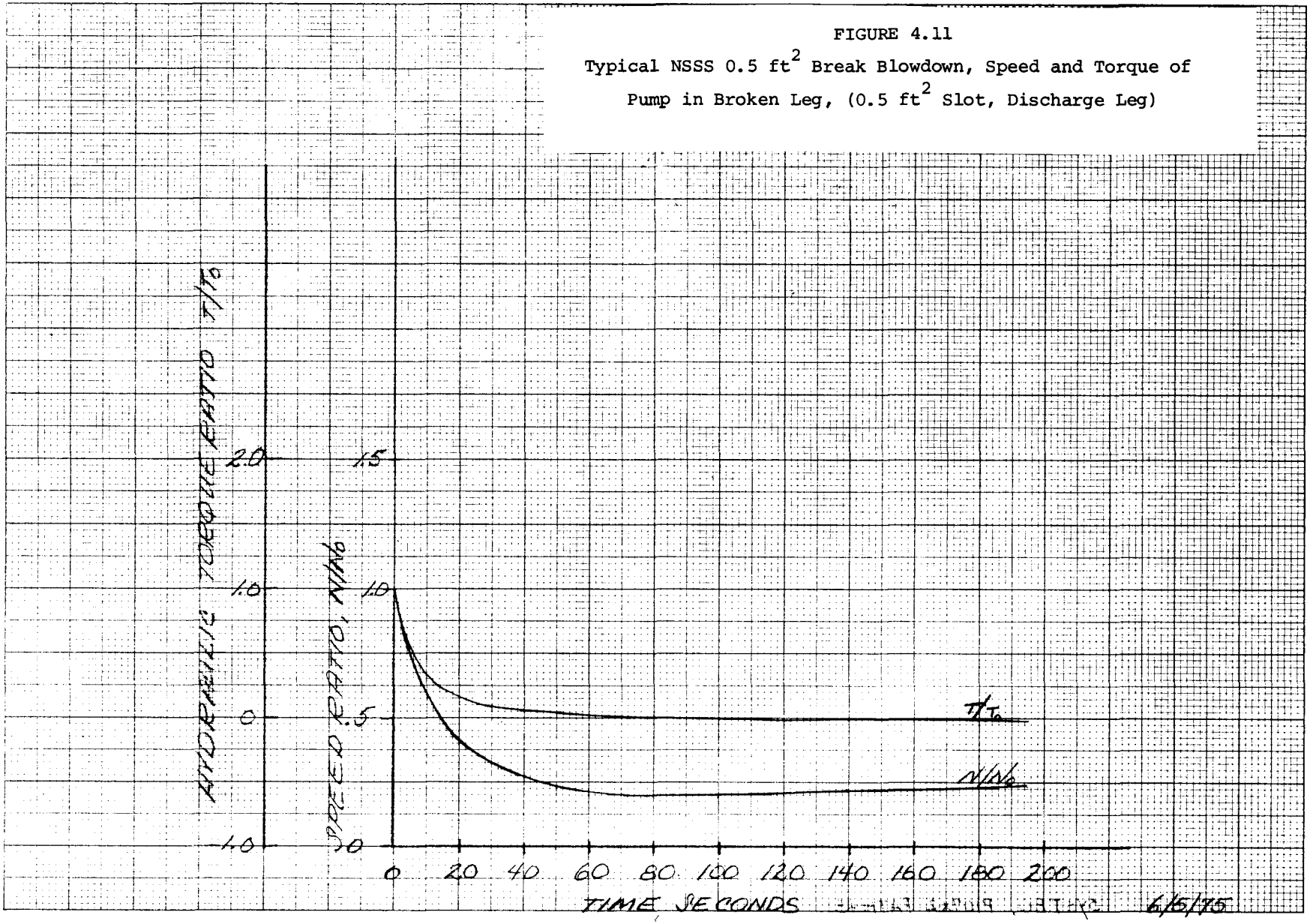

FIGURE 4.11

Typical NSSS 0.5 ft^2 Break Blowdown, Speed and Torque of Pump in Broken Leg, (0.5 ft^2 Slot, Discharge Leg)

torque degradation because of the lack of adequate degradation data. It should also be noted that the LOCA calculations use an unrealistically high discharge coefficient of 1.0 as dictated by NRC regulation.

Since this pump test program is particularly concerned with two-phase effects on performance, the region of the blowdown plots of special interest is the mid-span period in which quality and void fraction (x and α_F) rise from 0 to 1. The large brief fluctuations which appear toward the end of the larger-break blowdowns are generally a consequence of initiating safety injection of cold water and usually occur after the pump flow has returned to single-phase (steam) flow.

Discussion of how the pump and flow conditions in the ranges indicated are combined and evaluated for selecting operating points for the model pump tests is given in Sections 5, 6, and 7 below.

Pumps in the intact loop, being more remote from the break, experience transients less severe although generally similar in nature compared to the broken leg, as shown in Figures 4.12 to 4.21. Vaporization starts later and the flows are not enough to generate any significant pump acceleration. Consequently, the pump speed variation (Figures 4.17 to 4.21) amounts to extended coastdown to about 2/3 normal speed or less, much of which occurs before vaporization begins at the pump. The fluctuations accompanying safety injection in some cases are more marked and lead to temporary return to two-phase conditions, although void fraction remains close to 1.0.

Pump conditions in the intact leg of the broken loop are shown in Figures 4.22 to 4.31. The most distinctive difference here is the flow behavior involving sharp dropoff soon after vaporization begins and then for the larger breaks a persistent though mild flow reversal until injection disturbances occur.

For a large suction break, Figures 4.32 to 4.37 show that the intact loop pumps see about the same conditions as for a discharge leg break. In the intact leg of the broken loop the flow reversal is stronger than for a discharge break and stops the pump. In the broken leg the flow reversal is very strong, causing high reverse speed turbining of the pump if not stopped by an anti-rotation device.

FIGURE 4.12

Typical NSSS Large Break Blowdown, Flow Through Pump in Intact Loop, (0.8 DE Slot, Discharge Leg)

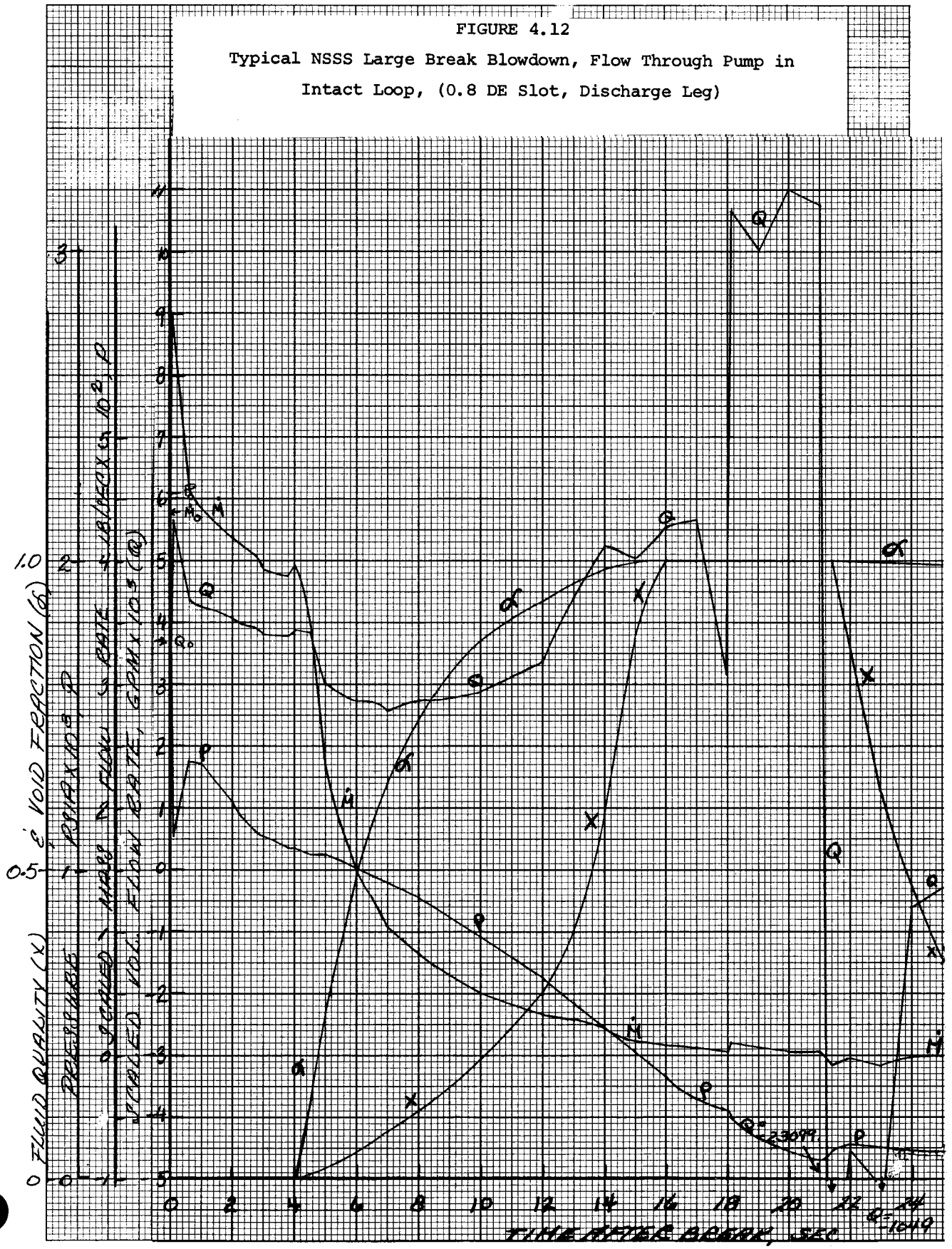

CLW 4/18/75

FIGURE 4.13

Typical NSSS Large Break Blowdown, Flow Through Pump in Intact Loop, (0.8 DE Slot, Discharge Leg), Alternate Design

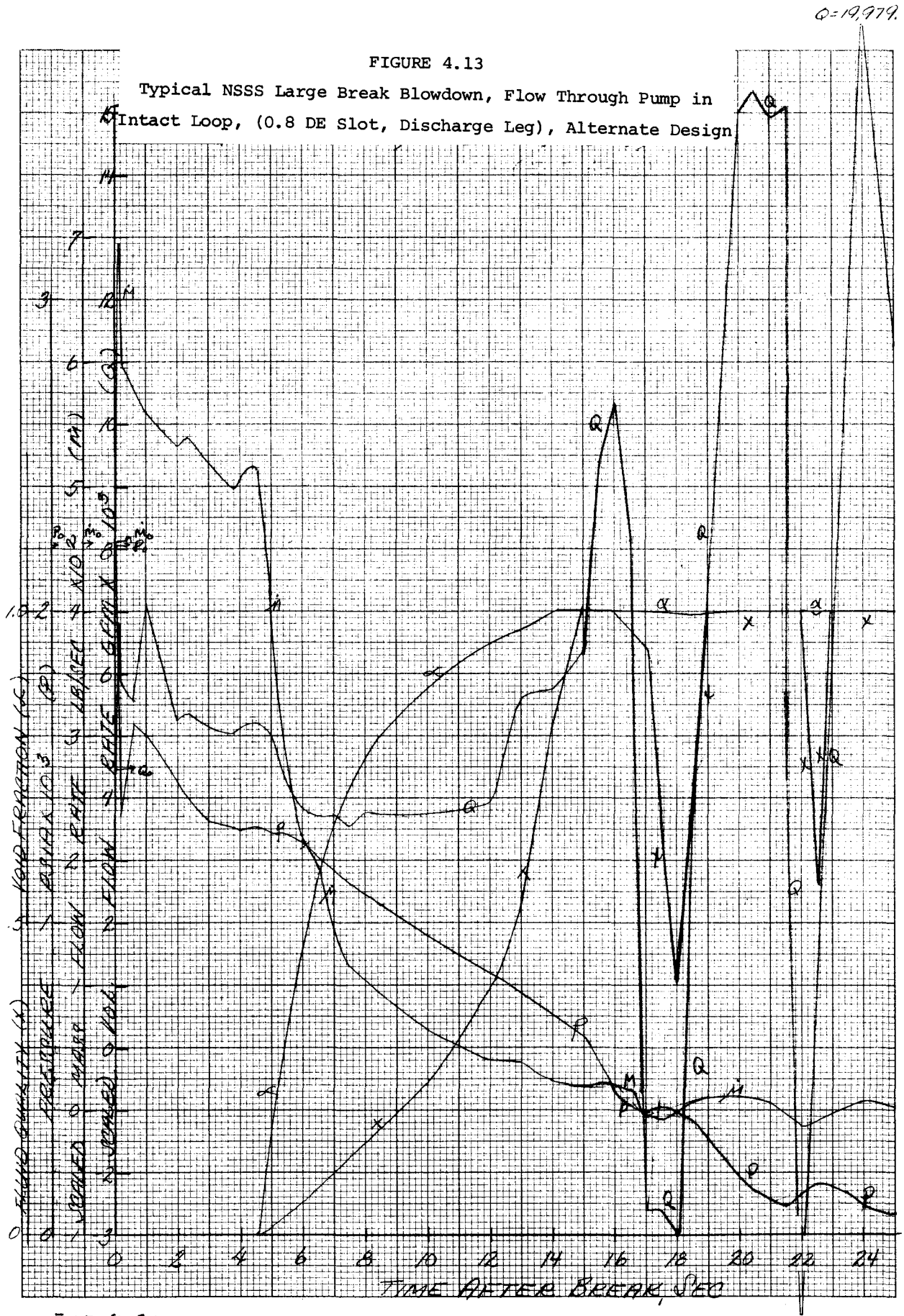

REV 7-8-75
KAHL 5-7-75

FIGURE 4.14

Typical NSSS Large Break Blowdown, Flow Through Pump in Intact Loop, (1.0 DE Guillotine, Discharge Leg)

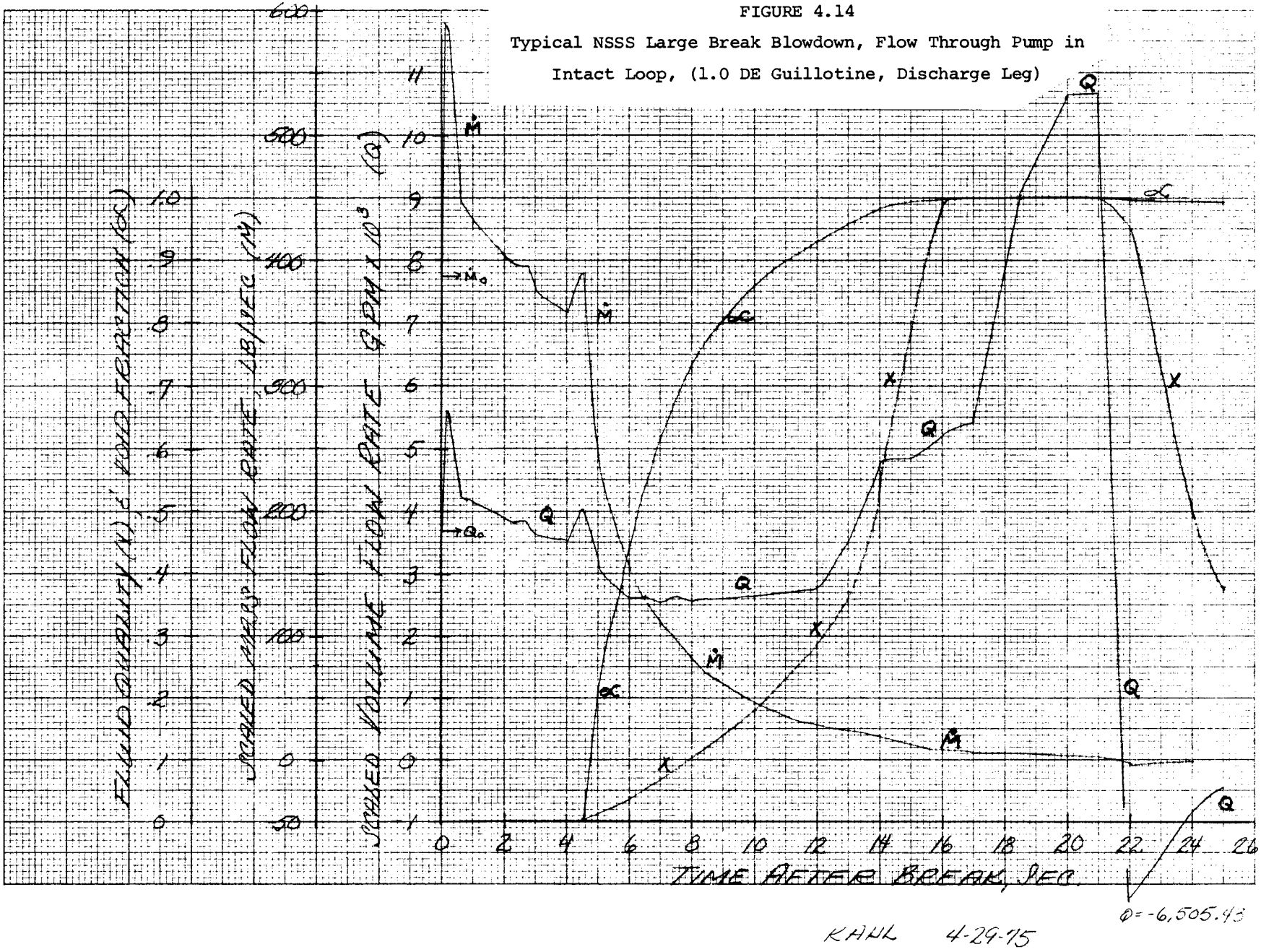

FIGURE 4.15

Typical NSSS 3.0 ft^2 Break Blowdown, Flow Through Pump in Intact Loop, (3.0 ft^2 Slot, Discharge Leg)

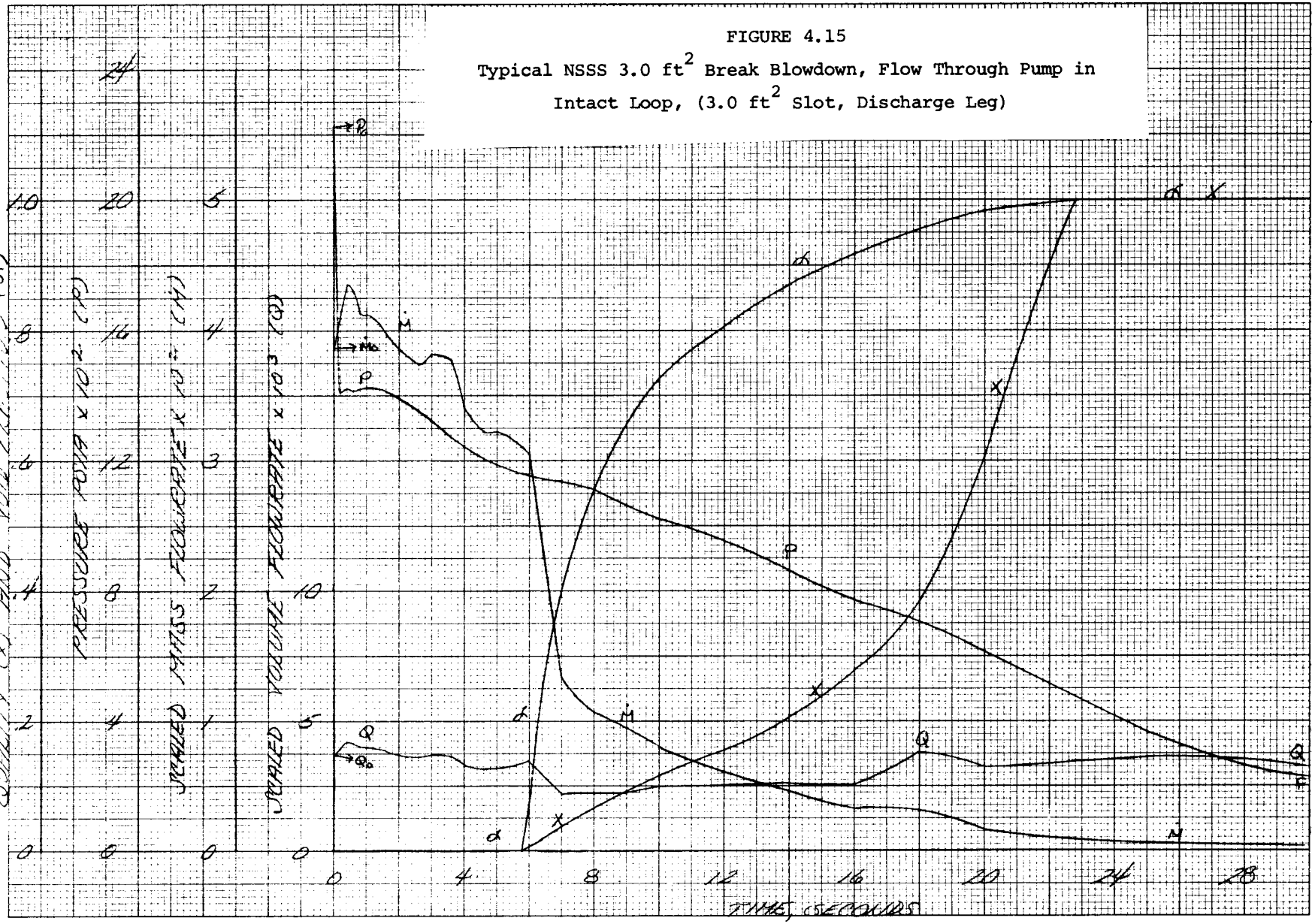

CLW 7-14-75 REV. 2-20-76

FIGURE 4.16

Typical NSSS 0.5 ft^2 Break Blowdown, Flow Through Pump in Intact Loop (0.5 ft^2 Slot, Discharge Leg)

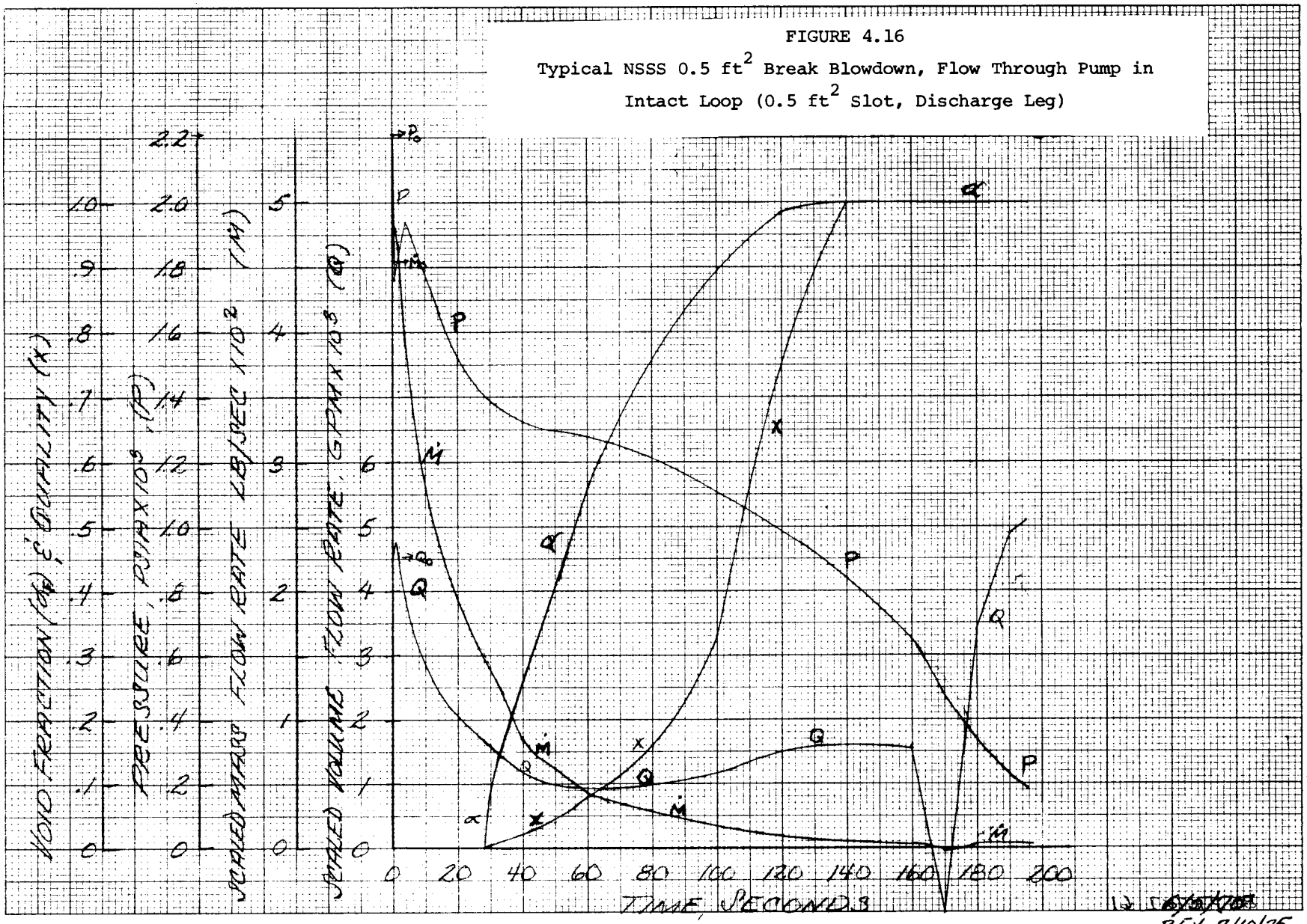

FIGURE 4.17

Typical NSSS Large Break Blowdown, Speed and Torque of Pump in Intact Loop, (0.8 DE Slot, Discharge Leg)

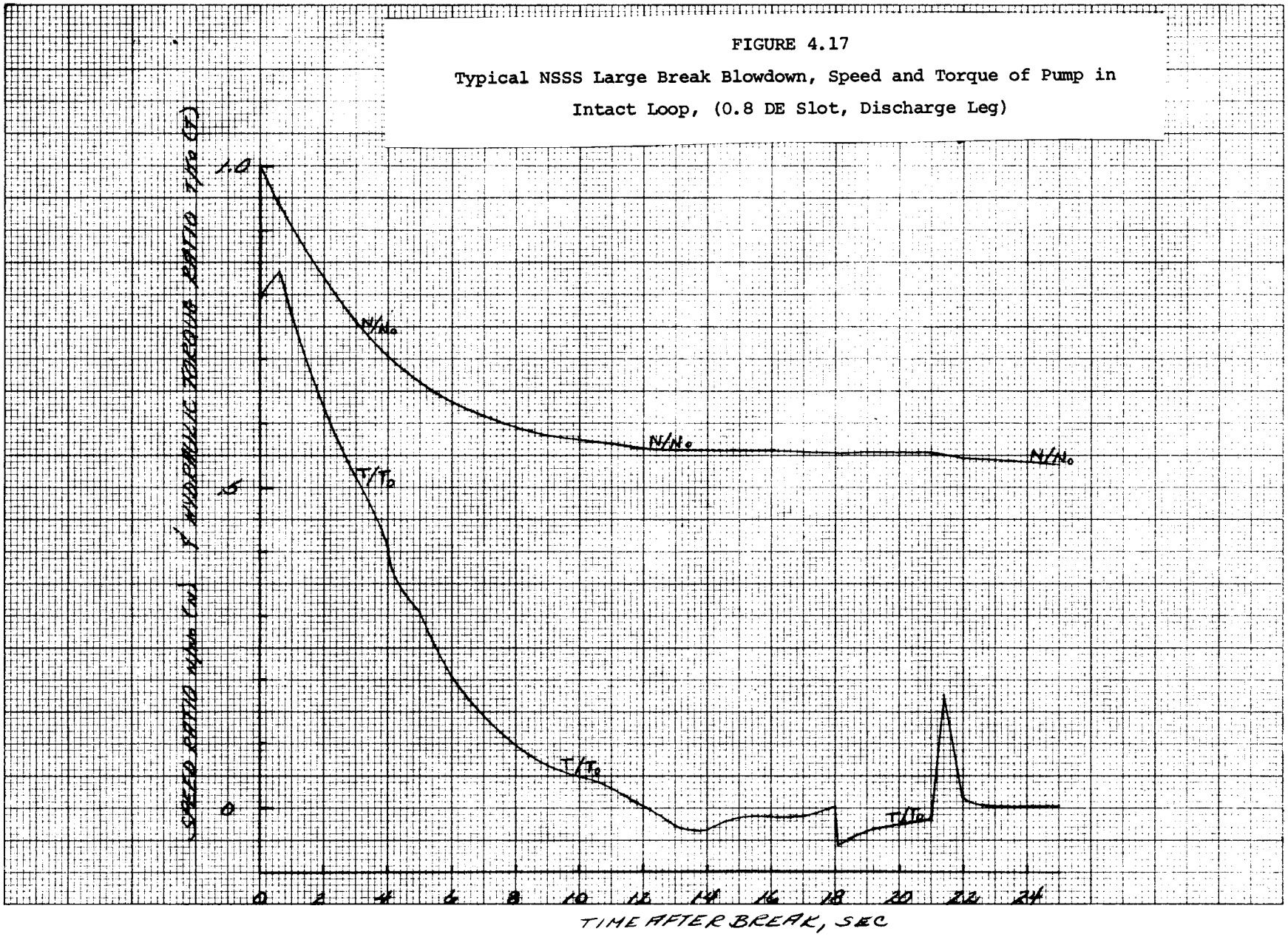

CLW 4/17/75

FIGURE 4.18

Typical NSSS Large Break Blowdown, Speed and Torque of Pump in Intact Loop, (0.8 DE Slot, Discharge Leg), Alternate Design

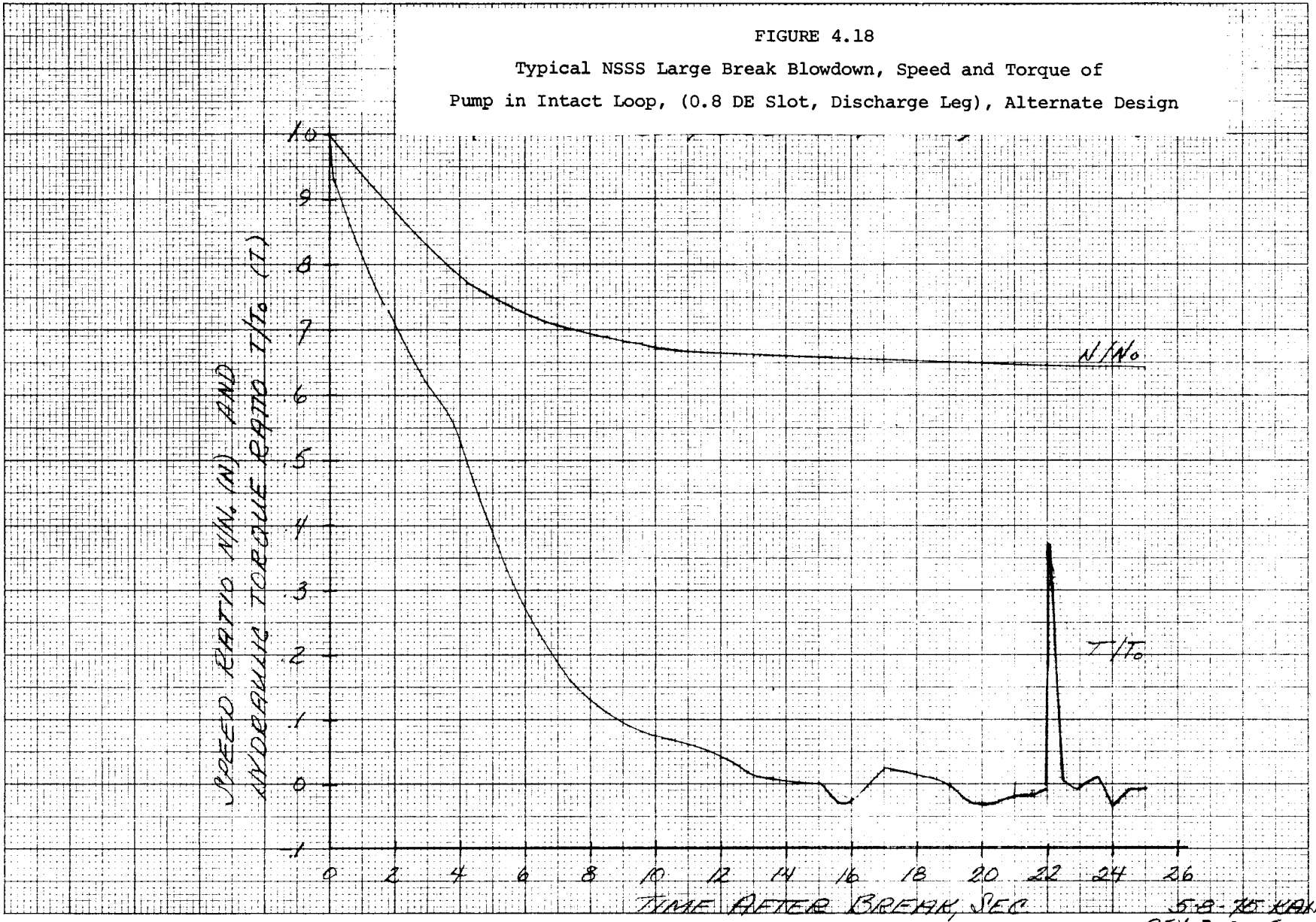

5-8-75 KAN
REV 7-8-75

FIGURE 4.19

Typical NSSS Large Break Blowdown, Speed and Torque of Pump in Intact Loop, (1.0 DE Guillotine, Discharge Leg)

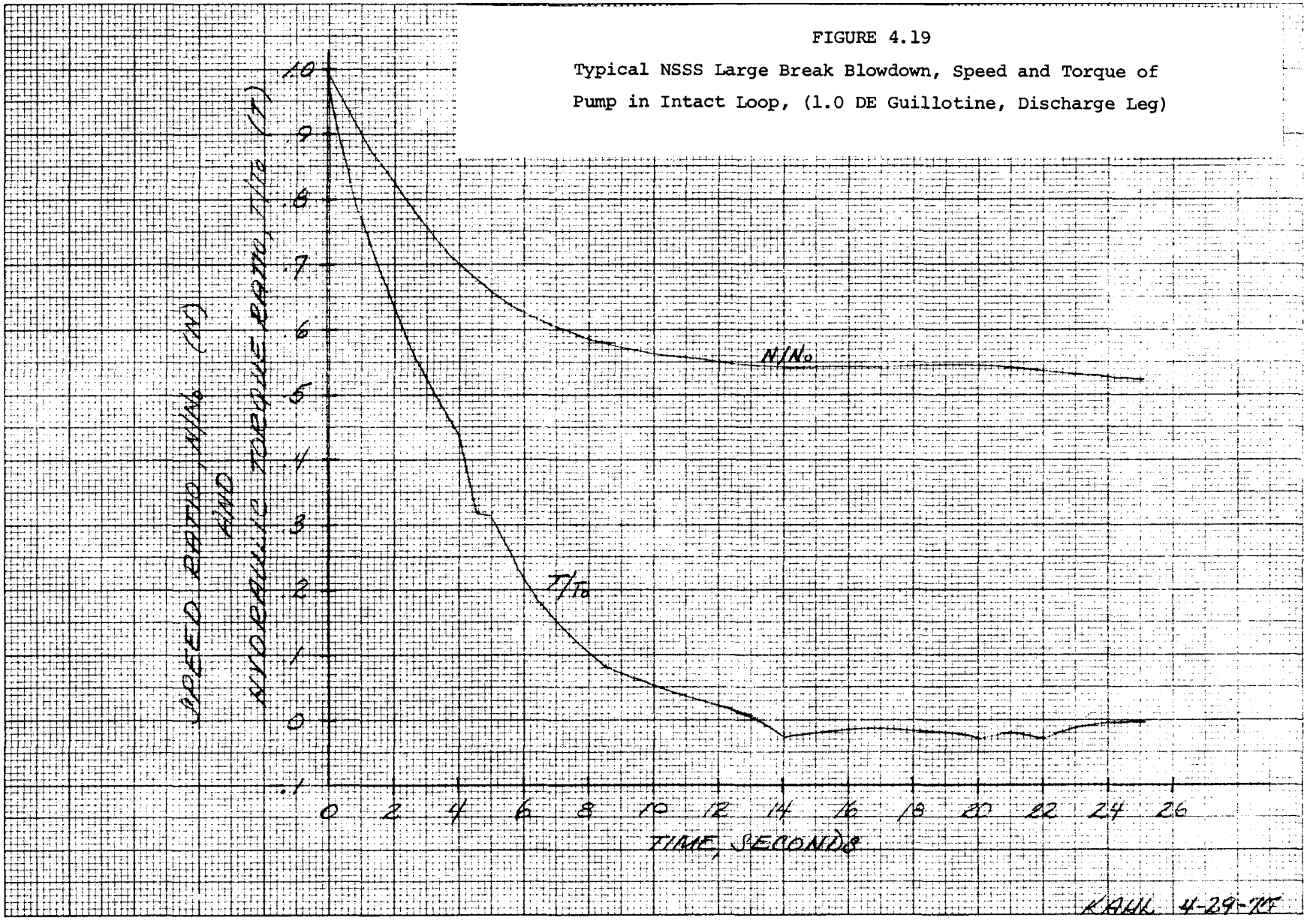

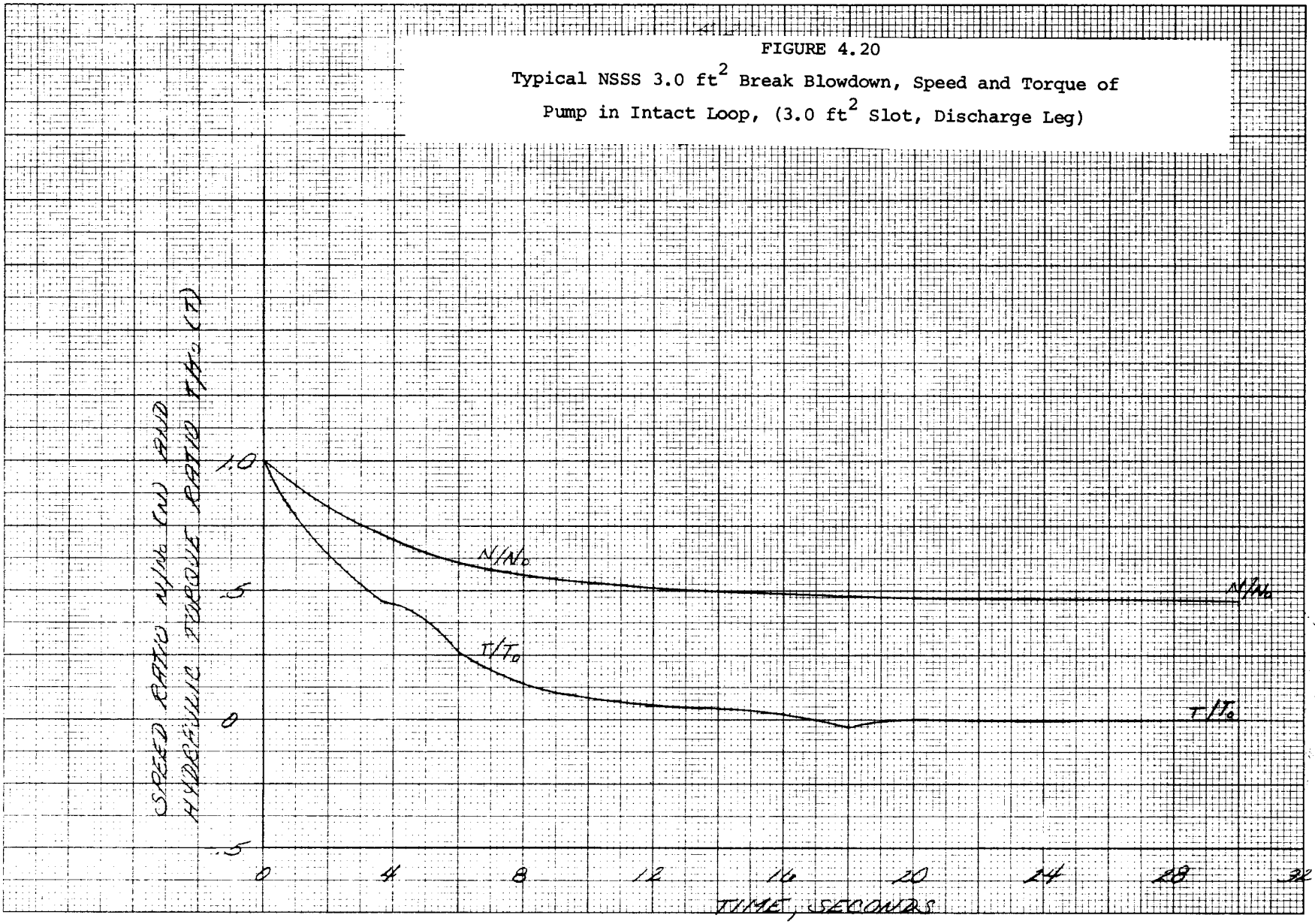

FIGURE 4.20

Typical NSSS 3.0 ft^2 Break Blowdown, Speed and Torque of Pump in Intact Loop, (3.0 ft^2 Slot, Discharge Leg)

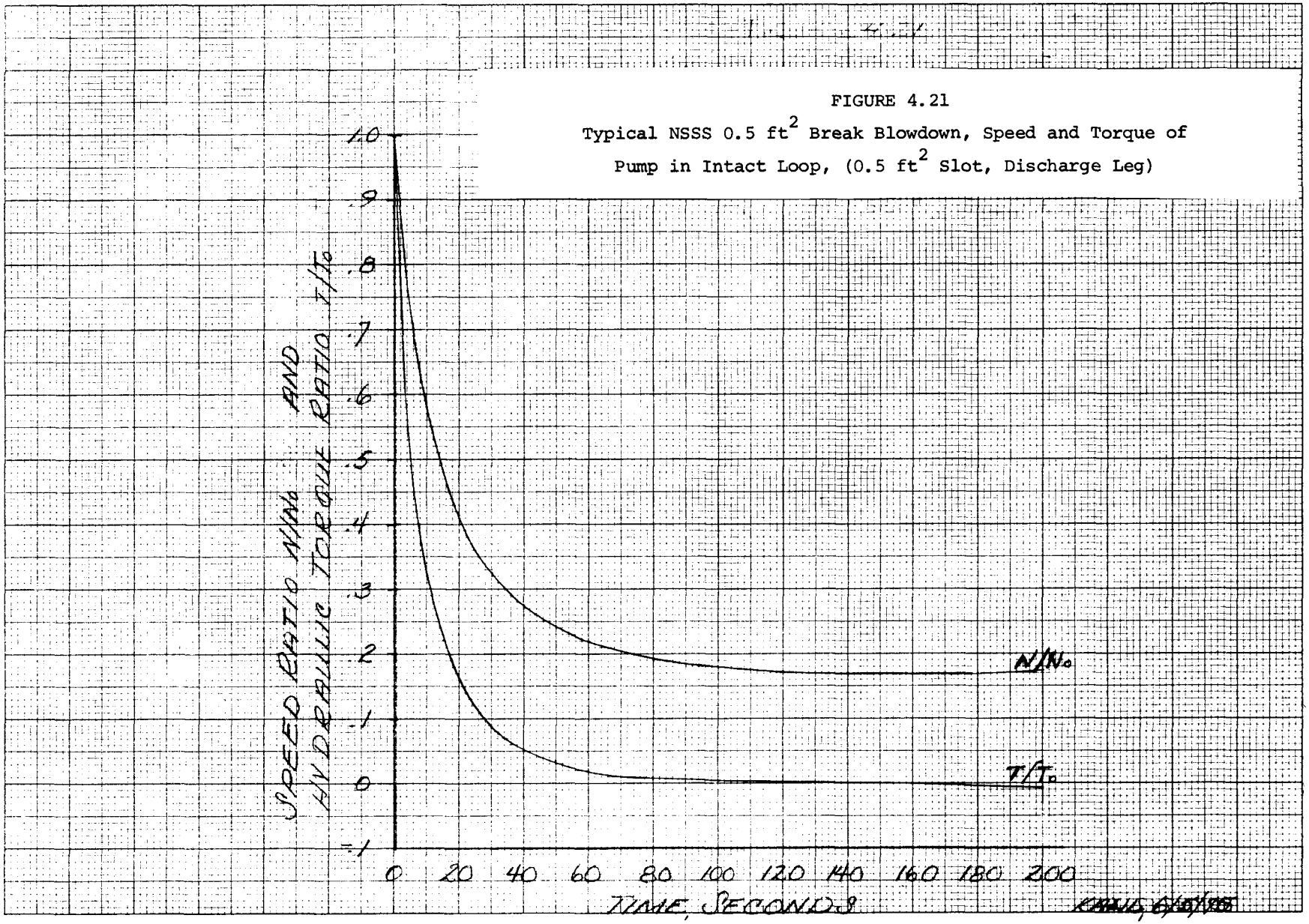

FIGURE 4.21

Typical NSSS 0.5 ft^2 Break Blowdown, Speed and Torque of Pump in Intact Loop, (0.5 ft^2 Slot, Discharge Leg)

FIGURE 4.22

Typical NSSS Large Break Blowdown, Flow Through Pump in Intact Leg, Broken Loop, (0.8 DE Slot, Discharge Leg)

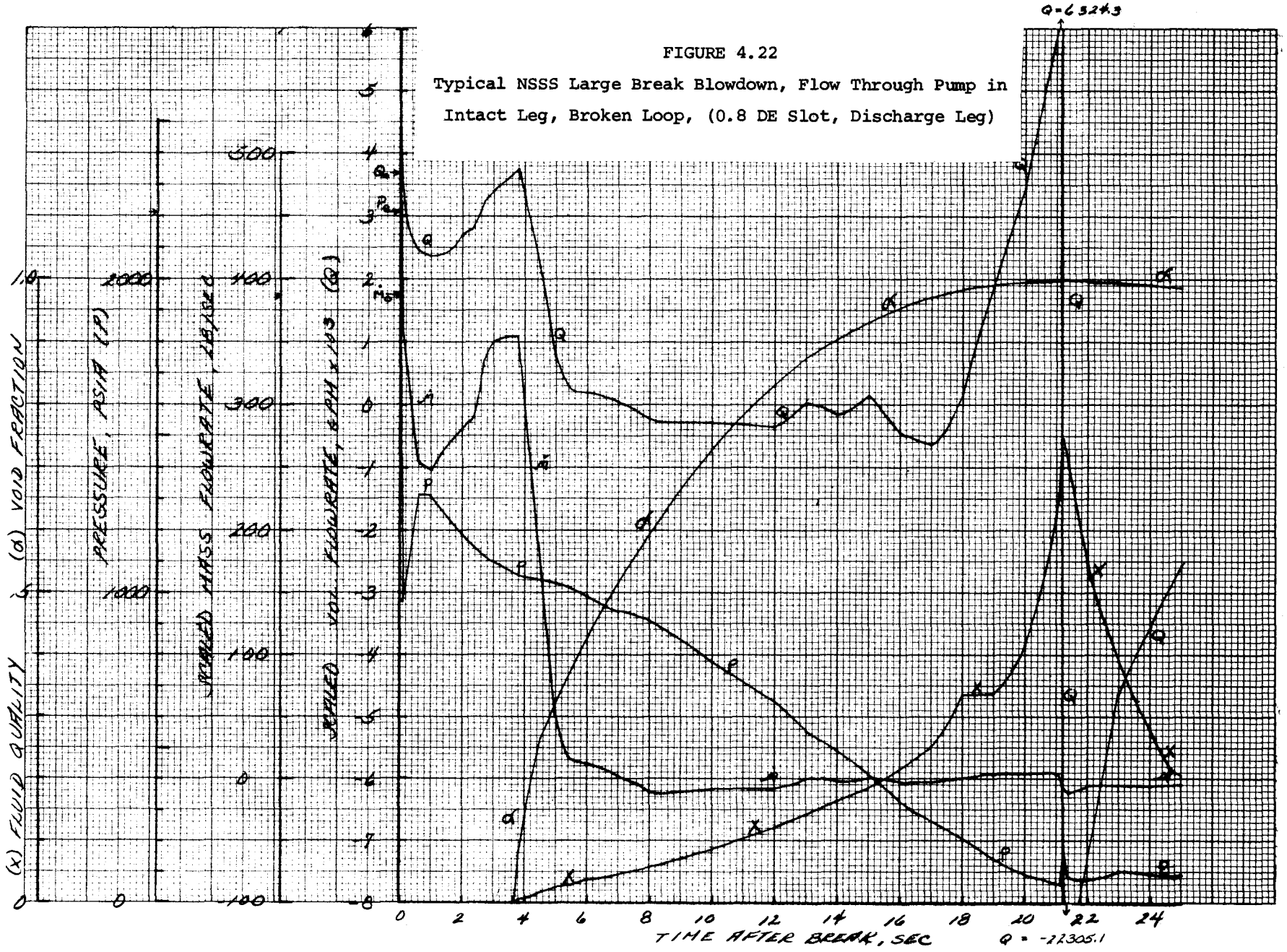

FIGURE 4.23

Typical NSSS Large Break Blowdown, Flow Through Pump in Intact Leg, Broken Loop, (0.8 DE Slot, Discharge Leg), Alternate Design

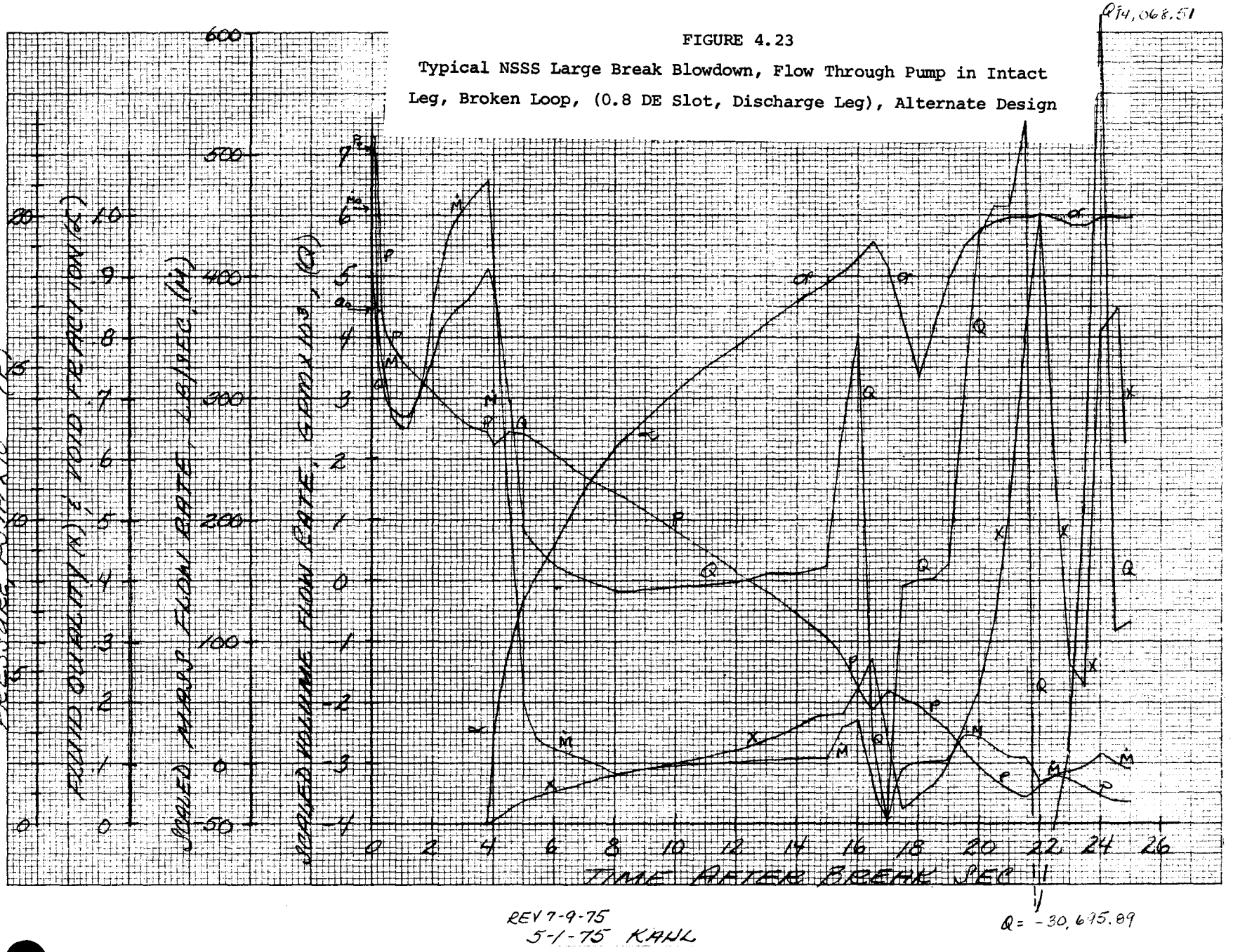

FIGURE 4.24

Typical NSSS Large Break Blowdown, Flow Through Pump in Intact Leg, Broken Loop, (1.0 DE Guillotine, Discharge Leg)

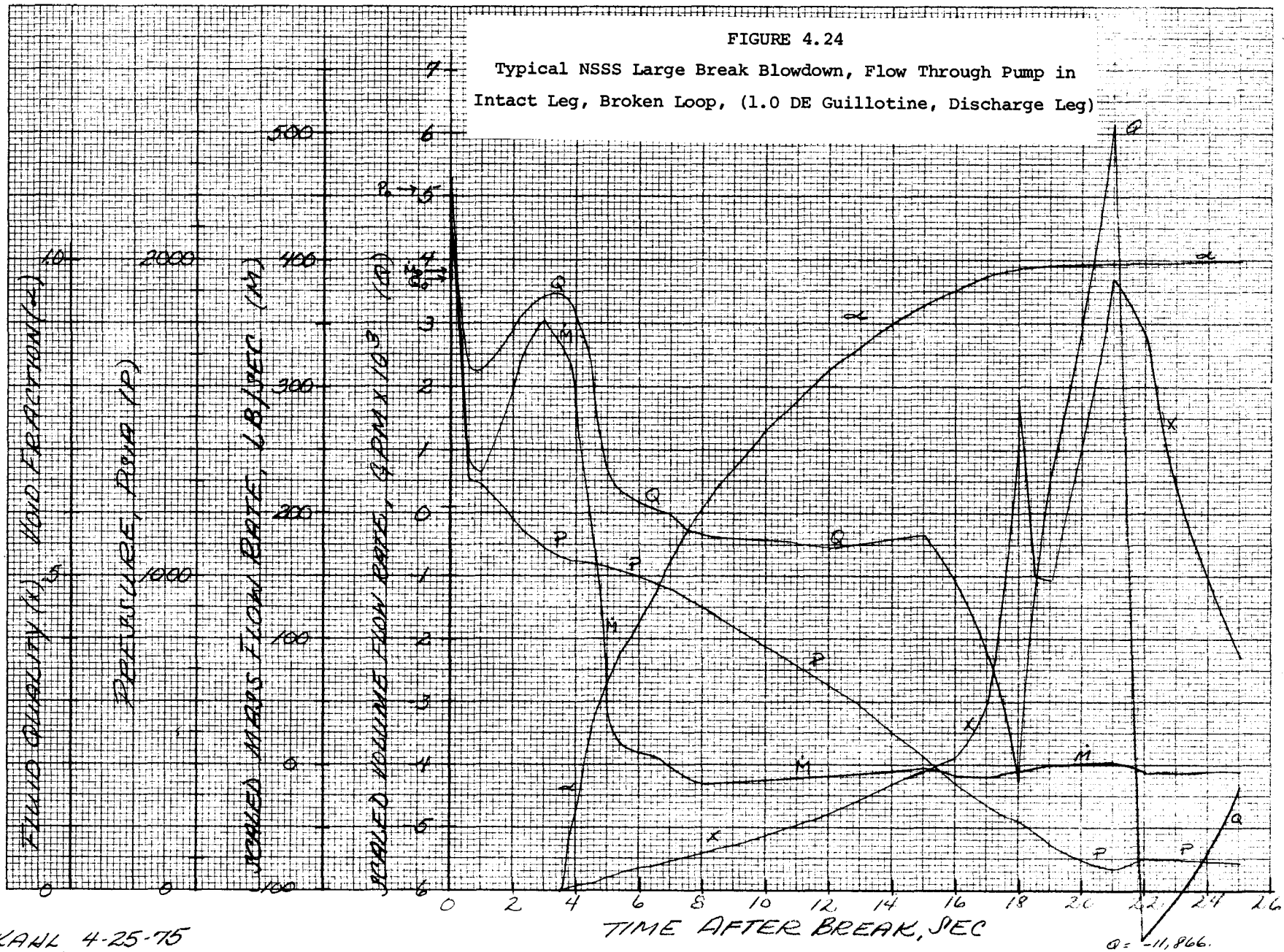

FIGURE 4.25

Typical NSSS 3.0 ft^2 Break Blowdown, Flow Through Pump in Intact Leg, Broken Loop, (3.0 ft^2 Slot, Discharge Leg)

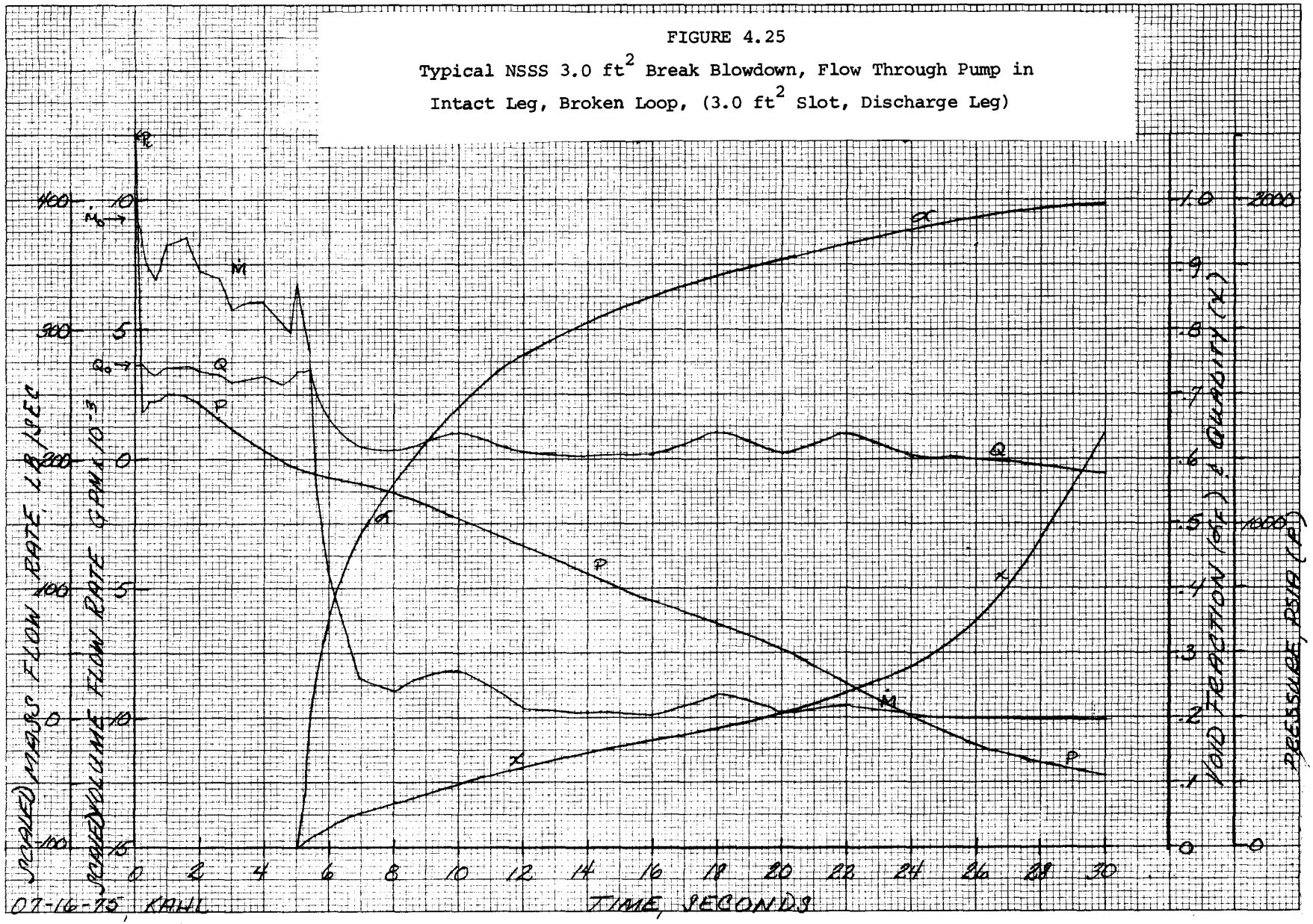

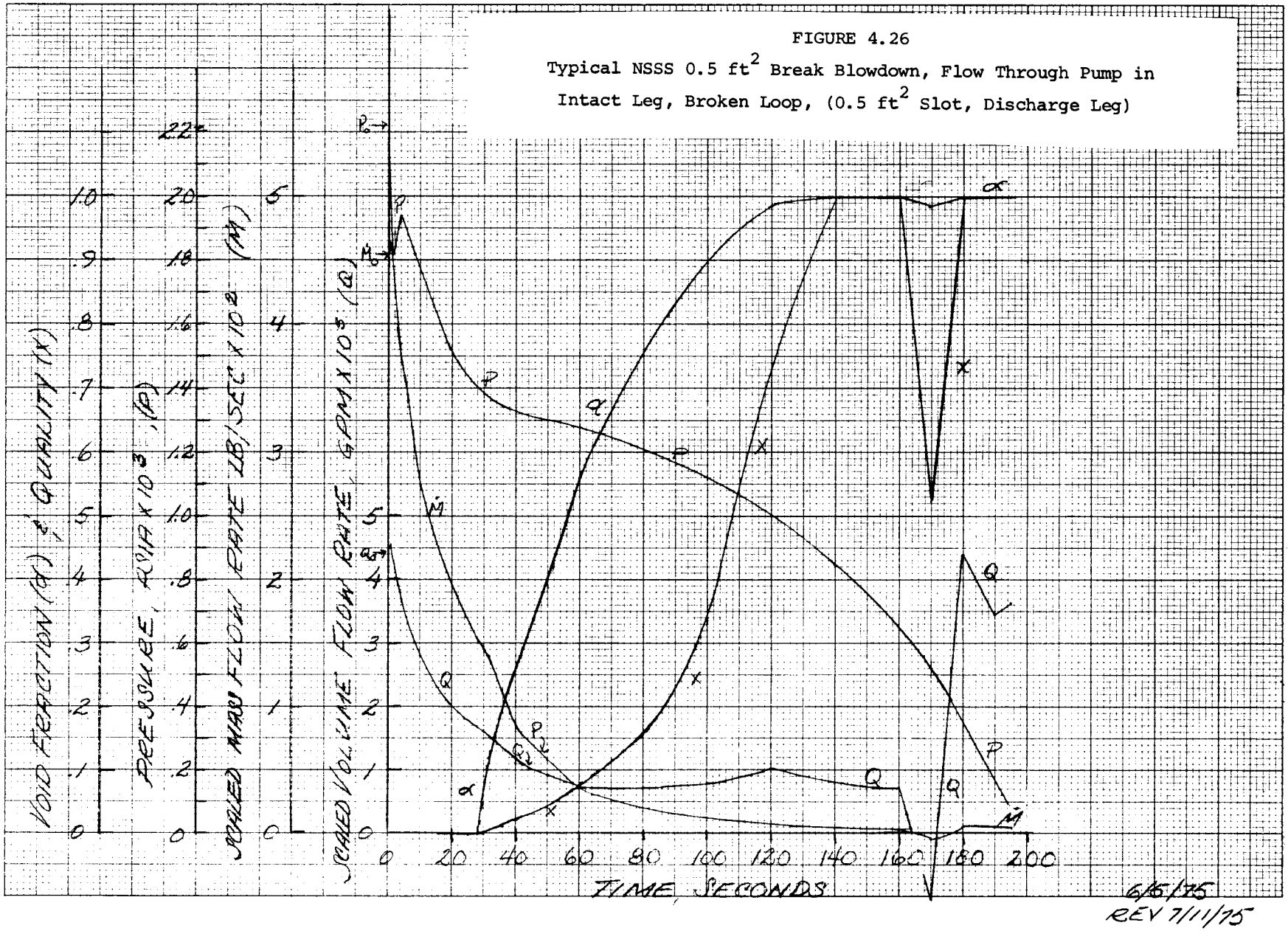

FIGURE 4.26

Typical NSSS 0.5 ft^2 Break Blowdown, Flow Through Pump in Intact Leg, Broken Loop, (0.5 ft^2 Slot, Discharge Leg)

FIGURE 4.27

Typical NSSS Large Break Blowdown, Speed and Torque of Pump in Intact Leg, Broken Loop, (0.8 DE Slot, Discharge Leg)

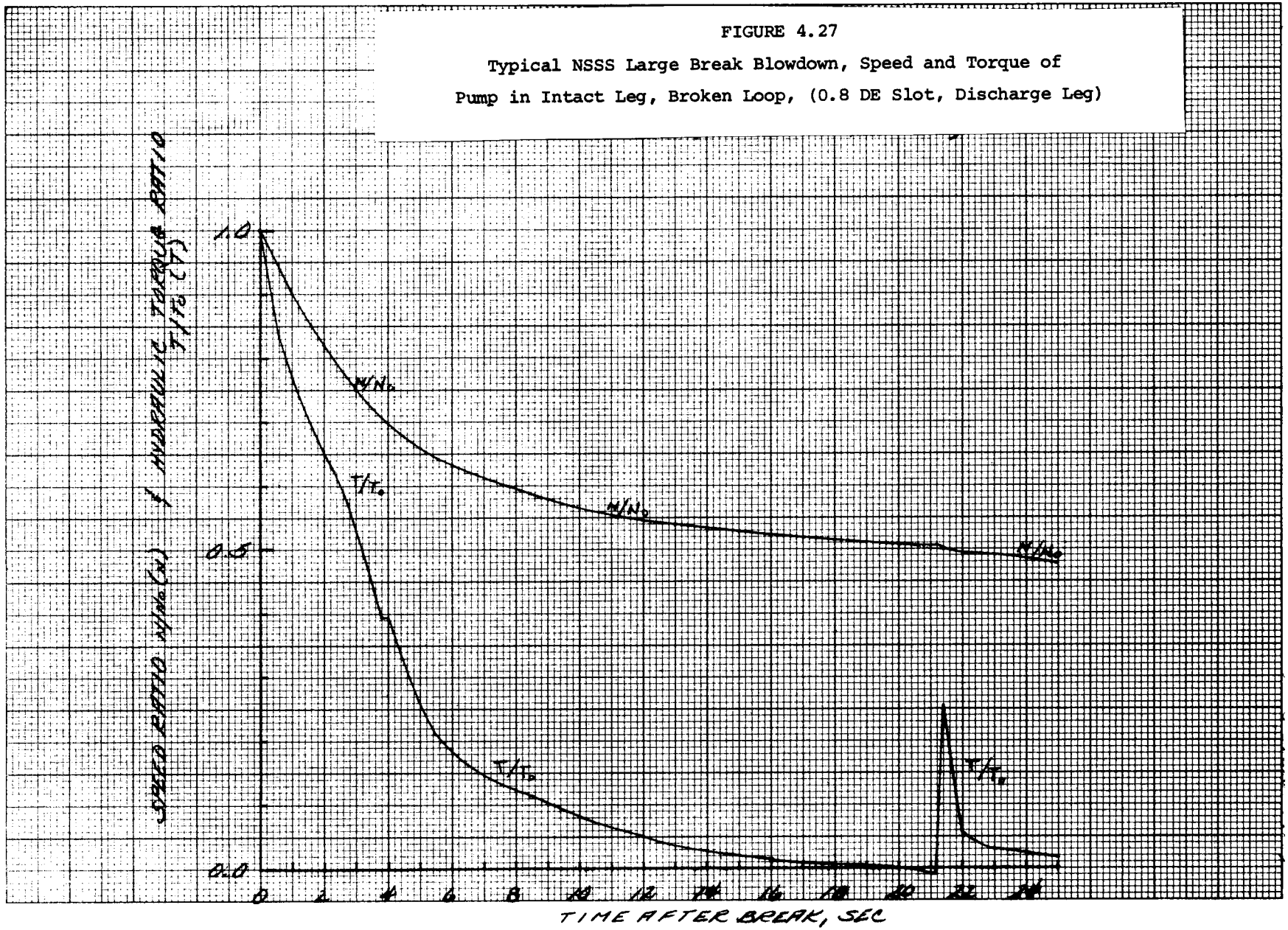

CLW 4/15/80

FIGURE 4.28

Typical NSSS Large Break Blowdown, Speed and Torque of Pump in Intact Leg, Broken Loop, (0.8 DE Slot, Discharge Leg), Alternate Design

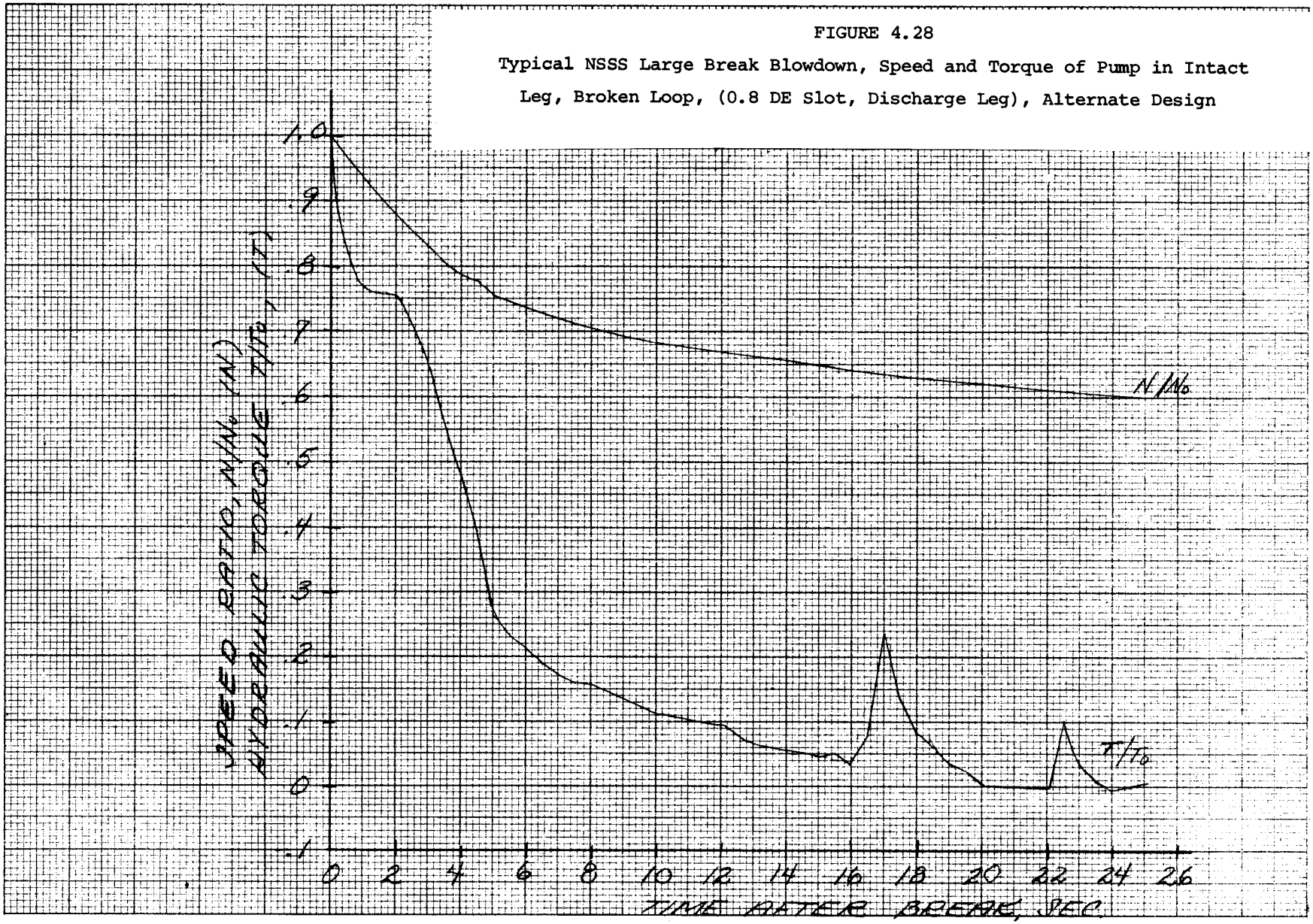

REV 7-9-75
5-1-75 KAHL

FIGURE 4.29

Typical NSSS Large Break Blowdown, Speed and Torque of Pump in Intact Leg, Broken Loop, (1.0 DE Guillotine, Discharge Leg)

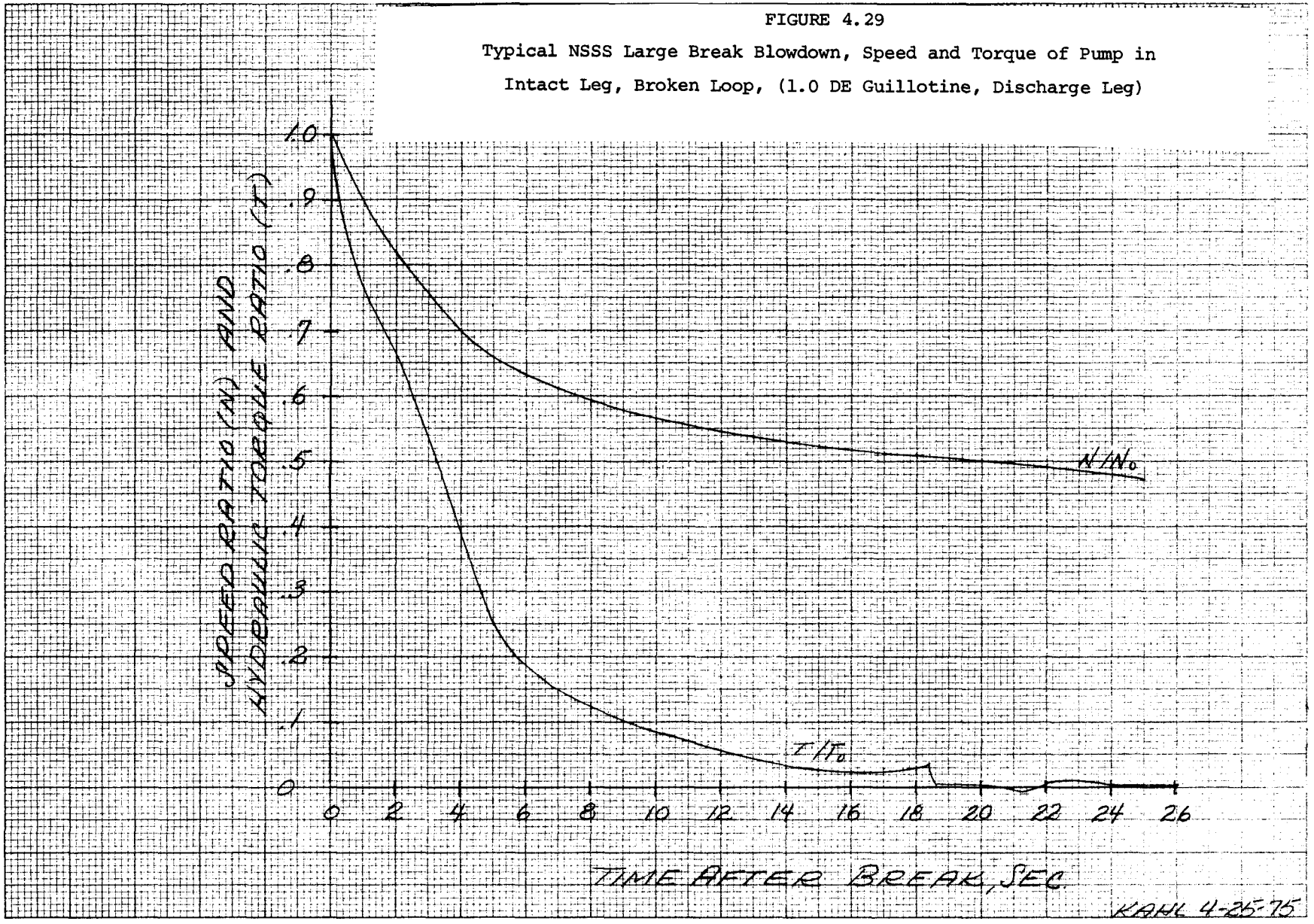

FIGURE 4.30

Typical NSSS 3.0 ft^2 Break Blowdown, Speed and Torque of Pump in Intact Leg, Broken Loop, (3.0 ft^2 Slot, Discharge Leg)

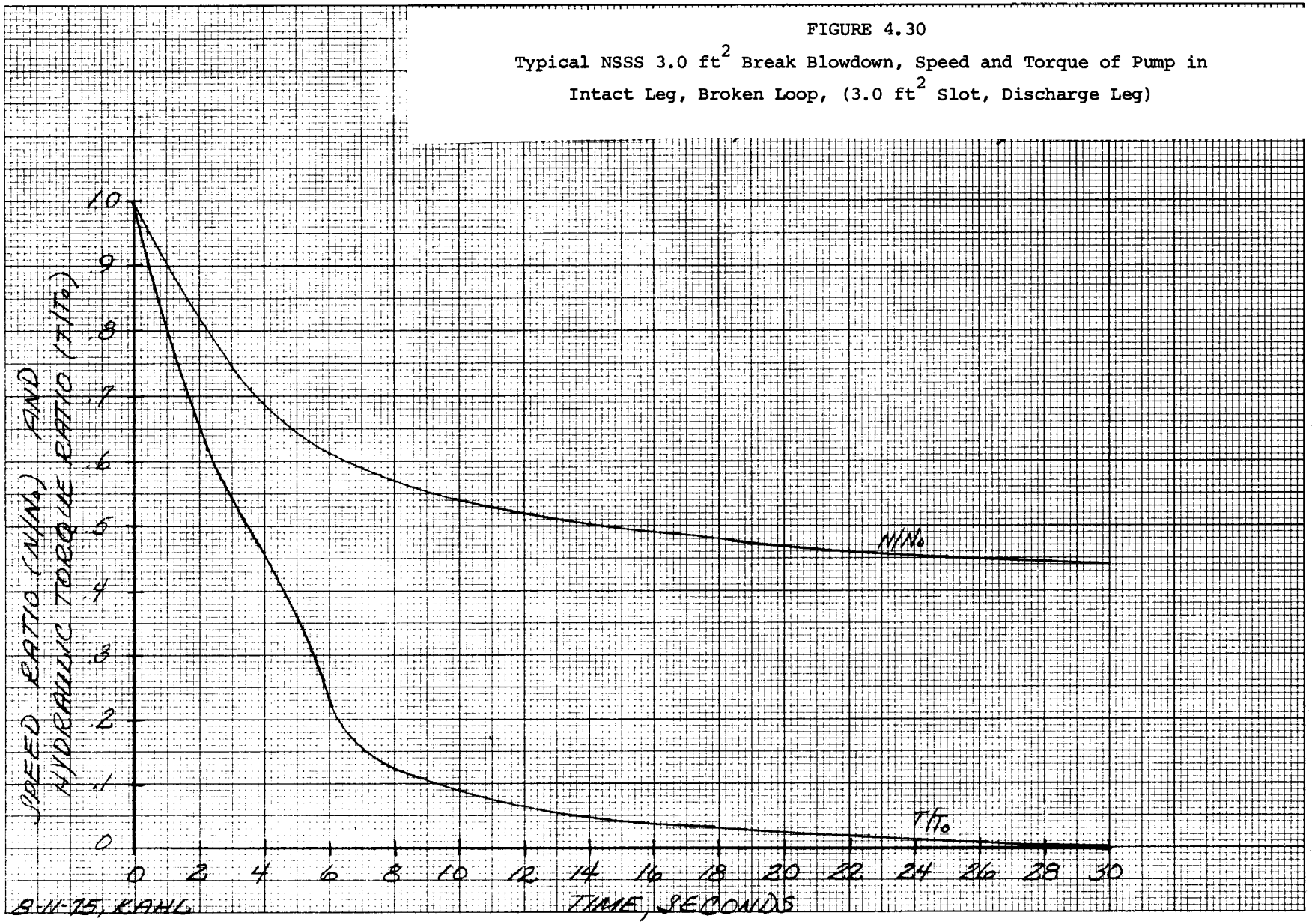

FIGURE 4.31

Typical NSSS 0.5 ft^2 Break Blowdown, Speed and Torque of Pump in Intact Leg, Broken Loop, (0.5 ft^2 Slot, Discharge Leg)

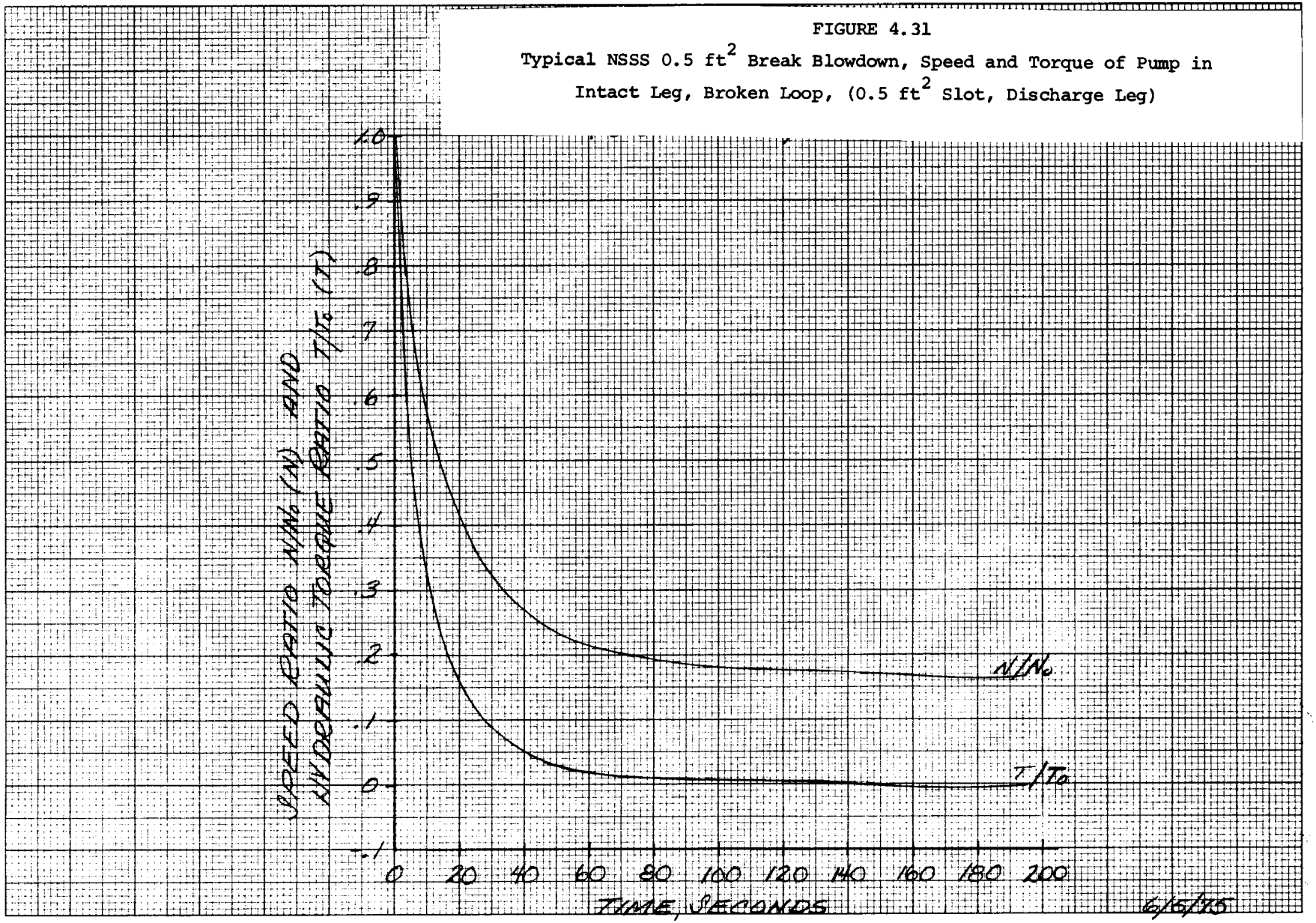

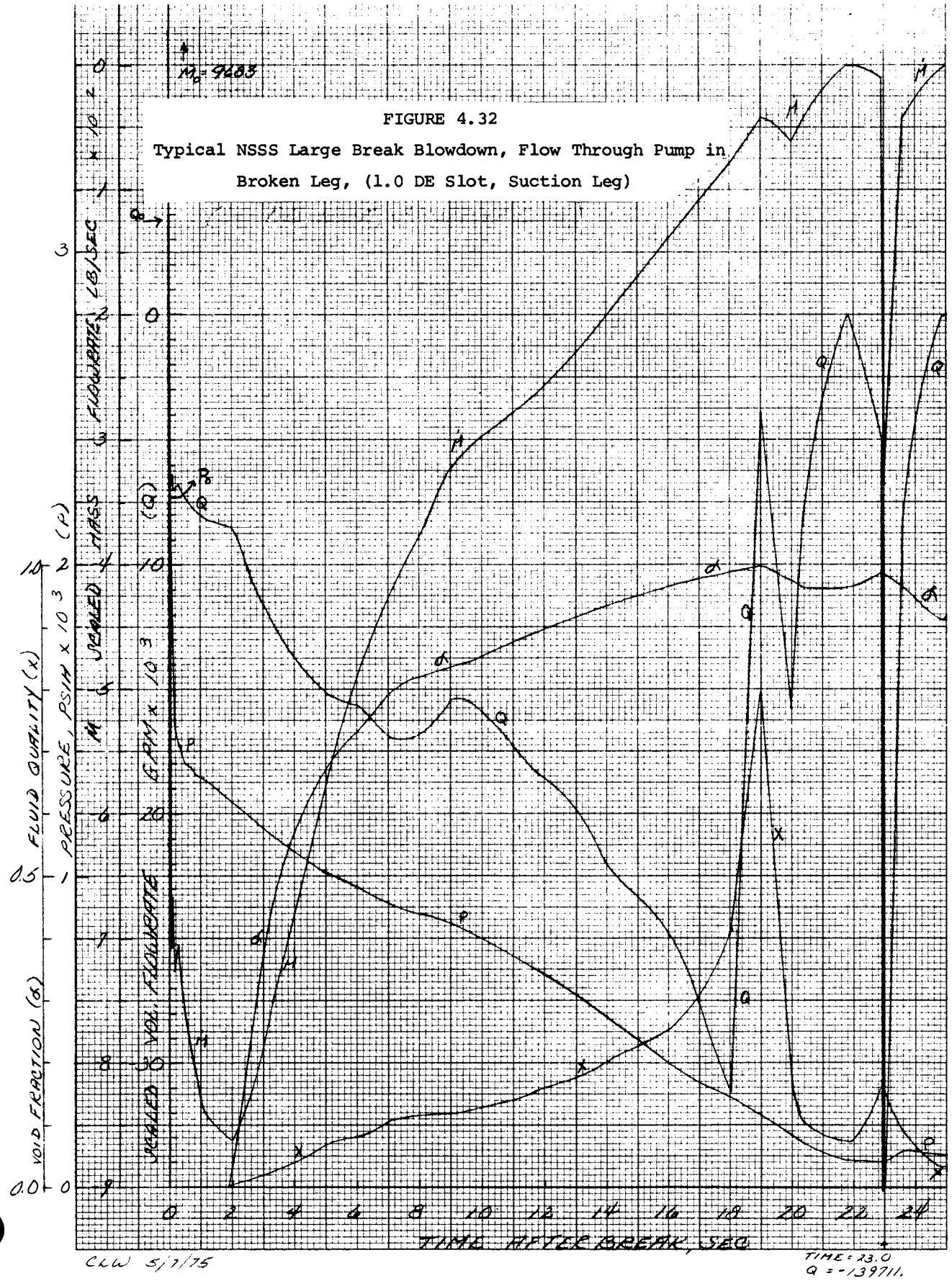

FIGURE 4.32

Typical NSSS Large Break Blowdown, Flow Through Pump in Broken Leg, (1.0 DE Slot, Suction Leg)

FIGURE 4.33

Typical NSSS Large Break Blowdown, Flow Through Pump in Intact Loop, (1.0 DE Slot, Suction Leg)

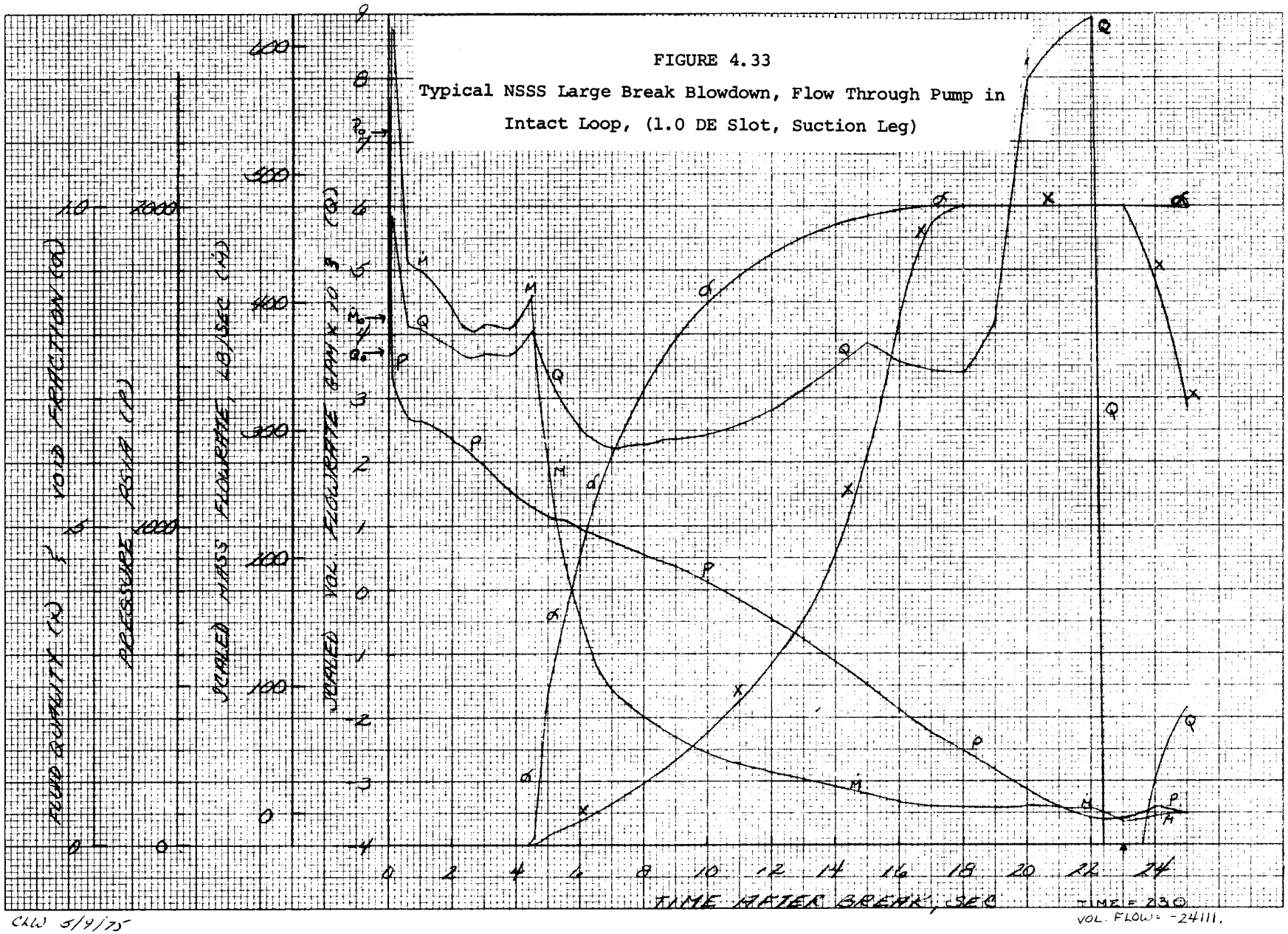

FIGURE 4.34

Typical NSSS Large Break Blowdown, Flow Through Pump in Intact Leg, Broken Loop, (1.0 DE Slot, Suction Leg)

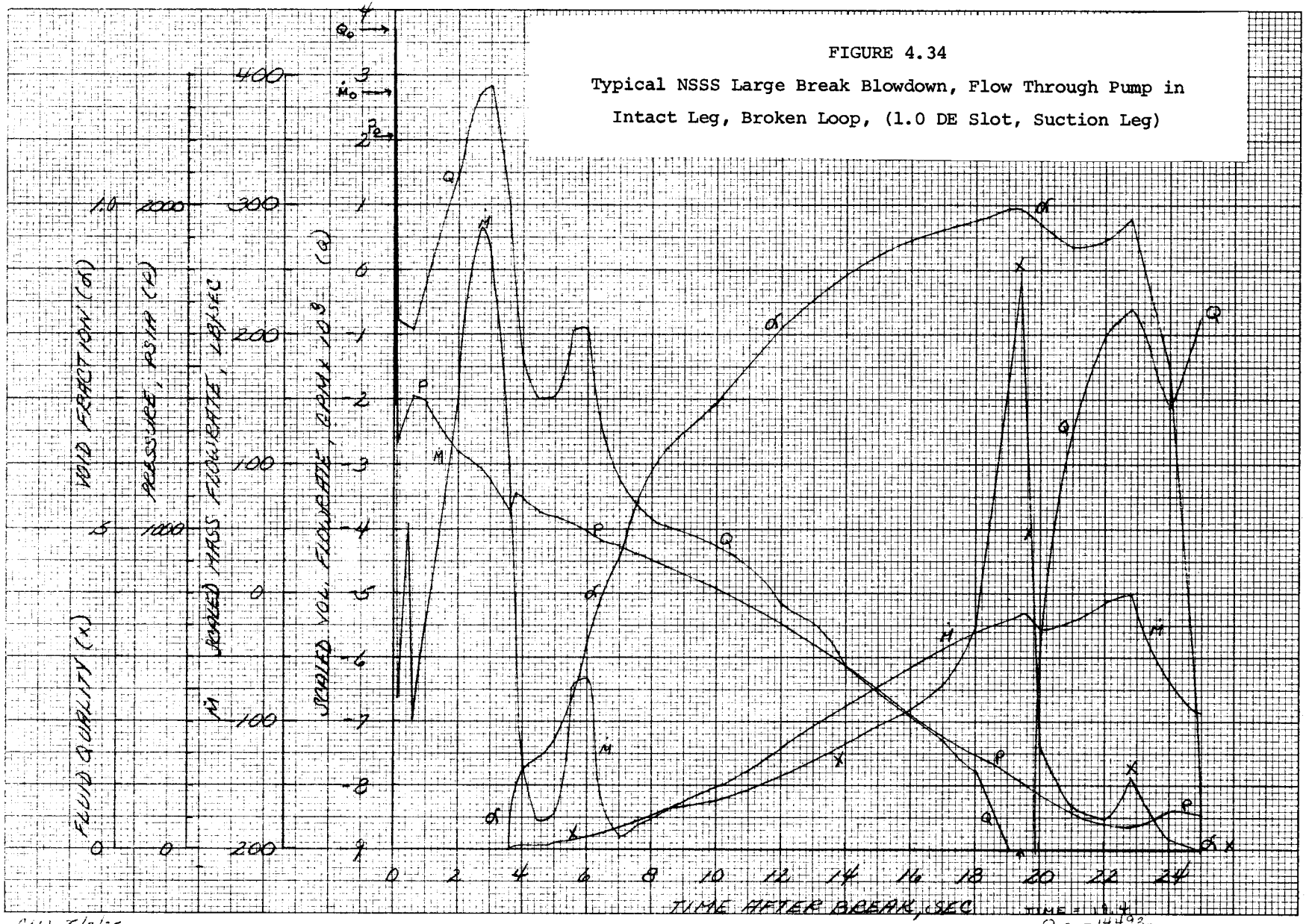

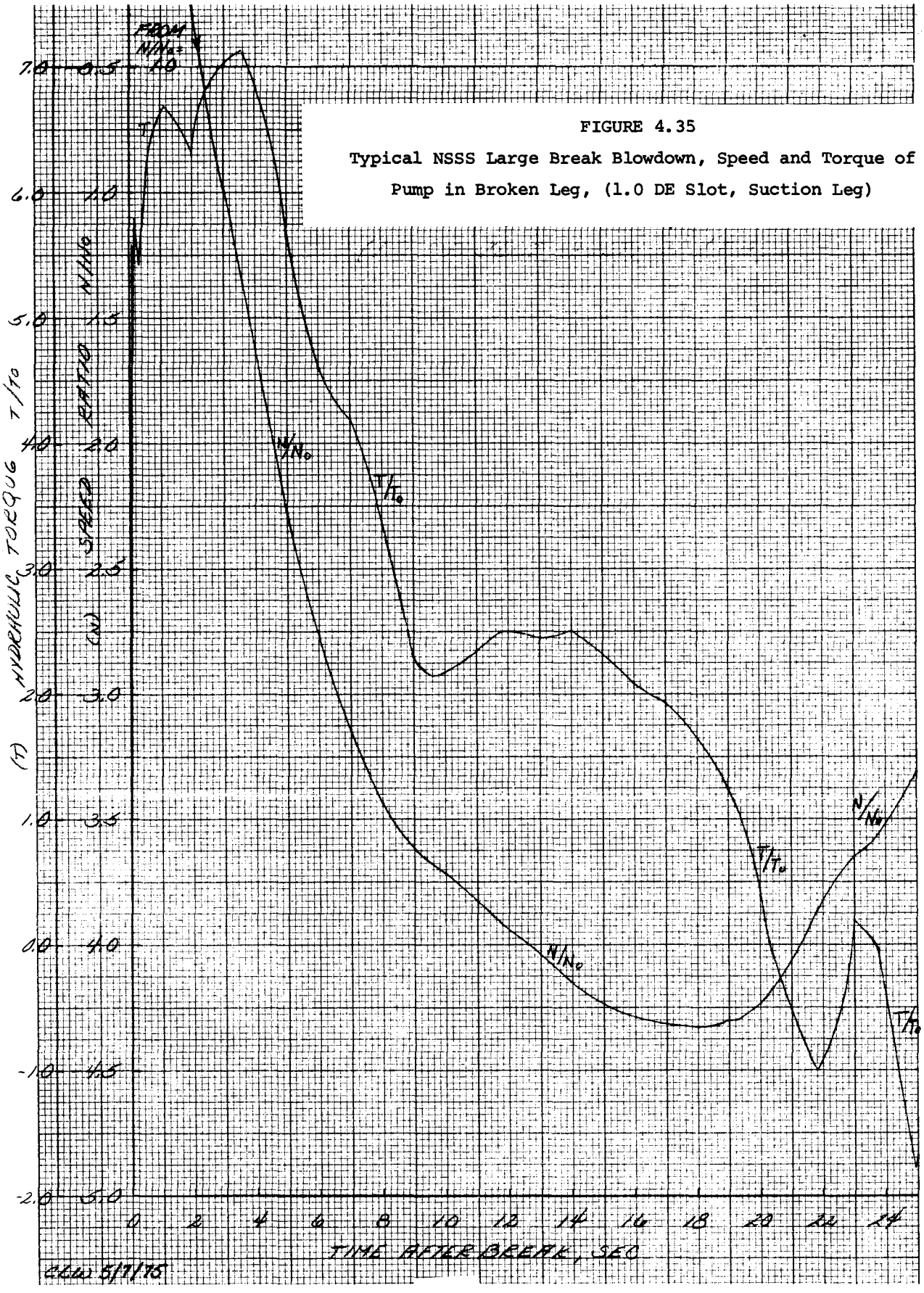

FIGURE 4.35

Typical NSSS Large Break Blowdown, Speed and Torque of Pump in Broken Leg, (1.0 DE Slot, Suction Leg)

FIGURE 4.36

Typical NSSS Large Break Blowdown, Speed and Torque of Pump in Intact Loop, (1.0 DE Slot, Suction Leg)

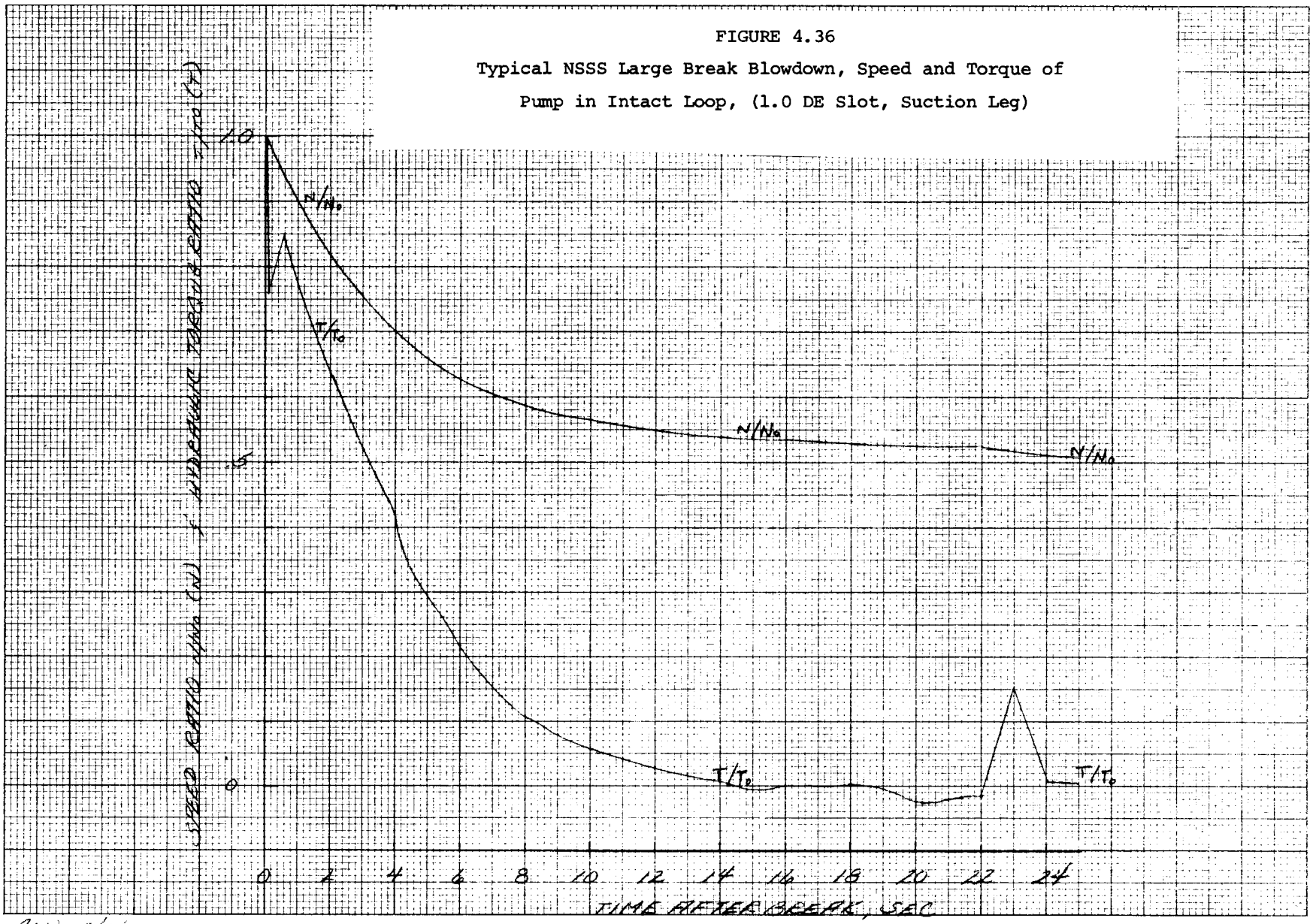

CWD 5/1/75

FIGURE 4.37

Typical NSSS Large Break Blowdown, Speed and Torque of Pump in Intact Leg, Broken Loop, (1.0 DE Slot, Suction Leg)

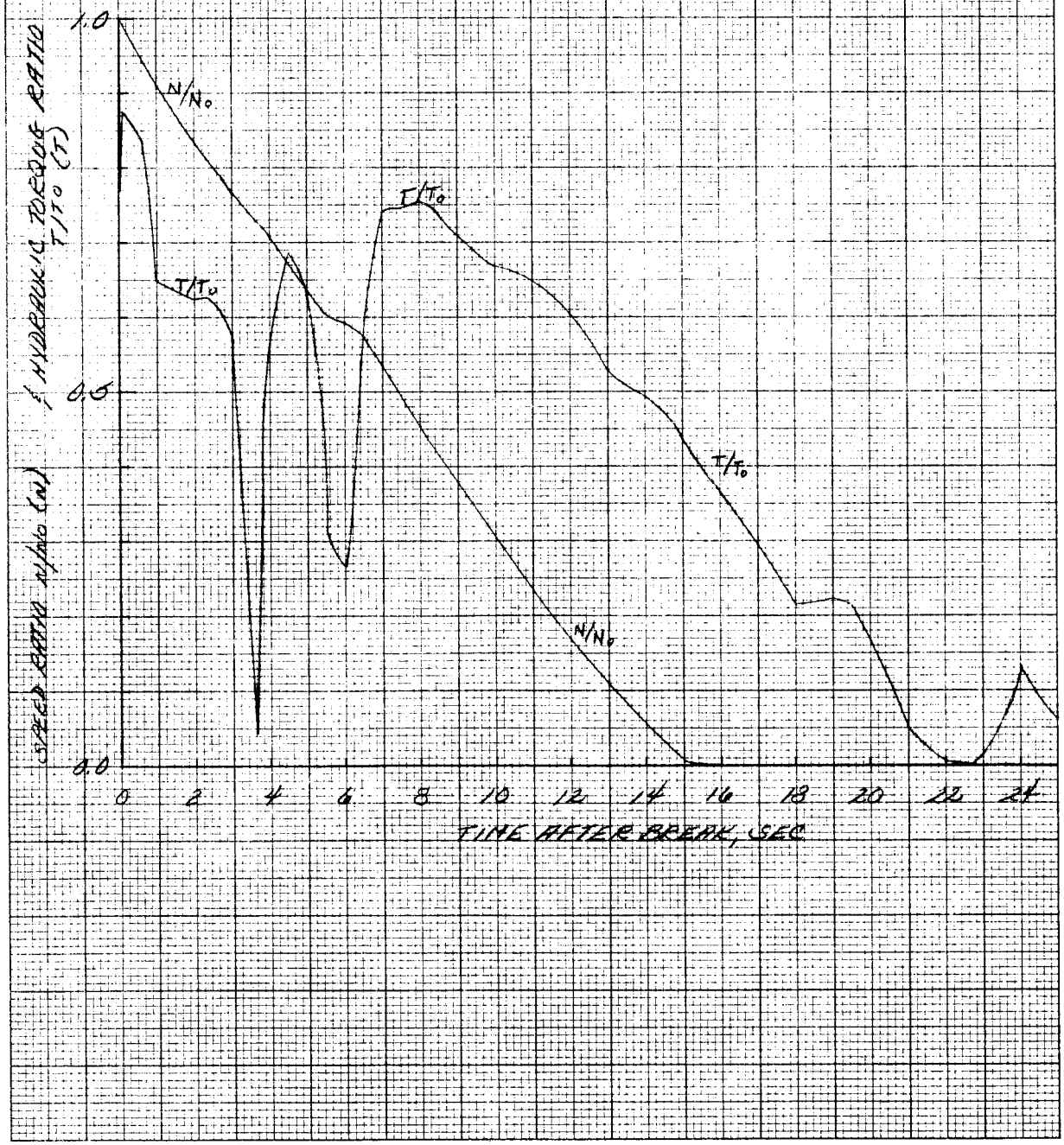

CLW 5/7/75

5. TEST PARAMETERS

5.1 Choice of Parameters

As stated above, single-phase pump performance is generally measured and described in terms of head and torques (hydraulic, friction and windage, and/or total) for a given speed, volume flow rate, and fluid density. For two-phase conditions pressure, void fraction and perhaps flow regime are also included. A straight empirical approach to performance testing would simply cover all combinations of these throughout the range of concern on a full-size pump. However, practical limitations require running the tests on a scaled-down model and obtaining as much information as possible from selected combinations of operating conditions within the capabilities of the test facility. This points to the need to understand the physical relationships among the parameters as a basis for scaling and to develop criteria for indicating the appropriateness of test conditions.

Flow paths and general dynamic actions in a given pump, or in scale model pumps, at different operating conditions with homogeneous fluids can be considered hydraulically similar when the vector diagrams relating fluid velocities to rotor velocities are geometrically similar. Since rotor velocities are proportional to ND (pump speed times impeller diameter) and fluid velocities are proportional to Q/D^2 (volume flow rate divided by area, or diameter squared), flow similarity is indicated by matching $\frac{Q/D^2}{ND}$ or $\frac{Q}{ND^3}$. This ratio is commonly normalized to give

$$\frac{Q/ND^3}{Q_R/N_R D^3} = \frac{Q/N}{Q_R/N_R} = \frac{Q/Q_R}{N/N_R} = \frac{\nu}{\alpha_N}$$

in which $\nu \equiv Q/Q_R$ and $\alpha_N \equiv N/N_R$ are called homologous flow and speed parameters. Thus, for the scale model test pump to be considered operating at the "same", or actually similar, hydraulic conditions as an NSSS pump, the model and NSSS values of ν/α_N, i.e., the indicator of ratio of fluid velocities to impeller velocities, should be matched. Pump head H is the net result of fluid dynamic head and hydraulic losses, both of which are generally proportional to square of fluid velocity, i.e., $H \sim V^2$.

For hydraulically similar conditions when the ratios of fluid and impeller velocities are matched, H is also proportional to the square of the impeller velocity, i.e., $H \sim (ND)^2$.

Thus, the head H_p for the full-sized power plant pump can be obtained from a measurement of head H_m of a scale model at hydraulically similar flow conditions by ratioing in proportion to $(ND)^2$, i.e.,

$$H_p = H_m \frac{(N_p D_p)^2}{(N_m D_m)^2} .$$

If these quantities are normalized to the rated conditions,

$$H/H_R \sim (N/N_R)^2$$

or $$h \sim \alpha_N^2$$

and $$h_p = h_m \, (\alpha_{Np}/\alpha_{Nm})^2,$$

in which $h \equiv H/H_R$ is called the homologous head parameter. This illustrates the significance and importance of using the fluid-to-impeller-speed parameter ν/α_N to indicate when test model operating conditions correspond to NSSS conditions.

In analogous fashion, hydraulic torque T_H which the impeller exerts on the fluid going through the passages is the result of causing momentum changes at each radius and is therefore proportional to mass flow rate, fluid velocities and impeller size, i.e.,

$$T_H \sim (\rho Q) \; (Q/D^2) \; (D).$$

For hydraulically similar conditions when the ratio of fluid and impeller velocities are matched as indicated by matching ν/α_N,

$$Q/D^2 \sim ND,$$

as above. This also can be expressed as

$$Q \sim ND^3.$$

Thus, $$T_H \sim (\rho ND^3)\ (ND)\ (D)$$

or $$T_H \sim \rho N^2 D^5.$$

Thus, the hydraulic torque T_{Hp} for a full-size power plant pump can be determined by measurement of T_{Hm} for the model at hydraulically similar conditions and then ratioing in proportion to $\rho N^2 D^5$, i.e.,

$$T_{Hp} = T_{Hm} \frac{(\rho N^2 D^5)_p}{(\rho N^2 D^5)_m}.$$

If these quantities are normalized to rated conditions,

$$T_H/T_{HR} \sim (\rho/\rho_R)\ (N/N_R)^2$$

or $$\beta_H \sim (\rho/\rho_R)\ \alpha_N^2 \quad \text{and}$$

$$\beta_{H_p} = \beta_{H_m} \left[\frac{\rho_p/\rho_{Rp}}{\rho_m/\rho_{Rm}}\right] \times \left[\frac{\alpha_{Np}^2}{\alpha_{Nm}^2}\right],$$

in which $\beta_H \equiv T_H/T_{HR}$ **is called the homologous hydraulic torque parameter.**

Hydraulic torque for the model will be calculated from measured quantities as follows:

$$T_H = T_{total} - T_{f\&w} - \frac{I}{g_c}\frac{d\omega}{dt}$$

in which T_{total} is total shaft torque, $T_{f\&w}$ is friction and windage torque, I is moment of inertia, and $d\omega/dt$ is angular acceleration.

The above discussion of hydraulic similarity and scaling and their application to head and hydraulic torque show that the similarity criterion parameter ν/α_N should be considered one of the test parameters.

It should be noted that head, torque, flow and speed expressed in percent of rated values are frequently used instead of the homologous parameters h, β, ν, and α_N, but the meaning is the same. Also, the names "similarity laws" and "affinity laws" are often given to relationships stated above as applying when hydraulic similarity exists, i.e.,

$$H \sim N^2D^2 \quad \text{or} \quad h \sim \alpha_N^2$$

$$Q \sim ND^3 \quad \text{or} \quad \nu \sim \alpha_N$$

and $$T_H \sim \rho N^2 D^5 \quad \text{or} \quad \beta \sim (\rho/\rho_R)\alpha_N^2 \ .$$

Deviations from hydraulic similarity can occur when scale models are used if some flow phenomena do not scale geometrically and are not compensated readily by adjusting the mode of operation. Such distorting effects can come from gravity, Mach number, or certain Reynolds number effects such as variation in friction coefficients. For scaling down by a factor of only 5, and unless choking is present, such effects are expected to be of secondary importance provided the fluid is essentially homogeneous. If inhomogeneity occurs to a significant degree, which is possible with two-phase flow, deviations from homogeneous fluid performance could result.

The pump test program is primarily concerned with how pump performance is affected by various two-phase mixtures of water and steam. The nature of a relatively uniform two-phase mixture is largely indicated if the void fraction α_F and density are specified. Tests will be made over a range of pressure levels, and the main indicator of the nature of the fluid is taken to be void fraction, α_F. Initial investigations by Aerojet Nuclear Company (ANC) on the Semi-scale system pump (Reference 5.1) have indicated that two-phase head degradation can be correlated fairly well as a function of inlet void fraction as shown in the following sketch.

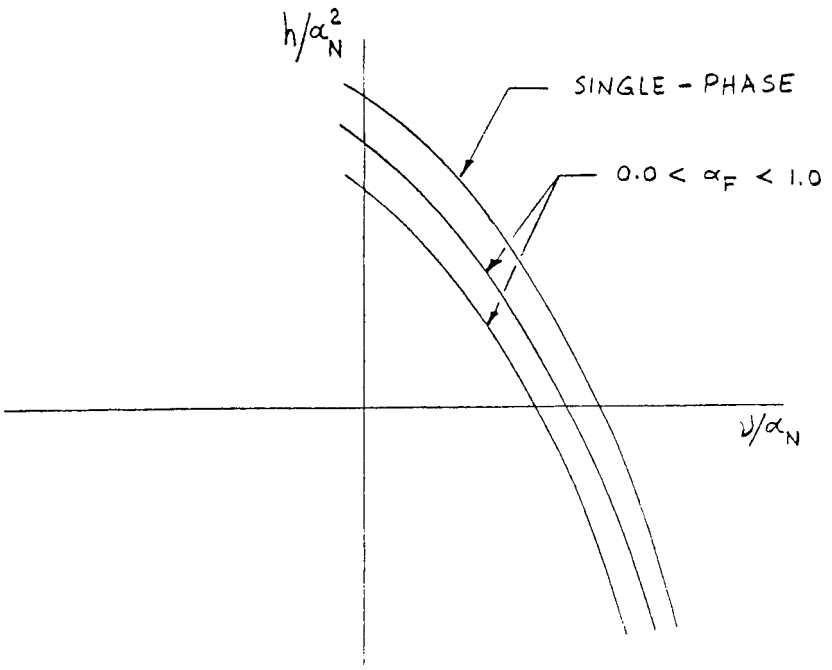

The average void fraction in the pump path, i.e., at average pressure between path inlet and outlet, have been used in CEFLASH analyses. At the present time, this seems to be an appropriate choice for a single parameter indicator of the kind of two-phase fluid flowing through the pump. It is expected that the test program will enable further evaluations of this choice.

The effects on pump performance of having two-phase mixtures instead of a single phase are expected to be different if the two phases do not remain thoroughly mixed or homogeneous. The type of two-phase distribution pattern or "flow regime" which will exist in a horizontal pipe (such as ahead of the pump) has been shown by various investigators to correlate approximately with the relative volume flow rates of the two phases. Govier and associates (References 5.2 and 5.3) recommend plotting superficial liquid velocity V_{SL} vs. superficial gas velocity V_{SG} on a log-log plot showing empirical regions corresponding to various flow regimes such as dispersed bubble flow, slug flow, and annular mist. Superficial velocity is defined as volume flow rate of the phase divided by total pipe cross-sectional area. If the liquid velocities are high enough, the mixture will be uniform enough to behave

essentially as homogeneous. As will be shown later (Section 6.4), for a major part of the transient associated with large breaks, homogeneous flow is expected in the pump suction pipes.

Pump performance during a blowdown transient could differ from steady-state performance, even though the same inlet conditions exist momentarily, if inertial or nonequilibrium phase change effects are significant. Past experience in the field, (e.g., Reference 5.1), indicates that for transients of interest, inertia effects are small and phase change effects are more likely to come into play. On this basis, the parameter chosen to indicate severity of a transient is the behavior of the pump average void fraction α_F, as indicated by a plot of α_F vs. time from which the change in void fraction $d\alpha_F/dt$ can be inferred.

For pump flow conditions in two situations to be considered similar, all of the above comparison criteria, i.e., ν/α_N, α_F, $d\alpha_F/dt$ and flow regime should be matched simultaneously. Combinations of ν/α_N and α_F are indicated by plotting α_F vs. ν/α_N. Comparisons of flow regimes are made from the flow regime maps showing the path of blowdowns with progressive times noted. These two comparisons apply to steady-state flow as well as to transients. As mentioned before, the steepness of the transients at the corresponding times can be compared on plots of α_F vs. time. Since the test system will start the blowdowns with essentially saturated fluid, it is convenient to compare transients on the basis of time after start of vaporization. Further comments on the significance of such comparison parameters will be given below in examining the behavior of an NSSS versus the test system.

5.2 Parameter Influences on Pump Performance

To assess the influence of various parameters on pump performance, it is appropriate to consider the pump calculational model employed in the LOCA analysis. This model is based on the homologous relationships between pumps of similar specific speeds and uses the Palisades one-fifth scale model pump single-phase test data as its foundation. The fundamental equation of the model is an angular momentum balance applied to the pump/motor/flywheel assembly.

The purpose of this analytical pump model is to calculate the pressure difference across the pump for use in the CEFLASH-4A conservation of momentum equation. Since the pressure difference, or head, is dependent on the pump speed, the speed is calculated throughout the transient, thus giving a pump head dependent on transient flow conditions. This is also the way in which any predicted overspeed is determined.

The equation which describes the change in the pump impeller speed is:

$$\frac{d\omega}{dt} = (T_{e\ell} - T_h - T_{f\&w}) \frac{g_c}{I} \qquad (5.1)$$

where:

ω = Angular velocity of the rotating assembly, rad/sec

t = Time, sec

$T_{e\ell}$ = Electrically induced torque acting on the rotor, ft-lbf (Torque is positive in normal direction of rotation)

T_h = Hydraulic torque exerted on the fluid by the pump impeller, ft-lbf

$T_{f\&w}$ = Torque exerted on the rotating assembly due to bearing friction and windage losses, ft-lbf

g_c = Gravitational constant, 32.174 lbm-ft/lbf-sec^2

I = Moment of inertia of the rotating assembly, lbm-ft^2

The three torques ($T_{e\ell}$, T_h, and $T_{f\&w}$) are calculated as follows:

(1) The hydraulic torque is calculated from the following equation:

$$T_h = \begin{cases} (\beta/\alpha_N^2)\ (\alpha_N^2)\ (T_R)\ (\rho/\rho_R)\ (m_t) & \text{for } \nu/\alpha_N \leq 1.0 \\ (\beta/\nu^2)\ (\nu^2)\ (T_R)\ (\rho/\rho_R)\ (m_t) & \text{for } \nu/\alpha_N > 1.0 \end{cases} \qquad (5.2)$$

where:

β = Ratio of the hydraulic torque to the rated hydraulic torque, $\beta \equiv (T_h/T_R)/(\rho/\rho_R)$, or T_h/T_R at rated density.

α_N = Ratio of the pump speed to the rated pump speed, $\alpha_N \equiv \omega/\omega_R$

ν = Ratio of the volumetric flow rate to the rated volumetric flow rate, $\nu \equiv Q/Q_R$

ρ = Density of coolant, lbm/ft^3

ρ_R = Density corresponding to pump rated conditions, lbm/ft^3

m_t = Torque degradation multiplier; the degradation multiplier is a function of the void fraction

Note that values of β/α_N^2 and β/ν^2 as a function of ν/α_N are obtained from a table of values representing the appropriate homologous torque curve similar to Figure 5.1.

The procedure for calculating the hydraulic torque is as follows:

(a) Calculate the ratio of the pump speed to the rated pump speed, α_N

(b) Calculate the ratio of the volumetric flow rate to the rated volumetric flow rate, ν

(c) Check the direction of the pump speed and the direction of the flow

(d) Knowing the direction of the pump speed and flow and the quantity ν/α_N, obtain the value of β/α_N^2 or β/ν^2 from the tables representing curves such as in Figure 5.1.

(e) Calculate the hydraulic torque using Equation 5.2 with the above values and the value of the density in the pump path.

If the flow direction is negative through a pump and the pump speed is zero, a check is made to determine if the hydraulic torque has exceeded the design torque of the anti-reverse device. If the hydraulic torque exceeds the design anti-reverse torque, the pump is then allowed to rotate in the reverse direction.

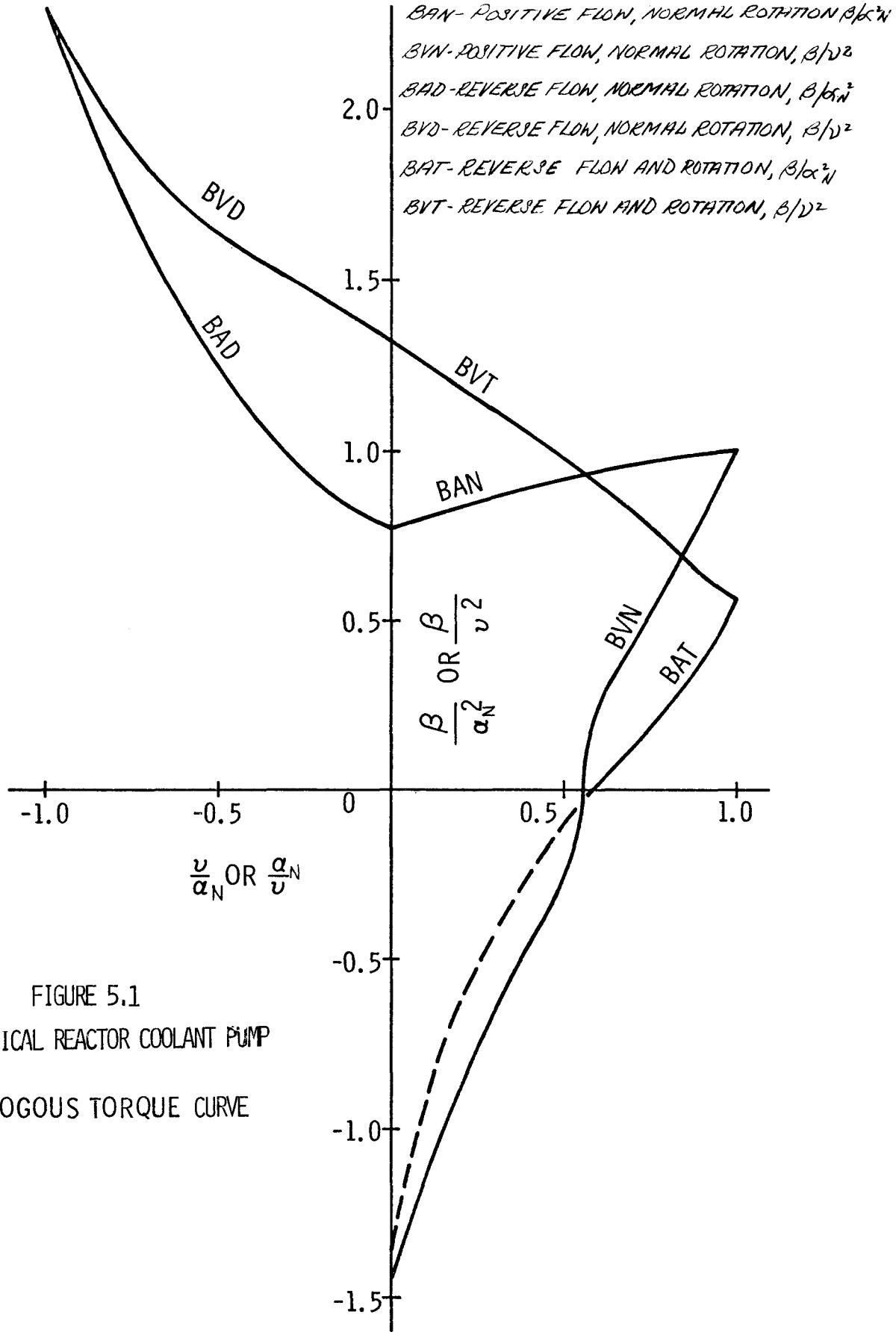

FIGURE 5.1

TYPICAL REACTOR COOLANT PUMP

HOMOLOGOUS TORQUE CURVE

(2) The friction and windage torque is calculated from the following equation:

$$T_{f\&w} = (K)\ (\alpha_N|\alpha_N|) \qquad (5.3)$$

where:

K = Input constant, ft-lbf

α_N = Calculated as in Step (a), above

(3) To solve for the electrical torque, the pump speed from the previous time step is used and an interpolation is done in a table of speed vs. electrical torque for the drive motor. A pump trip system is used to determine when the electricity supplied to the pump motor is interrupted. This system trips the pump power when any of several safety limits have been exceeded and subsequent time delays expired. In the cases cited in this report, the electrical power is assumed lost coincident with the pipe break.

With all quantities known in Equation 5.1, the change in the pump speed can be calculated. The pump speed is then changed by this amount for the next time step.

The pump head is calculated from the following equation:

$$H = \begin{cases} (\alpha_N^2)\ (H_R)\left[h/\alpha_N^2 - (m_h)\ (h/\alpha_N^2)_{TP}\right] & \text{for } |\nu/\alpha_N| \leq 1.0 \\ (\nu^2)\ (H_R)\left[h/\nu^2 - (m_h)\ (h/\nu^2)_{TP}\right] & \text{for } |\nu/\alpha_N| > 1.0 \end{cases} \qquad (5.4)$$

where:

H = Pump head, ft of fluid

H_R = Rated pump head, ft of fluid

h = Ratio of the pump head to the rated pump head, $h \equiv H/H_R$

m_h = Head degradation multiplier; the degradation multiplier is a function of the void fraction

$(h/\alpha_N^2)_{TP}$, $(h/\nu^2)_{TP}$ = Difference between single phase and "fully degraded" two-phase heads as obtained from the "difference" homologous head curve.

Note that the values of h/α_N^2 and h/ν^2 as a function of ν/α_N are interpolated from a table of values representing the appropriate homologous head curve similar to Figure 5.2. Values of $(h/\alpha_N^2)_{TP}$ and $(h/\nu^2)_{TP}$ as a function of ν/α_N are taken from a table representing Figure 5.3, which is the "difference" homologous head curve. This curve is a compilation of the difference between single-phase and fully degraded two-phase pump performance curves. The test data used in generating these curves was from the ANC Semi-scale 1-1/2 loop system pump (References 5.1 and 5.4).

The degradation multipliers allow the hydraulic torque and head to be expressed as a function of the two-phase flow properties. In Equation 5.2, the torque degradation multiplier is unity for single-phase flow and is a function of the void fraction for two-phase flow. In Equation 5.4, the head degradation multiplier is zero for single-phase flow and is a function of the void fraction for two-phase flow. The void fraction is evaluated at the average conditions in the pump flow path.

From Equation 5.2, it is seen that the torque degradation multiplier, the two-phase mixture density and the homologous torque value determine the hydraulic torque, and according to Equation 5.1, the hydraulic torque is employed to calculate the pump speed at any time. The pump head is determined from Equation 5.4 using the head degradation multiplier, homologous head value and the difference homologous head value. Thus, it is clear that knowledge of the degradation multipliers, the homologous head and torque values, the difference homologous head value and the fluid density are required for accurate prediction of the pump performance during a LOCA. The head degradation multiplier and therefore the degraded head were found to depend very strongly on the average void fraction for the ANC Semi-scale pump (References 5.1 and 5.4), as shown in Table 5.1 and Figure 5.4. Although the same relationship between the degradation and the void fraction is not expected to hold true for the reactor coolant pump (or the scale model), it is believed that the multiplier for the reactor pump would also be a function of the void fraction. The two-phase mixture density is also a function of this parameter as well as dependent on the pressure which is considered as another parameter affecting the pump behavior during the transient.

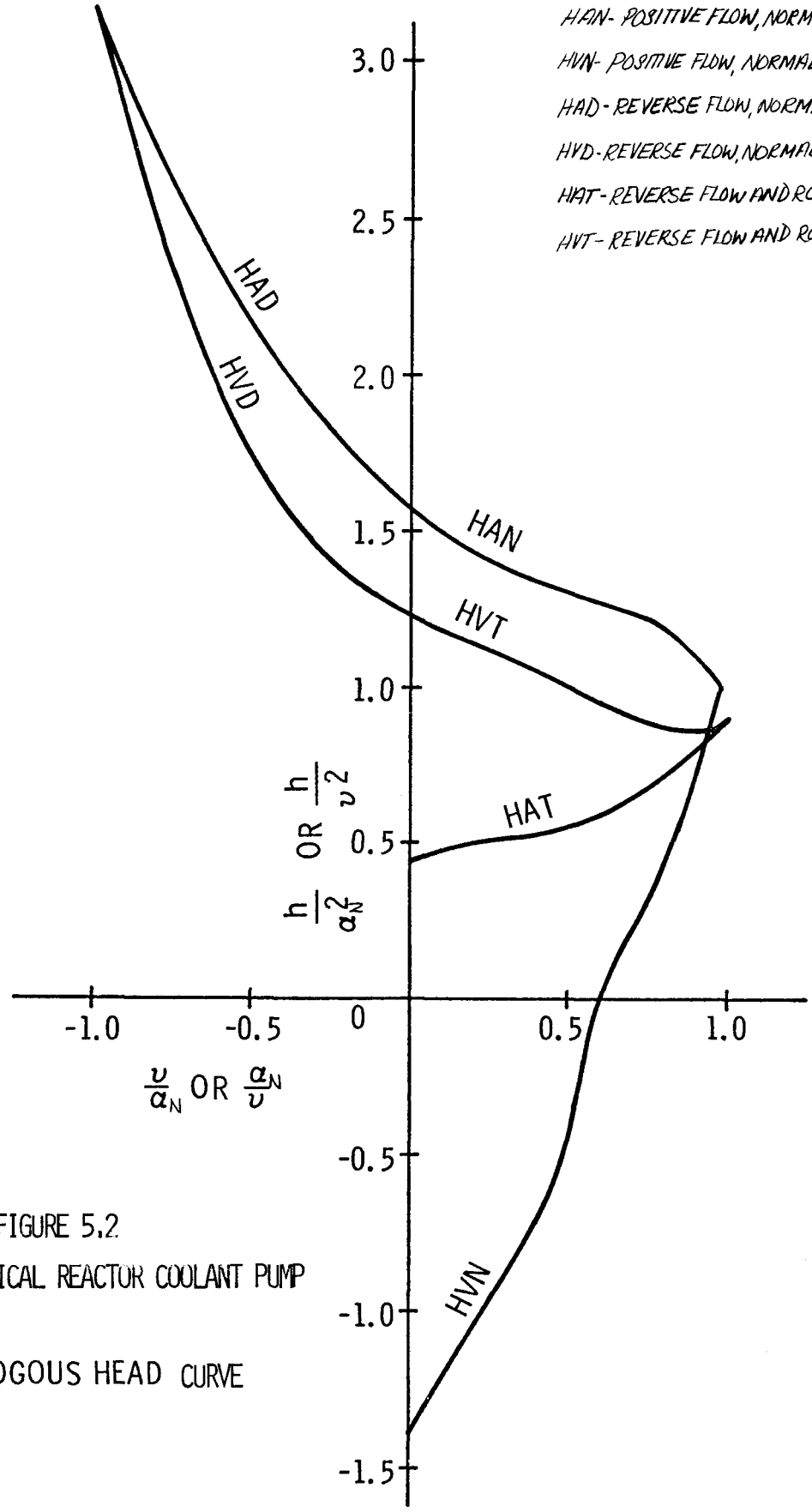

FIGURE 5.2

TYPICAL REACTOR COOLANT PUMP

HOMOLOGOUS HEAD CURVE

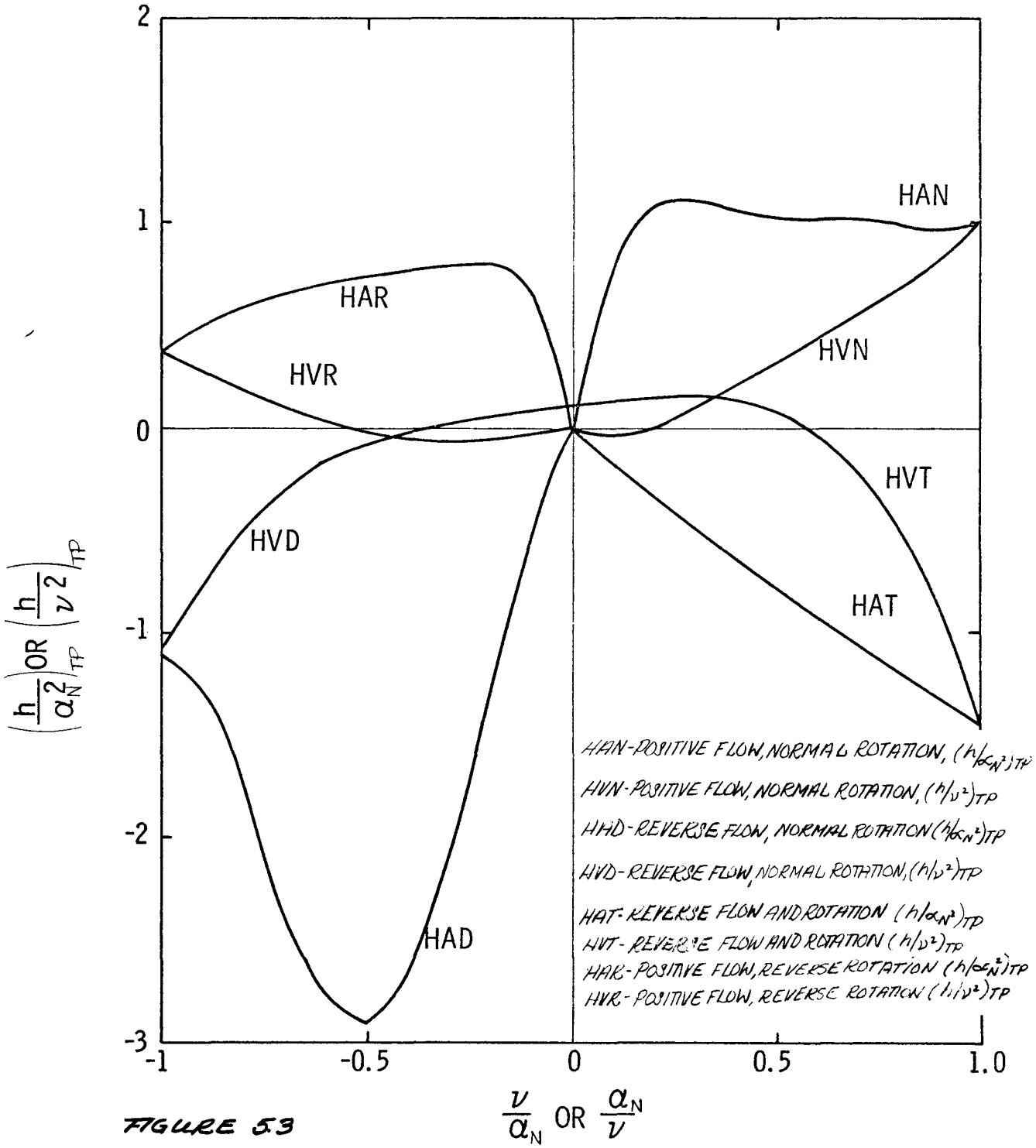

FIGURE 5.3

HOMOLOGOUS HEAD CURVE FOR THE DIFFERENCE BETWEEN SINGLE PHASE AND FULLY DEGRADED TWO PHASE HEADS BASED ON ANC SEMI-SCALE PUMP DATA

Table 5.1

PUMP HEAD DEGRADATION MULTIPLIER VS. VOID FRACTION

Void Fraction (α)	Degradation Multiplier (m_h)*
0.0	0.0
0.10	0.0
0.15	0.05
0.24	0.80
0.30	0.96
0.40	0.98
0.60	0.97
0.80	0.90
0.90	0.80
0.96	0.50
1.00	0.0

*m_h is designated as M3(α) in Reference 5.4.

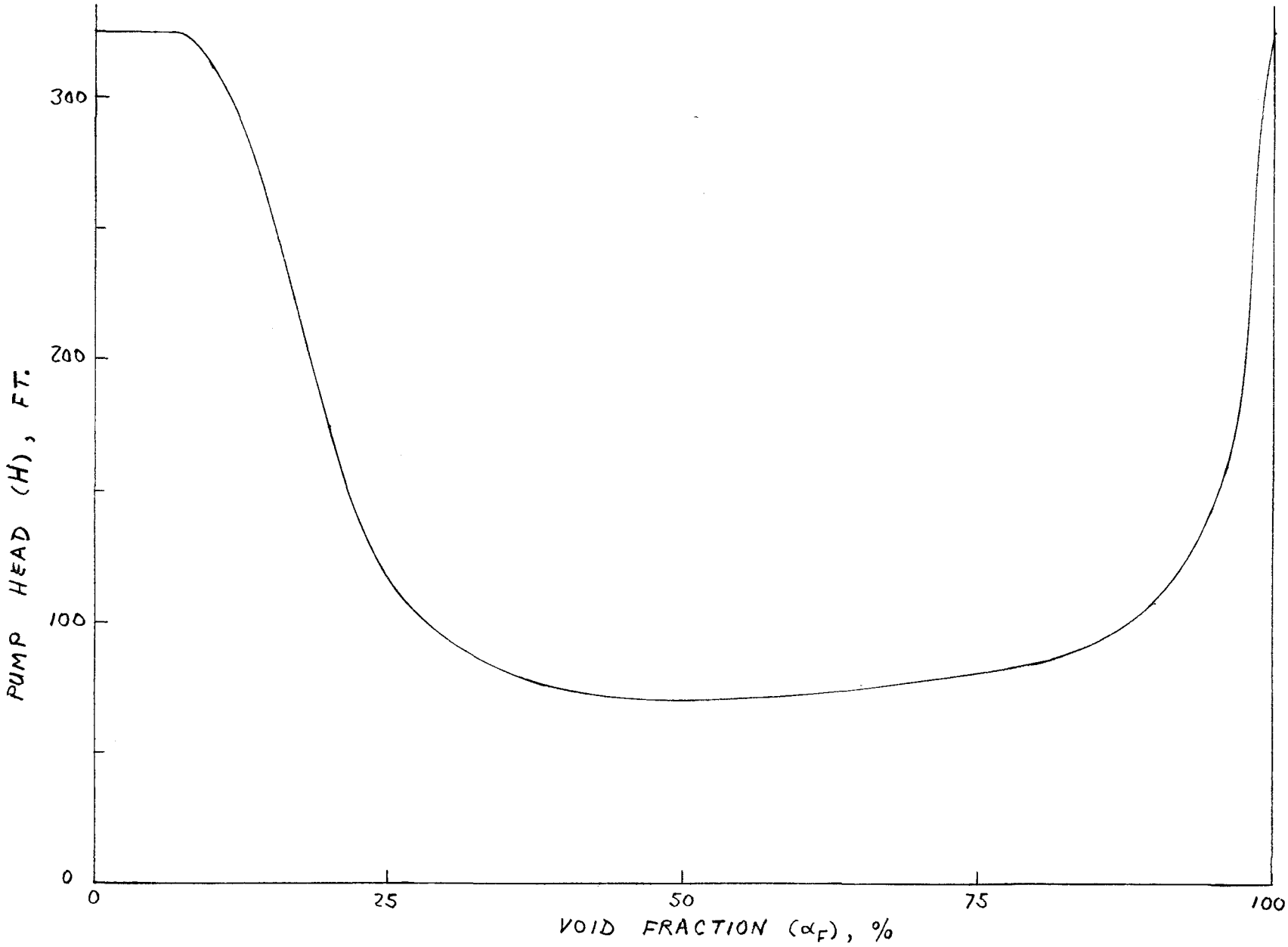

FIGURE 5.4

Degraded Pump Head as a Function of Void Fraction Based on ANC Degradation and Multiplier Data

In the ANC tests, the homologous head and torque values and the difference homologous head values were found to depend on the normalized flow/normalized speed (ν/α_N) ratio. This confirmed the expected significant effect of the ν/α_N ratio on pump behavior.

6. TEST MATRICES AND SEQUENCE

6.1 Overall Test Program

As a final step in the loop modification phase, the test system will be checked out and "de-bugged" in a series of shakedown tests. The system will be operated first with a pipe section in place of the model pump and then with the pump installed. Both steady state and transient runs will be conducted. In addition to general checkout of integrity and proper functioning of components, controls, and instrumentation, required in-place calibration of instruments will be performed as described in the Test Facility Description (Reference 3.1), and cross-checks of redundant measurements such as pump inlet density can be made. Data acquisition equipment will also be operated. Preview test loop performance information can be obtained on (1) test section heat losses for correcting quality and void fractions, (2) steady-state flow ranges to confirm system capability, (3) piping pressure drops to refine input to calculations of blowdown behavior. Data from the simplified blowdowns without the model pump will afford opportunity to "tune" the calculational blowdown model and give an initial check of loop blowdown characteristics.

The actual pump performance test program will begin with several single-phase (hot water) steady-state runs to spot check the applicability of the Byron-Jackson single-phase (cold water) data from Reference 3.1. Inlet water will be subcooled enough to avoid vaporization in the pump.

Subsequent testing will be divided into blocks of tests, or "phases", separated by intermissions which provide time for data evaluation, servicing of test equipment, and detailing and/or modification of plans and procedures for following phases. Current plans call for three test phases separated by two intermissions of 4 to 6 weeks each.

Phase I is planned to comprise the following:

(a) Sampling the effects of void fraction at constant pressure, speed, and volume flow.

(b) One full steady-state performance map at an intermediate pressure and void fraction, (Section 6.2).

(c) Additional forward flow points selected from the steady-state text matrix (Section 6.2) to correspond to conditions predicted for an initial blowdown transient run (Item e or f below).

(d) Additional reverse flow steady-state points similarly selected to correspond to conditions during an initial reverse blowdown (Item h).

(e) A mild forward flow blowdown run (discharge leg break).

(f) A medium forward flow blowdown run.

(g) A repeat of Item f to check reproducibility.

(h) A mild reverse blowdown (suction leg break).

These Phase I tests will thus include some of most kinds of testing and provide the information needed for initial comparisons of measured transient pump performance with performance predicted by the calculational model derived from steady-state data. This will provide a broad sampling of test operations, data analysis, and results, and is likely to reveal overall performance trends and any general problems in the methods or results so that appropriate adjustments can be included in rounding out the test coverage during Phases II and III.

The division between Phases II and III is rather arbitrary, being primarily a matter of pausing for evaluation. It is expected that Phase II will provide general coverage of most steady-state mapping and a range of transients, particularly discharge leg breaks, as laid out after reviewing Phase I results. Phase III will complete the general mapping and some larger blowdowns. Many of the "fill-in" points previously reserved for selective coverage as needed according to the evaluations after Phases I and II will be used during Phases II and III.

In the following two sections, the steady-state and transient test matrices will be discussed in detail. These matrices cover all those phases of the test program as presently envisioned.

6.2 Steady-State Test Matrix

The steady-state test matrix is an array of operating conditions at which pump performance will be measured. Selection of the operating conditions is aimed at (1) spanning the ranges of interest for calculating pump performance during postulated NSSS LOCA's, (2) spacing the test points to favor good interpolation and development of quantitative relationships which can be used in the calculational pump performance model, and (3) accommodating the practical limitations of test facility capabilities and a total of 300 steady-state test points. The test operator will set the points in terms of pump inlet pressure level, void fraction at the inlet or possibly averaged across the pump, volume flow rate, and pump speed. To achieve these he will manipulate the controls to vary pressure level, water and steam flows to the mixing tee, pump speed, and opening of the throttle valve in the return line, as described in more detail in the Facility Description Report (Reference 3.1).

The matrix points are derived from operating conditions selected in terms of the test parameters discussed in Sections 3.2 and 5.1 above, namely, pump inlet pressure, void fraction, pump speed, and volume flow rate, and also normalized or homologous ratios of these that relate to scaling. The ranges of interest for these parameters have been derived from the calculation results for typical postulated NSSS LOCA's compiled in Section 4.2 and also summarized below. Limitations of the test facility capabilities are also indicated where pertinent.

Thus, specifying the matrix combinations of pressures and void fractions in Figure 6.1 is based on using these parameters as the indices of fluid density and two-phase mixture. As stated previously, both inlet and pump path average void fractions are possible correlating parameters for two-phase effects on performance. At present it is proposed that the pump path average void fraction more nearly represents the two-phase mixtures throughout the pump, and Figure 6.1 is constructed on this basis.

The variations of inlet pressure versus pump path average void fraction calculated for the compiled representative NSSS LOCA's (Section 4.2) are summarized in the composite plots in Figures 6.2 to 6.4. These include both discharge and suction leg breaks. The shapes and ranges of the bands covered

FIGURE 6.1

Steady-State Test Matrix

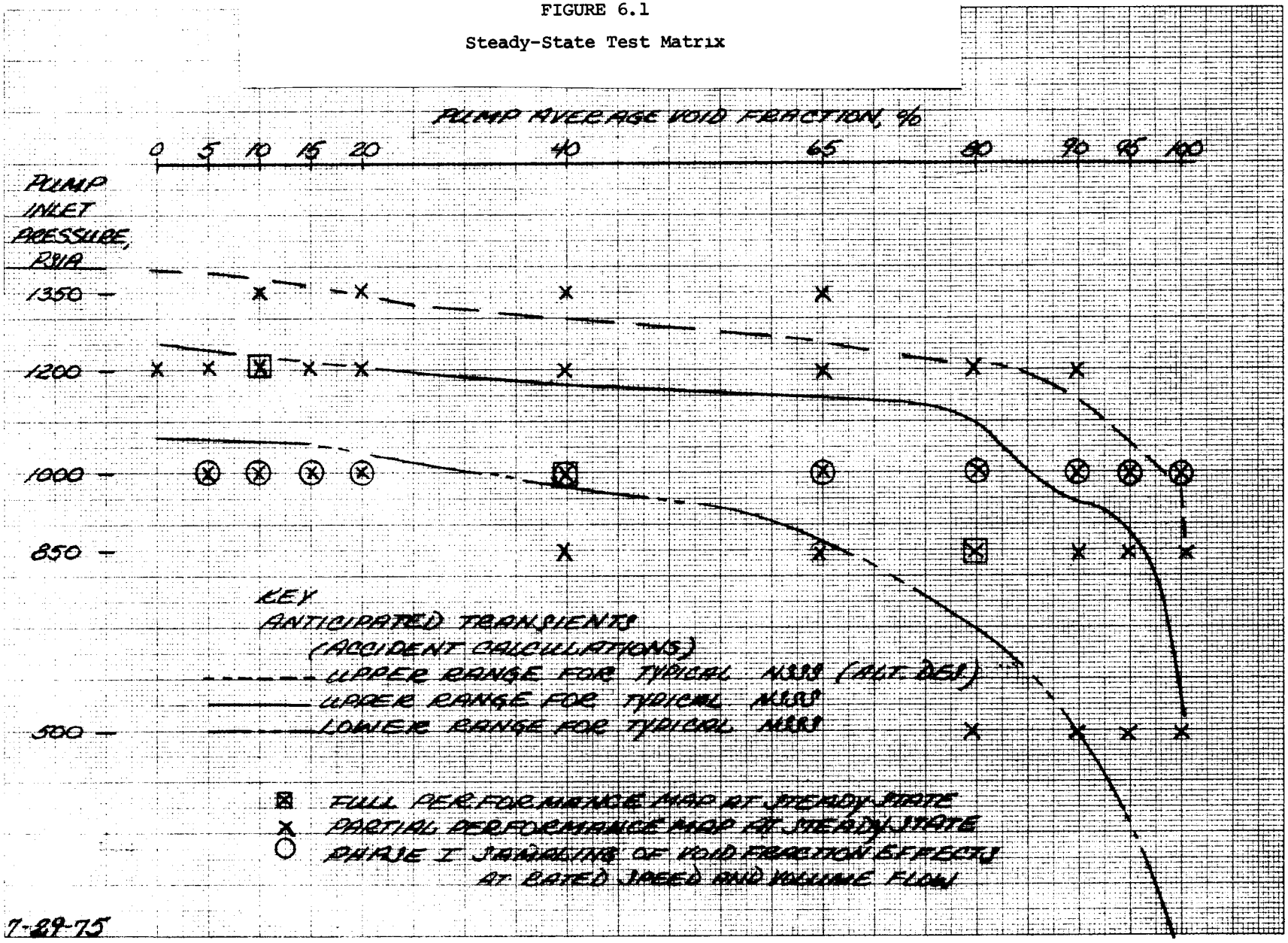

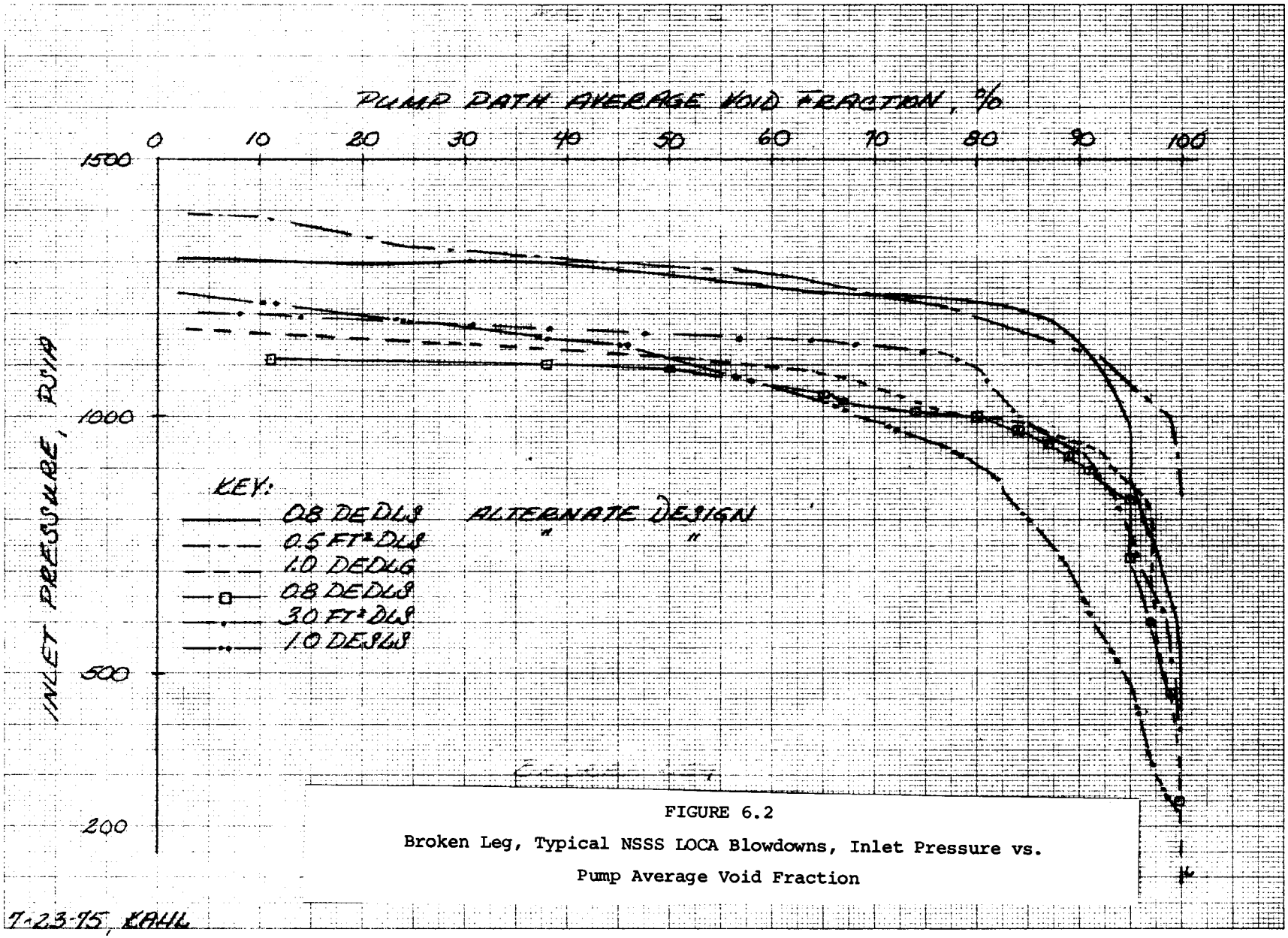

FIGURE 6.2

Broken Leg, Typical NSSS LOCA Blowdowns, Inlet Pressure vs. Pump Average Void Fraction

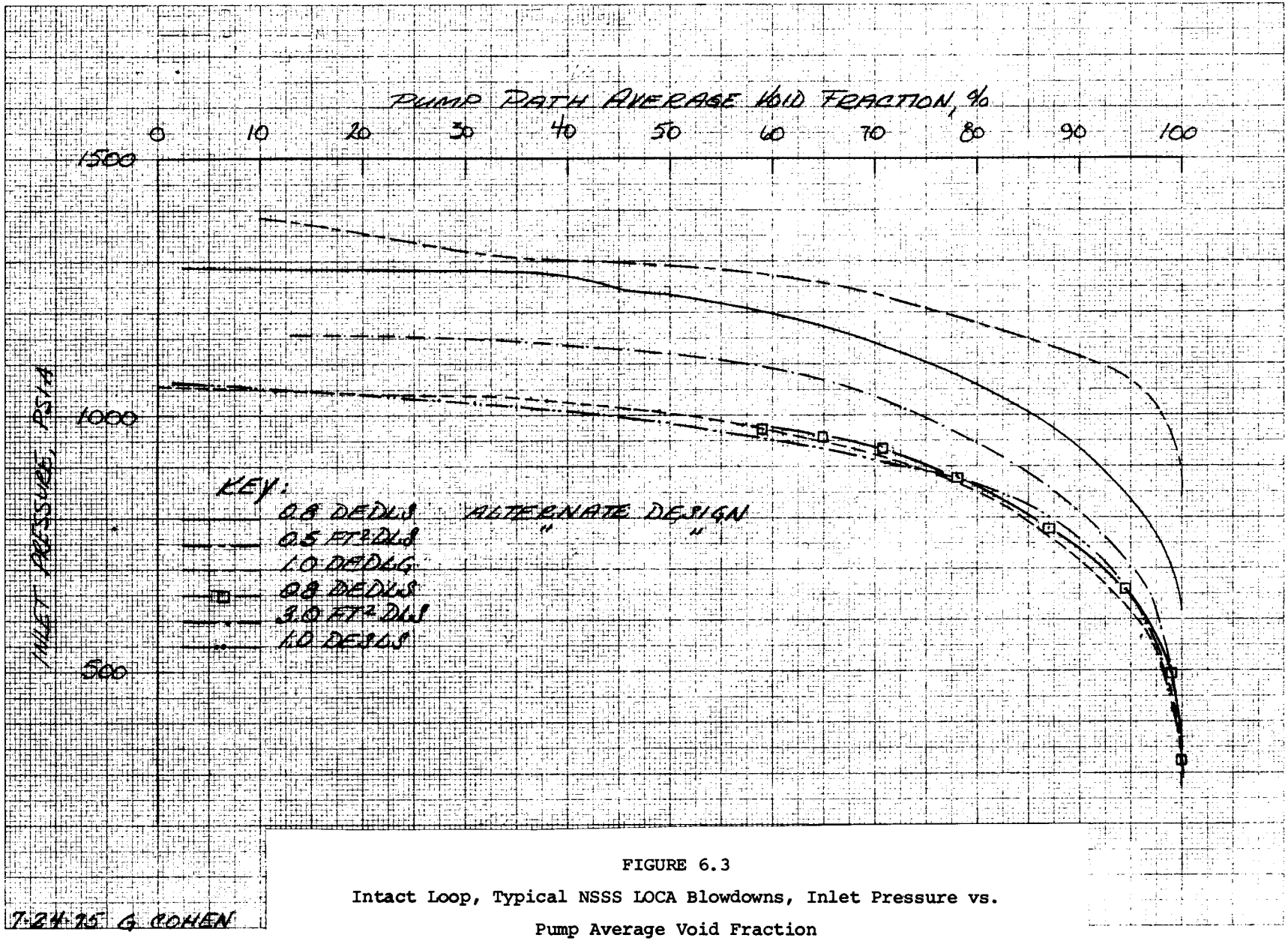

FIGURE 6.3

Intact Loop, Typical NSSS LOCA Blowdowns, Inlet Pressure vs.

Pump Average Void Fraction

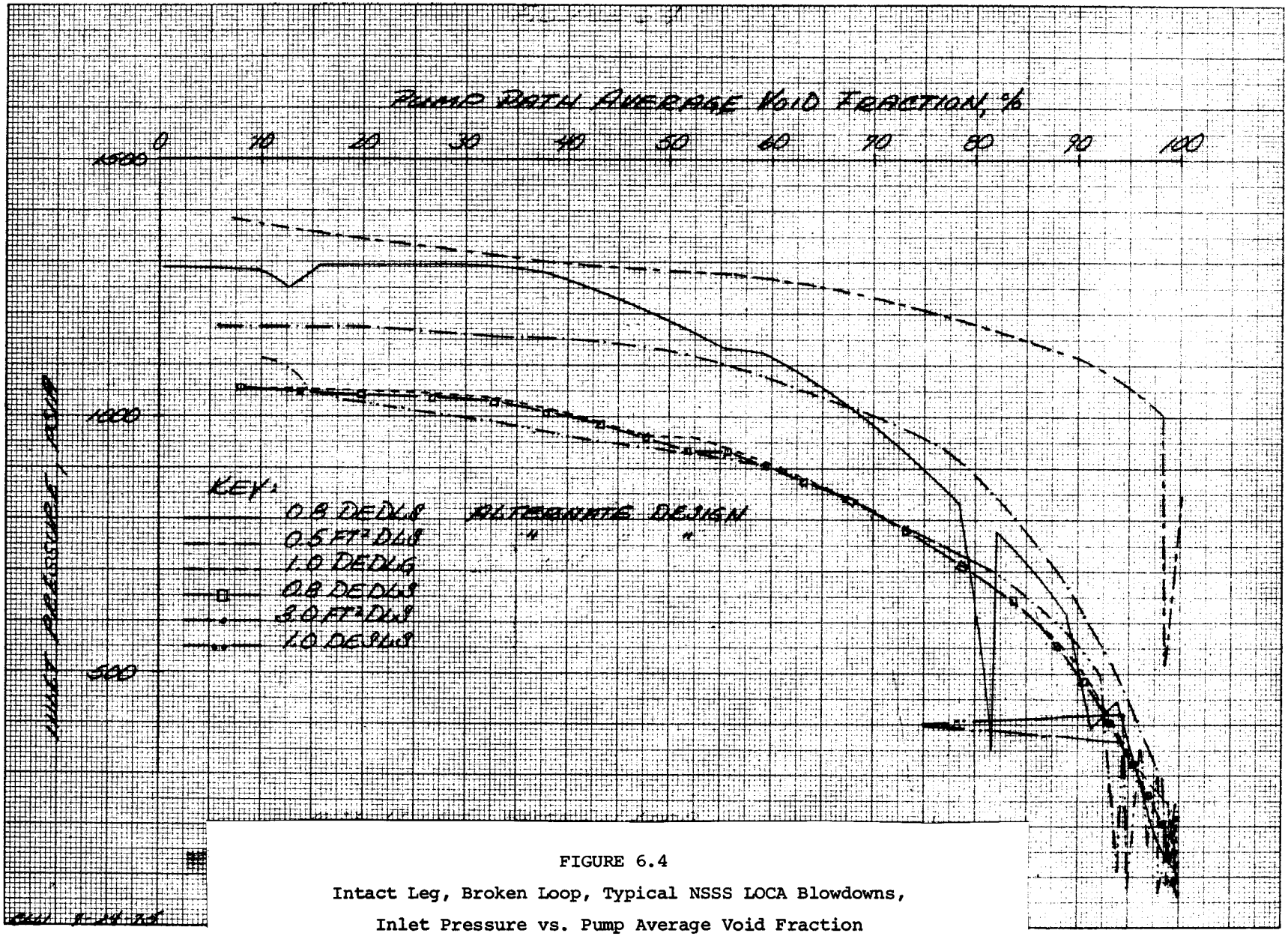

FIGURE 6.4

Intact Leg, Broken Loop, Typical NSSS LOCA Blowdowns,

Inlet Pressure vs. Pump Average Void Fraction

by the curves for the three locations of the pump relative to the break are roughly the same. Values for large and small breaks are sometimes similar, especially for the broken leg pump, although the timing for reaching the points during the blowdowns varies considerably. The terms in Figures 6.2 etc. have the following meaning:

(a) 0.8 DEDLS = DOUBLE-ENDED DISCHARGE LEG SLOT with break area = 0.8 x full area, i.e., 0.8 x 2 x pipe cross-sectional area.

(b) DLS = DISCHARGE LEG SLOT

(c) DESLS = DOUBLE-ENDED SUCTION LEG SLOT

(d) DEDLG = DOUBLE-ENDED DISCHARGE LEG GUILLOTINE BREAK

As mentioned before, the "spikes" at the higher void fractions as occurring in Figure 6.4 are associated with initiation of NSSS safety injection of cold water and are generally of such short duration and low mass flows to be of little importance to pump performance.

For the broken leg and intact loop pumps these spikes generally occur after the flow is all steam and therefore do not appear in the graphs. The envelope of these curves, indicating the range of interest, is superimposed on the matrix in Figure 6.1 and forms a basis for entries in the matrix.

The pump average void fraction could be converted to inlet void fraction for operational convenience, but conversion would require prior knowledge of pump performance. Also of note is that for high flows when there is a pressure drop (negative head) across the pump, vaporization will start in the pump when the inlet fluid is still subcooled, and to cover this situation operationally will require setting a specified amount of subcooling at the inlet.

The limited available experimental information on two-phase effects on pump performance now used in the calculational model indicates that any two-phase effects ensue over a narrow range of void fractions at low values, with little further change until diminishing rapidly in the final approach to all steam as shown in Figure 5.4. Whether this holds for the model test pump is to be checked, and extra matrix points are shown in the 0 to 20 and

80 to 100 percent void fraction ranges. Actually the plan is to "feel out" the presence and location of any performance gradients and adjust the void fraction settings accordingly before running the closest-spaced points. This procedure illustrates that the test matrix is part of a dynamic plan which maps out an approach but adjusts the specific settings in response to test results obtained.

Each "X" in the matrix in Figure 6.1 represents only one combination of inlet pressure and pump average void fraction, but any number of combinations of pump speed and volume flow ranging from one speed and flow to a full performance map. A full map for single-phase performance (Figure 6.5) from cold water tests is expected to be applicable to single phase hot water or steam with hydraulic torques scaled for fluid density.

Three additional full maps for two-phase conditions are planned for the pressure and void fraction combinations indicated in Figure 6.1 by [X]. These are expected to involve 55 speed and flow test combinations each, which leaves a total of 145 other test points for the rest of the X's, or an average of about five points for each.

The three full-map [X]'s in the matrix were placed as shown on the basis of (1) spacing the maps across the pressure and void fraction ranges, (2) recognizing the trend to higher void fractions at lower pressures, (3) determining one map at an intermediate void fraction for which two-phase effects might be near maximum and not very sensitive to small deviations in void fraction, (4) obtaining a map at low void fraction to show two-phase performance with small amount of vapor with presumably small effects, and (5) obtaining a map for high void fraction but before the final approach to single-phase all steam.

The other, "partial map" X's are spaced to sample performance over the rest of the pressure and void fraction ranges of interest and generate data for cross-plots at constant pressure or constant void fraction in order to separate the effects of the variables. This will provide information for interpolating between the full maps and for determining steady-state performance at conditions similar to those in selected test system blowdowns.

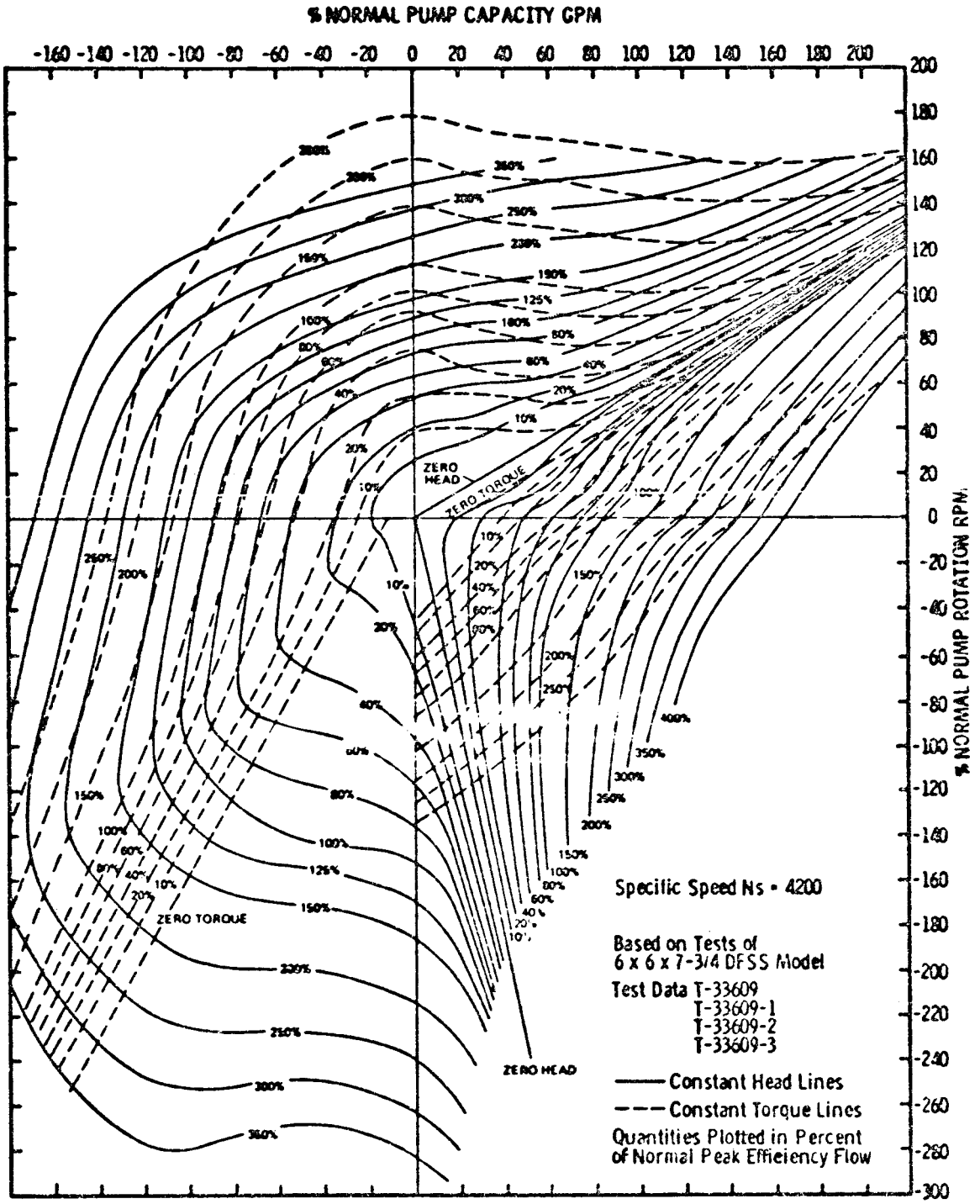

Single-Phase Full Performance Map for Test Pump

The initial spot checks of single-phase performance to confirm the applicability of the Byron-Jackson cold water data to hot water conditions and different loop configuration are planned for 1200 psia inlet pressure with somewhat subcooled inlet fluid to avoid any vaporization. These planned test points are as follows:

Speed	Volume Flow
100% of rated	100% of rated
100	120
100	50
120	100
50	100

A few more single phase points will occur later for all steam at inlet pressures of 1000, 850, and 500 psia as indicated in Figure 6.1.

Early in Phase I, the two-phase effects on performance as a function of void fraction will be sampled by running at constant inlet pressure, speed and volume flow for various void fractions from near-zero to 100 percent. It is planned to run these tests at 1000 psia, as indicated by the ⊗'s in the matrix (Figure 6.1). Speed and volume flow will be at normal rated values. This sampling will give early indication of the magnitude and "shape" of the performance variations with void fraction, and if only minimal effects are found, points will also be run at other flows and/or speeds. These points will tie in with the Phase I full performance map, which is planned for 1000 psia and 40 percent void fraction as indicated by the ⊠.

Additional Phase I runs will be made at steady-state conditions similar to transient pump operating conditions predicted to occur in initial forward and reverse test system blowdowns. This is shown in Figure 6.6, which is a reproduction of Figure 6.1, but with the addition of a calculated typical medium-strength forward blowdown trace and heavy dots at the matrix points which are nearest to the blowdown trace and at which tests would be run. The speeds and volume flows for these steady-state runs will be set at values close to those for the adjacent regions of the blowdown curve, or if a blowdown speed or flow cannot be duplicated directly in the pertinent steady-state test, then the normalized transient flow/speed ratio ν/α_N will be matched as a basis for scaling to the blowdown condition. Steady-state

FIGURE 6.6

Steady-State Test Matrix, (with Phase I Blowdown)

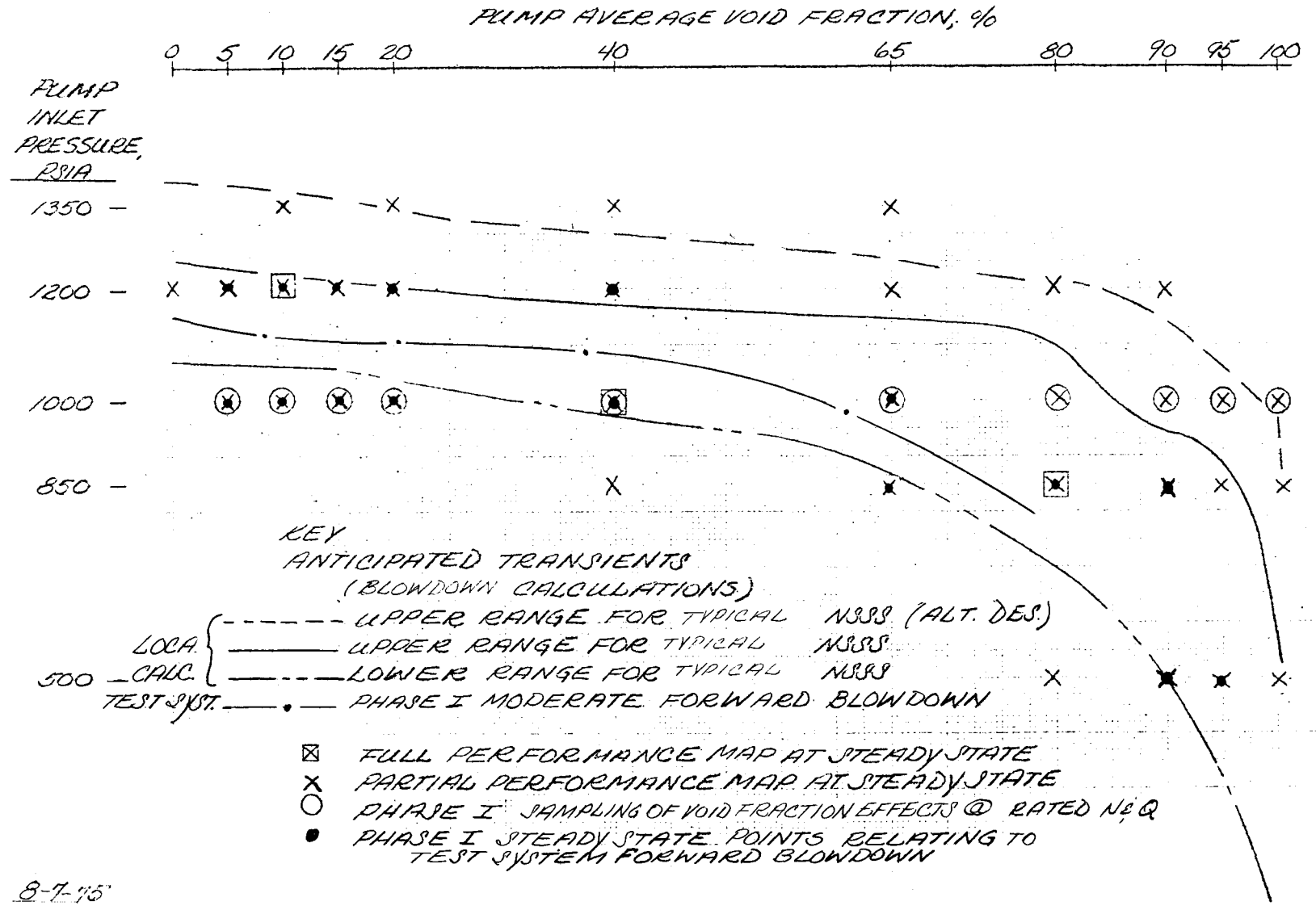

points relating to an initial mild reverse blowdown will be selected in a similar fashion from pending reverse blowdown calculations.

For generating a full performance map at any given combination of inlet pressure and pump average void fraction, the speed and volume flow combinations will be laid out in a fashion illustrated in Figure 6.7. The coordinates of rated speed vs. percent rated volume flow provide the framework for a "four-quadrant" performance map of constant percent head and torque lines. Typical lines for zero head and torque are shown. The area in which tests will be made is bounded as shown by (1) the highest positive and negative volume flows which can be achieved in the test loop at the model pump when the combined heads of the two booster pumps and the model pump just balance the pressure losses in the system with the throttle valve in the return line wide open, (2) the highest (twice the rated) positive or negative speed at which the speed controller will operate the test pump, and (3) the limit of interest to those combinations of speed and flow considered possible or likely in postulated LOCA's, which excludes positive flow with negative speed and negative torque with negative flow and speed.

Within the selected test area, several lines of constant speed will be selected, including rated, twice rated positive and negative, and zero (locked rotor) speeds.

Along these lines, various volume flows will be selected based on a blend of the following factors: (1) space several (preferably 6 to 9) points along each full length positive or zero speed line; (2) include maximum forward and reverse flows attainable; (3) use some of the same flow settings on several speed lines to allow checking speed and flow effects separately; (4) set the same flow/speed ratio ν/α_N on different speed lines to check the effectiveness of flow similarity parameters and scaling; (5) reserve at least 20% of the points for filling in where needed as indicated by the early results. The fill-in process of additional test points will include some points along the homologous head and torque curves developed from the measurements. This will require some additional measurements at low speeds in order to achieve the higher ν/α_N values as indicated in Figure 6.7 at the (A)'s.

FIGURE 6.7

Steady State Performance Map
Boundaries and Point Locations
(Sample, Estimated for Low α_F)

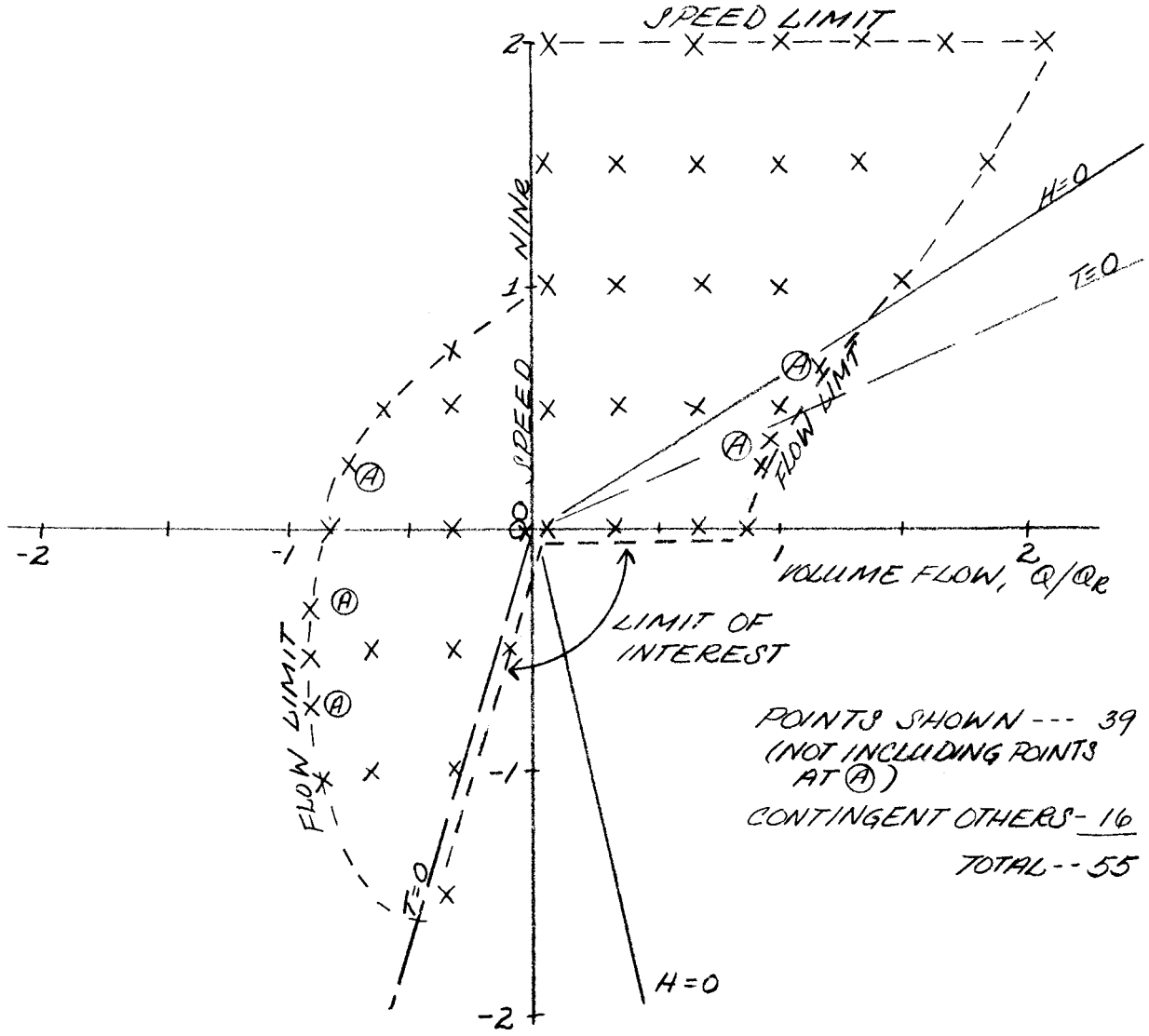

Maximum volume flow rates available in the test section are listed in Reference 3.1 for several void fractions and two values of model pump head, i.e., 0 (neutral) and -252 ft (loss) across the pump. Actually, as indicated above, the test pump head is different for each test condition and thereby affects the shape of the flow limit boundaries as in Figure 6.7. Since the model pump two-phase performance is yet to be determined from the test program, the flow limit boundaries shown in Figure 6.7 are simplified estimates for illustration of the plans to cover the actual achievable flow ranges.

Based on the above approach for laying out test points, Figure 6.8 shows the estimated boundaries and point locations for the Phase I full performance map at 1000 psia and 40 percent void fraction. Since the amount of two-phase head degradation for the model pump is not known yet, estimated flow boundaries are drawn first for undegraded test pump peformance. Degradation would then result in shifting of the flow limits in a manner indicated by the additional lines, with the amount of shift dependent on the amount of degradation. The first stage in running the tests in either the forward or reverse flow direction will be to determine experimentally the maximum flows achievable at each speed. Then the test points near the boundaries of the map can be adjusted to give the actual achievable pattern. For the estimated boundaries the planned test points for this Phase I performance map will be distributed as shown in Table 6.1 below.

6.3 Transient Test Matrix

The transient test matrix is an array of starting conditions from which test system blowdowns will proceed and the effective break sizes and flow routing to be used. Transient blowdown tests are generally planned to start from steady-state operation with liquid in the test loop at slightly subcooled conditions. The booster pump rotors will be locked during the blowdown runs, and therefore initial steady-state circulation will be generated by running the model test pump. Rupture of the diaphragms at the end of the blowdown line (see Figure 3.1) will then initiate depressurization of the loop, and the fluid will vaporize to progressively higher void fractions until the flow through the pump is all steam.

FIGURE 6.8

Phase I Steady State Performance Map
Boundaries and Point Locations
(Estimated, for 1000 psia and 40% Void Fraction)

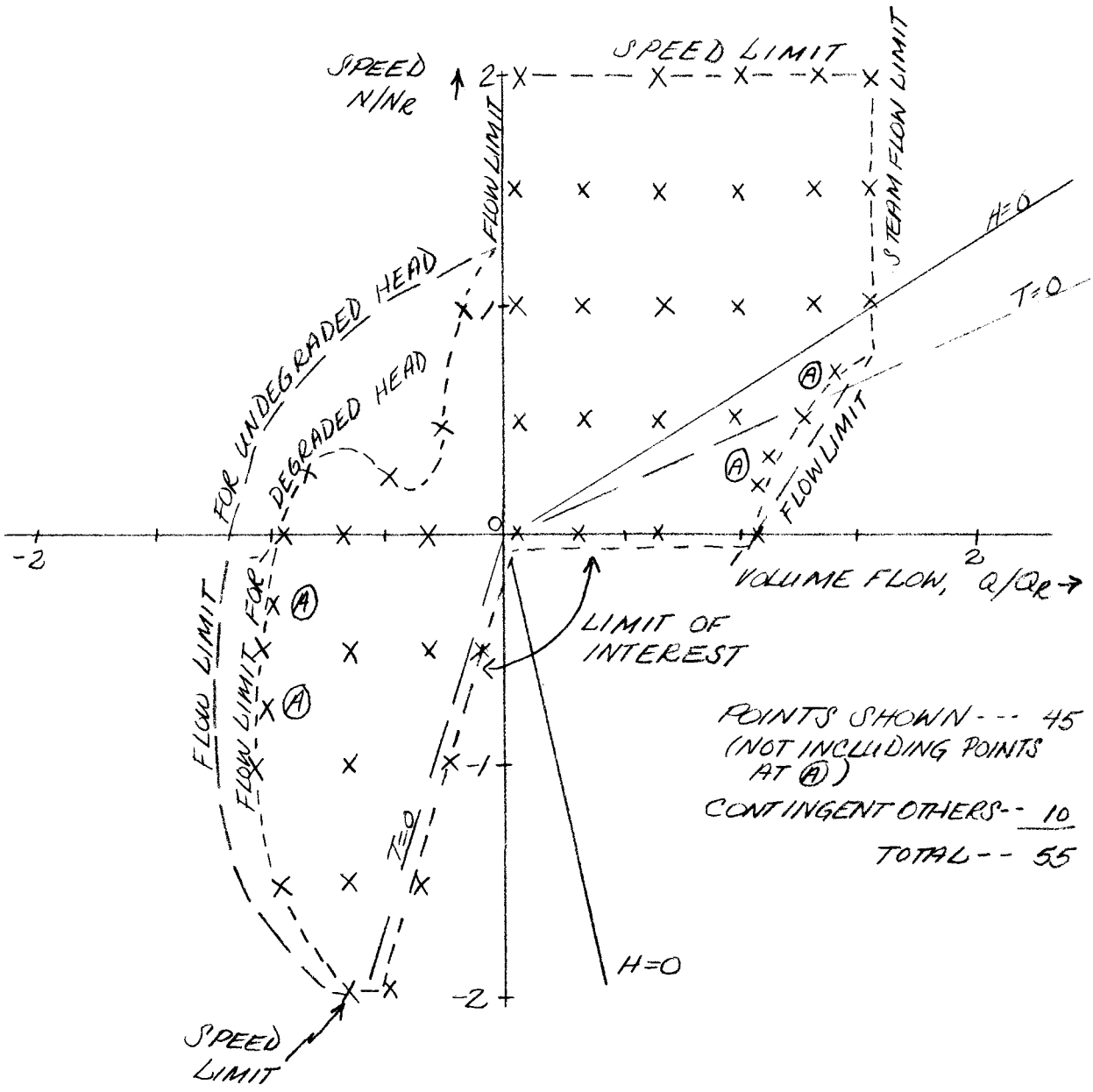

8-22-15

Table 6.1

PHASE I PERFORMANCE MAP POINTS

Speed % N/N_R	Volume Flow Rate, % Q/Q_R									
200					5		70	100	130	Max
150					5	35	70	100	130	Max
100			Max		5	35	70	100	130	Max
50			Max		5	35	70	100	Max	
25	Max	Min								
0	Max	-70	-30		5	35	70	Max		
-50	Max	-70	-30	$T=0^-$						
-100	Max	-70	$T=0^-$							
-150	Max	-70	$T=0^-$							
-200	Max	$T=0^-$								

The test operator will set the test points in terms of model pump inlet pressure level, inlet temperature (corresponding to desired amount of sub-cooling), volume flow rate, pump speed, steam drum water inventory, and size of throttling orifice in the blowdown line. He will manipulate the controls, including the throttle valve in the return line, to achieve the desired steady-state operation (Reference 3.1). Then, with the blowdown isolation valve open, blowdown will be initiated by triggering rupture of the diaphragms at the end of the blowdown line. Electric power to the pump drive motor may or may not be left on after rupture. If left on, the pump would run at nearly constant speed if the motor controller torque limit is not exceeded. Fluid from the high pressure drum will be able to reach the blowdown line by flowing backwards through the return line as well as by going through the test pump. When this bypass flow through the return line is present, the blowdown flow through the pump will be reduced because both flows will share the one blowdown line. However, this bypass flow can be interrupted by tripping the power-actuated throttle valve in the return line to close within one second, thereby increasing the pump flow and giving a more vigorous pump transient. Closing of the "bypass" throttle valve thus becomes one of the test specifications, but unless stated otherwise for a given case, it is assumed that the throttle valve will be closed in one second after blowdown is initiated.

As discussed in Section 9.3 below, the purposes of the test system blowdown runs do not require that any one test blowdown reproduce the time history of any one calculated NSSS LOCA blowdown. Rather, it is sufficient that somewhere in the assortment of test system blowdowns there are a number of times when the model pump operating conditions at least momentarily pass through the range of conditions typical of NSSS LOCA blowdowns and that at these times the severity of the test transients be sufficiently representative of LOCA's to check the applicability of a calculation model based on data from steady-state tests. Thus, the objective of selecting the matrix combinations of initial operating conditions and kinds of blowdown as shown in Figure 6.9, is to generate a series of pump transients, portions of which will pass with appropriate vigor through various parts of typical NSSS LOCA pump operating ranges, and which can be compared with results of steady-state test measurements ranging over some of the same or similar operating conditions.

FIGURE 6.9

Transient Test Matrix

BREAK LOCATION	DISCHARGE LEG			SUCTION LEG		
INIT. PUMP SPEED, RPM	0	4500	4500	0	4500	4500
MOTOR POWER AFTER RUPTURE	OFF	OFF	ON	OFF	OFF	ON
A. INIT. PRESSURE: 850 PSI						
BREAK SIZE 25% OF 8" PIPE AREA		X				
50%	X			X	X	
100%		X	X			
B. INIT. PRESSURE: 1000 PSI						
BREAK SIZE 25%		X			(X)	
50%	X	X		X	X	
100%	X	X	X			
C. INIT. PRESSURE: 1200 PSI						
BREAK SIZE 25%		(X)		X		
50%		(X)	X		X	X
100%	X	X	X	X		
NUMBER OF TRANSIENTS TEST SHOWN				25 PTS		
CONTINGENT ADDITIONAL TRANSIENTS TESTS				17 PTS		
TOTAL NUMBER OF TRANSIENT TESTS				42 PTS		

(○) = PHASE I TESTS

Pump conditions to be expected during test system blowdowns are calculated using the CEFLASH-4A computer program. Figure 6.10 shows a node and flowpath diagram indicating schematically how the test system has been modeled in such calculations. It is desired that predictions of test system blowdown rates be realistic, and therefore, the discharge coefficient is set at 0.6, a value generally agreed to come closer to matching experimental data than the 1.0 required in LOCA calculations. As discussed in Sections 5.1 and 6.2 above, pump performance in the different situations (NSSS LOCA's, transient tests, and steady-state tests) can be compared by matching operating conditions, (i.e., P_{inlet} and α_F, plus N and Q in percent of rated values) as far as possible or, when further scaling is required, using certain key parameters and homologous ratios (α_F, ν/α_N, and flow regime) as comparison criteria for both steady-state and transient cases, plus $d\alpha_F/dt$ for transients.

The variations of pump average void fraction α_F versus time after start of vaporization were shown for the compiled representative NSSS LOCA's (Section 4.2) in Figures 4.2 to 4.6, 4.12 to 4.16, 4.22 to 4.26, and 4.32 to 4.34. The envelope of these curves and some examples of intermediate curves are shown in Figure 6.11, along with representative test system forward flow blowdowns with a full-area break. As discussed in Reference 6.1, comparisons of the criterion $d\alpha_F/dt$ can be derived from these curves and indicate that the test system can produce blowdowns with $d\alpha_F/dt$ up to one-half of large break LOCA rates, which is severe enough to check applicability of the dynamic pump calculational model which uses steady-state data. Typical variations of ν/α_N versus α_F for NSSS and test system blowdowns are plotted in Figure 6.12, showing how the test system behaves in the NSSS range.

Representative variations of N/N_o, the ratio of pump speed to initial speed, are shown in Figure 6.13 as compiled from NSSS LOCA calculations (Section 4.2) and three test system blowdowns. N/N_o is not regarded as a primary transient parameter since (1) the main effects of speed are included in the normalized flow/speed parameter ν/α_N, and (2) the rotational inertia of the pump impeller and the drive system is large enough that velocity changes associated with impeller acceleration are considered to be small compared to fluid inertial response rates. Furthermore, it is not intended that a test system blowdown duplicate the time history of any LOCA blowdown, and thus speed variations during a test blowdown are not to be used to indicate LOCA overspeeds. Instead, as described in Section 5.2, LOCA overspeeds

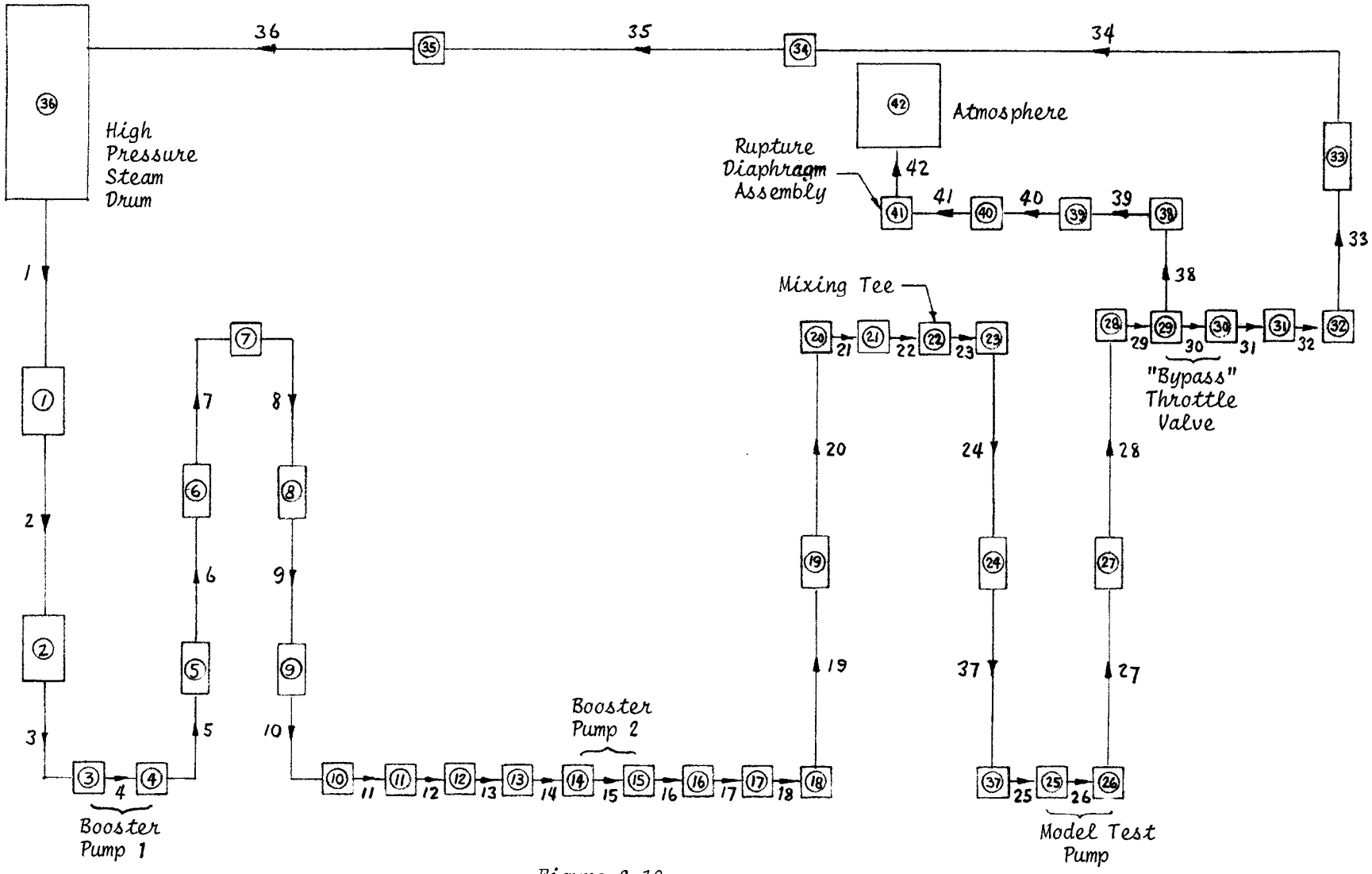

Figure 6.10
CEFLASH-4A Nodal Map of the Pump Test Facility

FIGURE 6.11

Typical NSSS and Test System Blowdowns,

Pump Average Void Fraction vs. Time

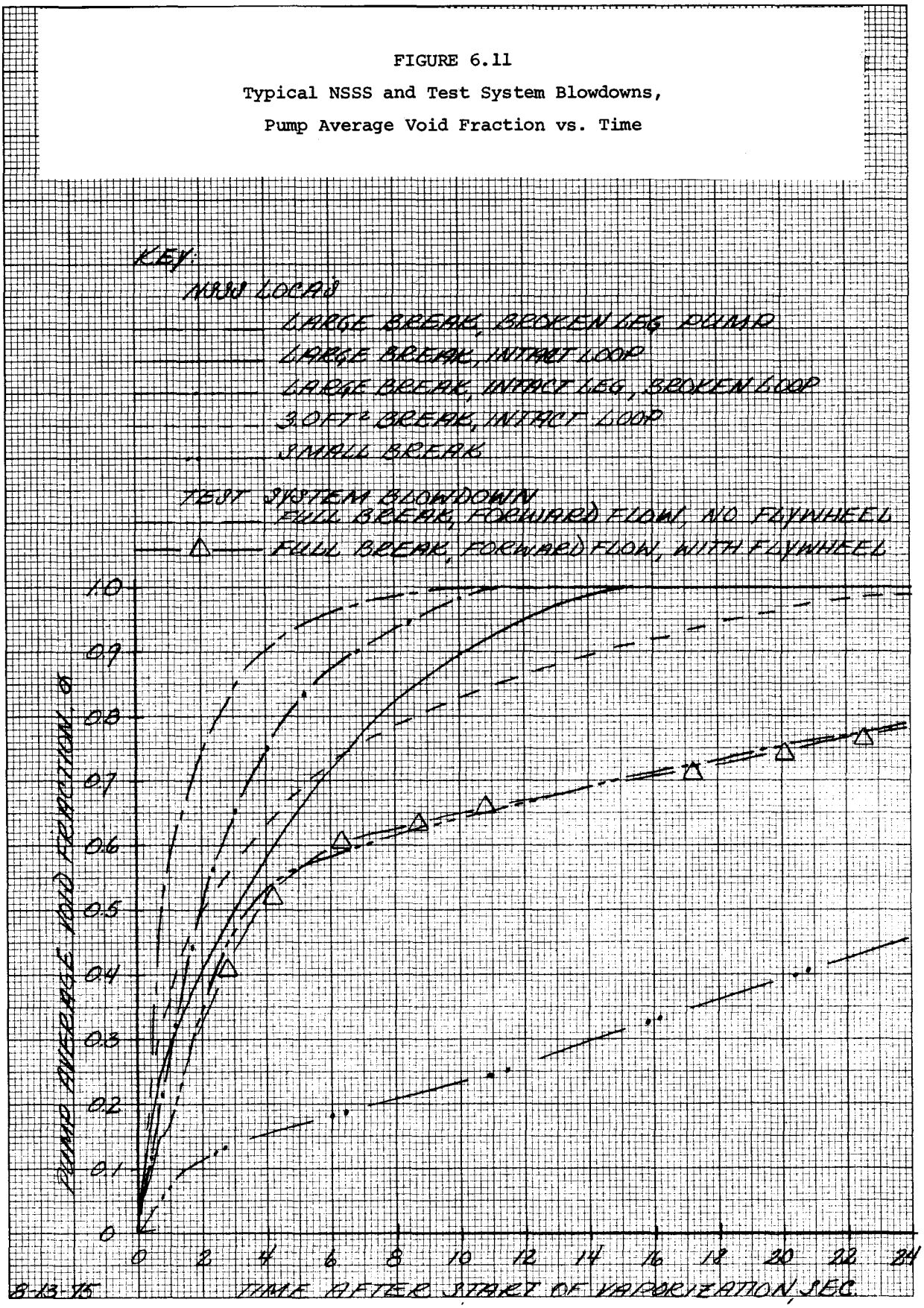

FIGURE 6.12

Typical NSSS and Test System Blowdowns for Discharge Leg Breaks, Pump Flow/Speed Ratio, ν/α_N, vs. Void Fraction, α_F

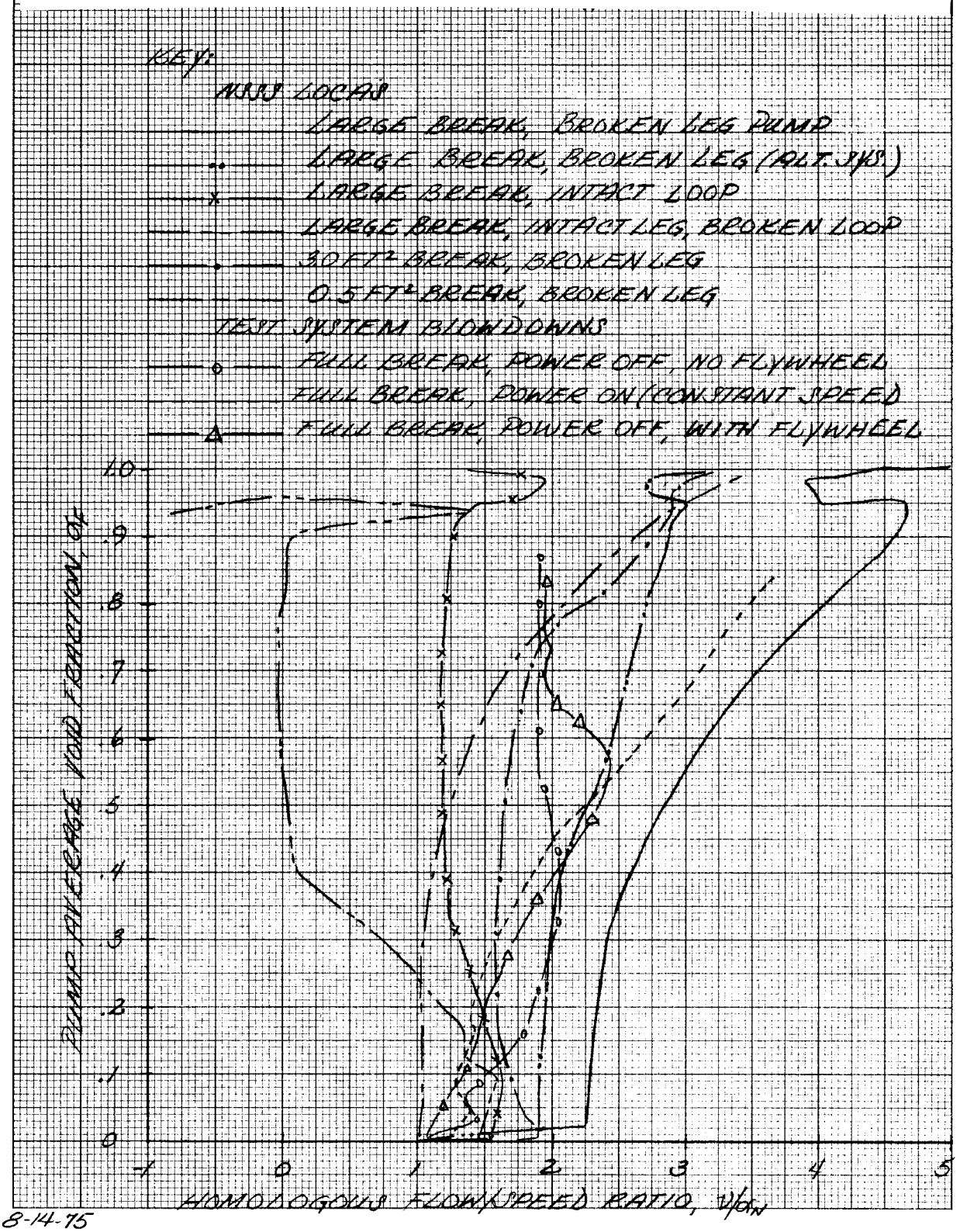

8-14-75

FIGURE 6.13

Pump Speed Ratios for Typical NSSS and Test System Blowdowns

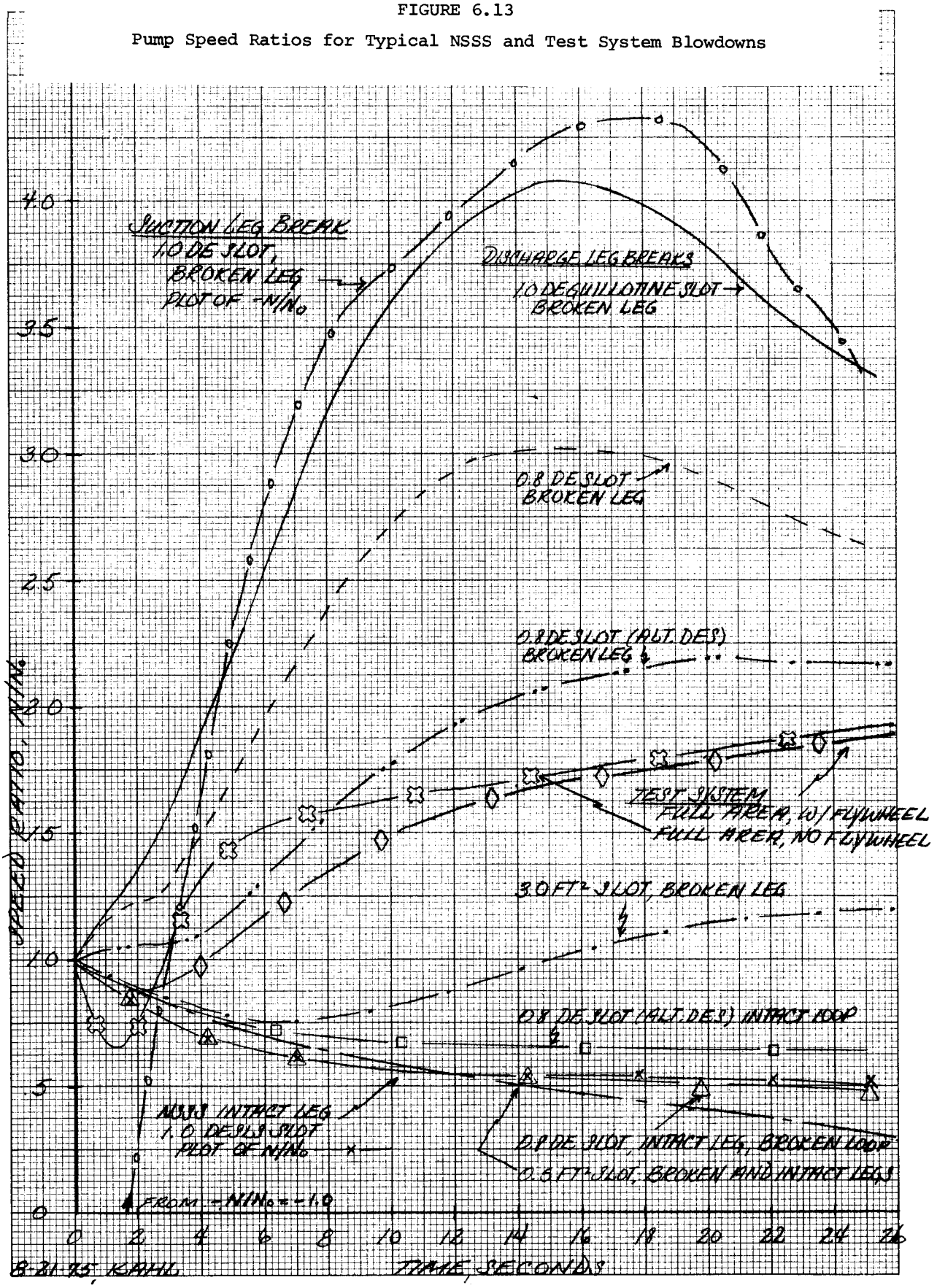

are predicted by the calculational model as the cumulative effect of angular accelerations dependent on net torque and moment of inertia. Therefore, hydraulic torque at various operating conditions is the key empirical information needed to calculate overspeed, and this is what will be determined in the transient tests to check the calculational model. Thus the addition of a flywheel to achieve scaled inertia is not necessary for obtaining the data required for predicting overspeed. Without a flywheel, the acceleration of the test pump will be more rapid and there can be a question from an operational standpoint whether there will be sufficient time for adequate measurements before reaching the facility safe speed limit. However, inspection of Figure 6.13 shows that for a test system full area forward flow blowdown test, the final pump speed is the same with or without a flywheel and the rates of change of speed are not excessive for good measurement. Further assurance that appropriate test conditions will be achieved without a flywheel is given by Figure 6.11, which shows that α_F versus time after start of vaporization is nearly identical with and without a flywheel. Also, Figure 6.12 shows that the possible useful variation in ν/α_N versus α_F occurring at intermediate α_F's from the addition of a flywheel can be equalled by running a blowdown at constant speed. For the above reasons, a flywheel is not included in the current test plans.

Pump speed versus time can be of interest as an additional general indicator of the strength of the initial surge and subsequent sustained rates of volume flow. Figure 6.13 shows the contrast between speed changes in the intact loop and broken leg pumps. The test system transients shown for full area forward flow blowdowns indicate that the test system does achieve significant accelerations and reach speeds approximately twice the rated speed, about as high as allowable in the test facility.

Calculated predictions of test system blowdown characteristics such as those exhibited above will continue to be made to evaluate cases as they are planned -- both before and during the actual test program -- taking advantage of the test results in order to "tune" the calculational description of the test system and to add new blowdown traces which will pass through additional conditions of interest.

The transient test matrix with 25 specified points and 17 reserve points as currently laid out is shown in Figure 6.9. Any one X could represent more than one initial flow, initial drum inventory, or option for

closing the bypass throttle valve in the return line. Until more blowdown calculations or test results suggest otherwise, it is assumed that the conditions to be used are rated flow, a full drum, and closing the valve within one second. Blowdown calculations for many of the cases listed are still pending, and test results and more analysis are expected to suggest and guide modifications and additions to the matrix in keeping with the concept of a flexible test program. For example, the break sizes shown as 50 and 25 percent, respectively, of the 8-inch blowdown line area are nominal indications of what might achieve mild and intermediate strength blowdowns relative to the full area blowdowns. If blowdown severity is to be judged by $d\alpha_F/dt$, and if for instance slopes at $\alpha_F = 0.3$ such as 1/4 and 1/2 of the slope for full break area are desired, additional calculations and early tests will help translate these into appropriate break (throttling orifice) sizes. Some additional calculations, including reverse blowdowns, will be made before the testing begins, but follow-on calculations as test data on test loop and model pump characteristics become available will have added meaning and be necessary anyway to provide predictions for evaluation.

Operating safety limits will restrict the pump shaft torque to about 4.5 times rated torque and the speed to 2.3 times rated. These are expected to be compatible with most of the forward flow breaks but may be more of a restriction for reverse blowdowns in which pump turbining tends to be stronger.

The early blowdown transients to be run in Phase I are indicated in the matrix (Figure 6.9) by (X)'s and comprise mild and medium forward flow (discharge break) blowdowns and a mild reverse (suction break) blowdown. As explained in Section 6.2, these will be tied in with early steady-state test conditions to enable early comparisons of steady-state and transient results (see Figure 6.6). Saturation pressures for these blowdowns may be adjusted somewhat to get operating conditions close to the early steady-state points.

6.4 Flow Regimes

As indicated in Section 5.1 earlier, the type of two-phase flow regime which will exist at the pump inlet is checked with regard to the applicability of the hydraulic similarity laws. Furthermore, average property values can be employed to characterize fluid conditions if the flow is truly homogeneous. Using the recommended methods of Govier and associates (References 5.2 and

5.3), the flow regime maps have been developed for typical NSSS blowdowns, steady-state pump operating conditions (occurring in the steady-state test matrix) and typical test facility blowdowns. These flow regime maps are log-log plots of the superficial liquid velocities V_{SL} versus the superficial gas velocities V_{SG} showing the cases of interest superimposed on empirical regions corresponding to different flow regimes. These superficial velocities are defined as the volume flow rates of each phase divided by the total pipe cross sectional area.

For typical NSSS blowdowns, the two-phase distribution patterns are indicated in the flow regime map of Figure 6.14. A comparison of the flow regimes shows that all breaks start well up in the dispersed flow regime, and for a large break the broken leg pump remains in the well-mixed flow regimes. For the pumps in the intact loop during a large break and all pumps during the 0.5 ft^2 break the flows later in the transient are low enough to indicate passage into other flow regimes.

For steady-state test operating conditions, the flow regime map is developed for sample pressures, void fractions, speed, and the corresponding maximum volume flow rates available in the test facility. The pump performance for two-phase flow is estimated using the different homologous head values and degradation multiplier of the ANC Semi-scale Pump as in References 5.1 and 5.4. Figure 6.15 shows the steady-state flow regime map for the rated speed and maximum achievable flows. It is seen that for most of the cases considered, the flow regime is of the dispersed flow type which is expected to be well-mixed. For some of the higher void fraction cases, the flows may be in the slug flow regime. This results mainly from the steam flow limit. It is worthwile to note that at lower pressures ($\leq$ 500 psia), the flow regime remain in the dispersed flow regime even at higher void fractions ($\geq$ 65%) due to the availability of additional steam flow from the low pressure boiler.

In Figure 6.16, the flow regime map for the pump inlet flow is indicated for typical test facility blowdowns. The path of the transient is noted with progressive times in this figure. It shows that the flow in the pump inlet pipe for all the transients starts well into the dispersed flow region and in some cases cuts through the slug flow regime for later part of the blowdowns, apparently in a similar manner to the NSSS (see Figure 6.14). It

FIGURE 6.14

TYPICAL NSSS BLOWDOWN
FLOW REGIME MAP

△ 0.8 DE Slot, Discharge Leg, Broken Leg
◇ 0.8 DE Slot, Discharge Leg, Intact Leg
□ 0.5 FT^2 Slot, Discharge Leg, Broken Leg

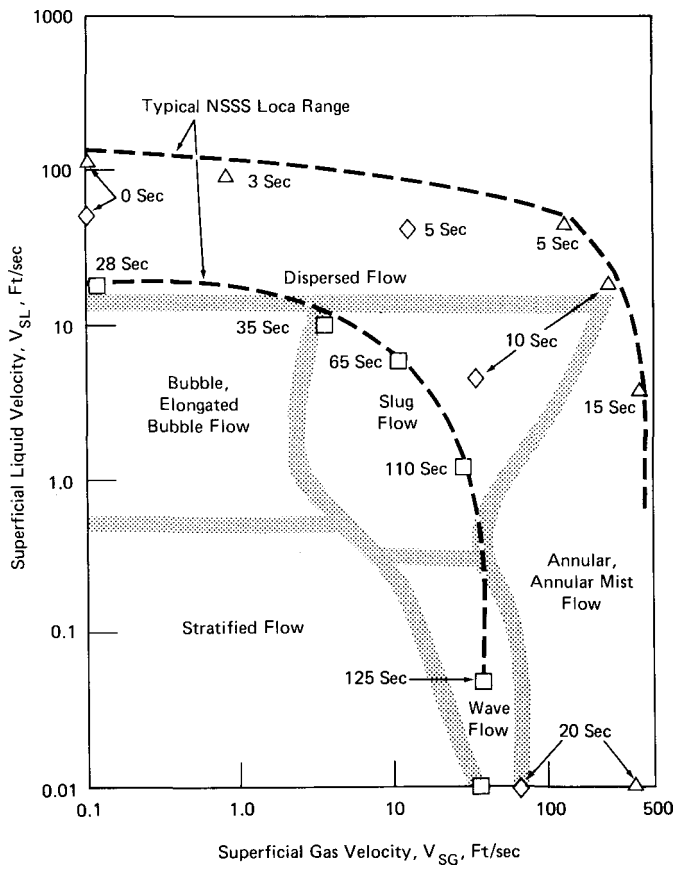

FIGURE 6.15

STEADY STATE FLOW REGIMES

IN TEST LOOP PUMP SUCTION LEG

FOR MAXIMUM FLOW RATES AT RATED PUMP SPEED

NOMINAL VOID FRACTION:

☆ α = 0%
◇ α = 5%
◇ α = 10%
▽ α = 20%
◇ α = 40%
△ α = 80%, 1200 psia (Steam Limit)
○ α = 80%, 1000 psia (Steam Limit)
□ α = 65%, 850 psia (Steam Limit)
α = 65%, 500 psia (two boilers)

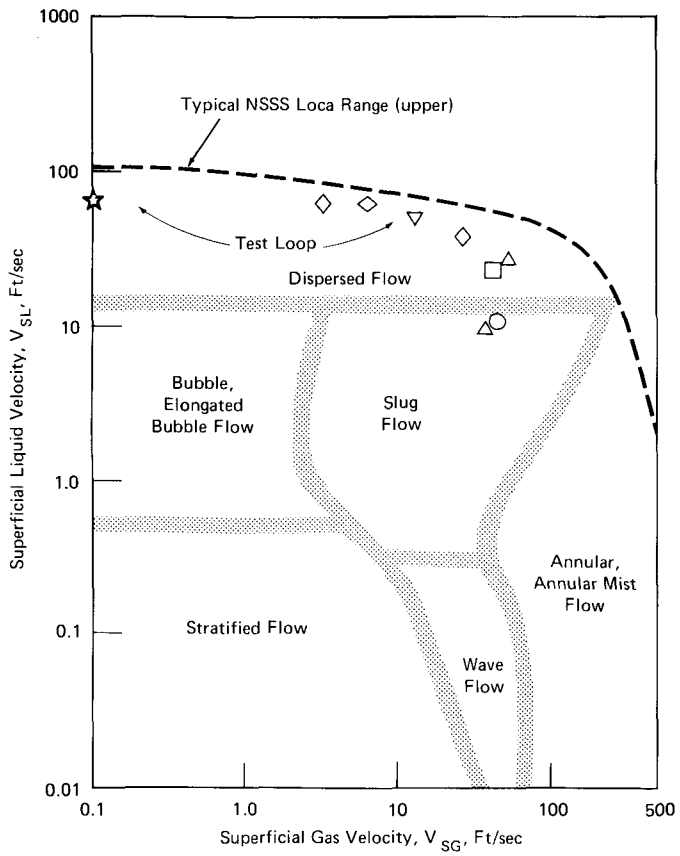

FIGURE 6.16

BLOWDOWNS OF TEST FACILITY

IN FLOW REGIME CHART

1 - ○ BYPASS VALVE OPEN

2 - △ BYPASS VALVE CLOSED IN 1.0 SEC

3 - ◇ 10% INVENTORY IN DRUM;
BYPASS VALVE OPEN

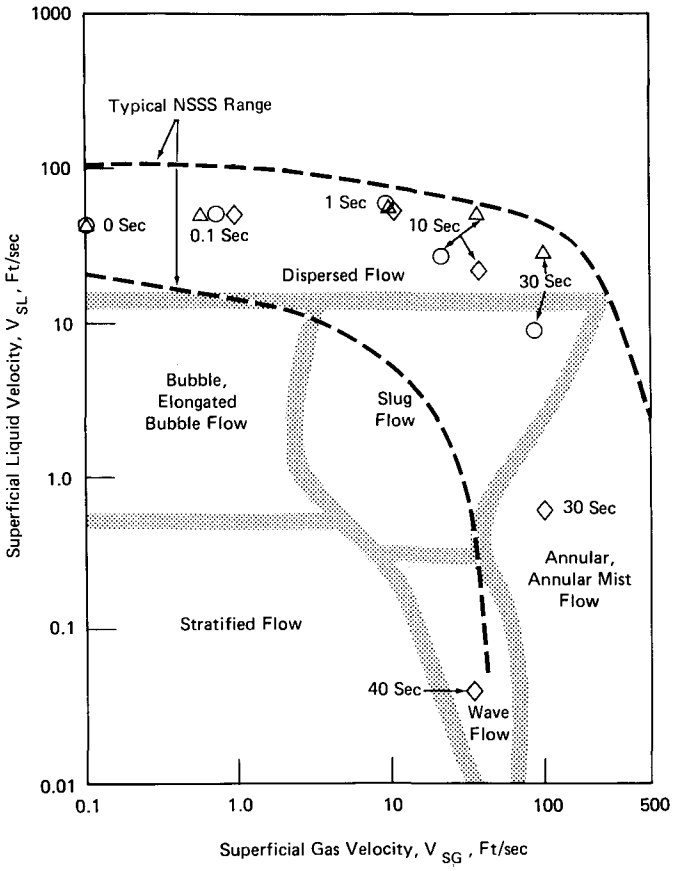

should be pointed out that for mode of operation 2, the two-phase flow distribution is of the dispersed flow type for over 30 seconds of the transient, suggesting good mixing of the two phases.

With the use of two three-beam γ-ray densitometers, located in the pump suction and discharge pipes, additional indication of density and phase distribution in the pipe can be obtained during the test program as described in Section 8.1 below.

6.5 Test Sequence

The sequence of test runs will be determined before the start of testing, with the intent of modifying the sequence during the course of operation if the results obtained indicate this to be advantageous. The test sequence within any block of tests will be primarily governed by the range of test conditions allowed for particular test loop configurations. Those test conditions requiring little change between successive conditions will be grouped together. The time required for various changes is given in rank from shortest to longest as:

(a) Change pump speed
(b) Change water flow (within orifice range)
(c) Change steam flow (within orifice range)
(d) Change pressure
(e) Change orifice plates (large flow changes)
(g) Change torque meter
(h) Change piping to reverse flow

An additional criterion for the test sequence will be the data needed to complete a portion of the pump curves during data analysis.

7. DATA REQUIREMENTS

7.1 Identified Data Need

As indicated in Section 5.2, the pump model employed in the CEFLASH-4A code for LOCA analyses requires the knowledge of the head and torque degradation multipliers, and the difference homologous head values. The U.S. Nuclear Regulatory Commission (NRC) has required that the ANC Semi-scale 1-1/2 loop system pump test data (Reference 5.1) be used to formulate the pump degradation model when two-phase flow occurs in the pump. However, the typical reactor pump differs greatly from the Semi-scale pump. The differences are in the shape of the pump impeller and hence the specific speed. The Semi-scale pump specific speed and that of a typical C-E reactor coolant pump compare as follows:

Semi-scale pump . . . . . N_S = 926 rpm
C-E pump . . . . . N_S = 4200 rpm

Since the specific speed is a characteristic number describing the type of the pump and the performance characteristics, a difference of this magnitude can result in distinct differences in performance.

The reactor pump has a mixed flow impeller while the Semi-scale pump has a radial impeller. Therefore, the two-phase flow distribution pattern in the reactor pump is expected to be different than for the Semi-scale pump.

Thus, it is believed that the Semi-scale pump test data for the degradation multipliers and the different homologous head values are not directly applicable for the case of the reactor pump. The data required of the pump tests include: the degradation multipliers over the range of two-phase void fractions and the difference head and torque values for a wide range of the ν/α_N-ratio to develop the four-quadrant difference homologous curves. This will involve both steady-state and transient tests at various void fractions, flows, speeds, and pressure ranges and conversion of the resulting heads and torques into homologous parameters. The test matrices and sequences described in Section 6 are designed to satisfy these data requirements.

7.2 Required Measurements and Instrument Locations

As stated above (Sections 3.2 and 5.1), pump performance is generally measured and described in terms of head and torque for a given speed, volume flow rate and fluid density, plus pressure, void fraction, and perhaps flow regime for two-phase flow. For transient tests these are all measured as a function of time. These parameters are listed in the first column of Table 7.1, and they are determined directly and/or calculated from combinations of quantities measured by instruments as indicated in the other columns. The required measurements at each location are summarized in Table 7.2. Details of the instrument measurements, data conversion and calculation of the performance parameters are given in the Test Facility Description Report (Reference 3.1) and Section 8.1 below.

For determining pump friction and windage torques several alternates are still under consideration. Since the seals in the model pump are of labyrinth type and not rubbing seals, the seal drag should be fairly low and perhaps vary along with windage as speed squared. Bearing manufacturer's data and comparing torques from runs with high and low densities (water and steam) at different pressures will help separate windage from bearing drag. Runs at zero hydraulic torque are what are needed, but this can only be approximated by estimating impeller approach and discharge scroll losses.

The pump suction and discharge conditions are measured in instrument sections of the 6-inch nominal pipe as indicated schematically at points 1 and 4 in Figure 3.1 and as detailed in Reference 3.1. This places the instruments in straight runs of pipe long enough to provide reasonably straight and symmetrical flow for good measurements. It also means that the pump inlet conditions as measured at point 1 will differ from what enters the pump casing at point 2 by the losses and changes in flow distribution induced by the intervening two elbows. Actually, this could be advantageous because the two-bend suction line is nearly the same as in a typical NSSS (see Reference 3.1) and so the test measurements will provide the calculational model with representative experimental data input for a pump path all the way from point 1 to point 4. However, in case it seems desirable to evaluate the losses in the suction line separately, pressure taps will be provided at point 2, located horizontally on both sides of the pipe flange. Discharge pipe station 4 is only a few diameters of straight pipe away from the pump

casing discharge at point 3 and therefore it does not appear essential to provide extra measurements at point 3, although a pressure tap fitting is provided.

It is also proposed to make some additional pressure and differential pressure measurements around the test loop so that the pressure loss characteristics used in blowdown calculations can be based on actual measurements. These call for provisions to measure (at least part-time) pressure differences such as from the high pressure drum to the suction line of the first booster pump, across each booster pump, to the water orifice, to the mixing tee, across the mixing tee, to the mixing plate, across the plate to the pump inlet instrument pool, across the test pump (as above), from pump discharge to the return line throttle valve, across the throttle valve, and from the valve to the drum.

7.3 Required Measurement Accuracy

A complete sensitivity study of how the peak fuel clad temperature in a postulated NSSS LOCA is affected by variations in each pump performance parameter would be a very sizeable task and is beyond the scope of this test program. Furthermore, such a study would be more meaningful after the two-phase performance test data for the model NSSS pump is obtained.

Instead, a single sample case was run comparing the results for a large break LOCA calculated with and without pump two-phase head degradation. No torque degradation effects were involved in this comparison. The head degradation used was taken from ANC Semi-scale pump test results as currently required by NRC until more appropriate data is obtained. For the Semi-scale pump, the head degradation was considerable, and more than might be expected in the less radial high flow-density NSSS pumps. For the head degradation assumed, the increase in peak clad temperature during blowdown was about 150°F. However, this peak was not the limiting clad temperature because with current NRC regulations on subsequent reflood and refill calculations, the limiting peak temperature occurs in these later phases. In the sample case, the presence of head degradation raised this maximum temperature only about 30°F.

From the results of the sample case cited it would appear that any reasonable accuracy in determination of head degradation, such as $\pm$10 or

TABLE 7.1

TEST MEASUREMENTS REQUIRED

Performance Parameter	Required Quantities		Required Measurements	Measurement Locations
Flow regime	ρ distribution - γ-densitometer		3 beam ρ's	Pump suction
	or V_{SL}, V_{SG}	Q as above α_F as above A pipe, direct		Pump discharge
Drum inventory	Liquid head & density		ΔP	Drum bottom to top
			°F	Lower drum
Special for transient tests -				
Q	V_{avg}	V at a point (turbine meter) Assumed V profile	V	Pump suction
				Pump discharge
	A_{pipe}			
ρ	V_{avg} as above			
	ρV^2	Drag disk at a point Assumed profile	ρV^2	Pump suction
				Pump discharge
	γ-ray attenuation Phase distribution	γ-densitometer as before		
time	direct	- data recorder		
Pump shaft acceleration	N	as before		
	time	as before		

TABLE 7.1 (cont.)

TEST MEASUREMENTS REQUIRED

Performance Parameter	Required Quantities		Required Measurements	Measurement Locations
Q	$\dot{M}$ mixture	$\dot{M}$ water	°F, P, ΔP	Water line orifices
		$\dot{M}$ steam	°F, P, ΔP	Steam line orifices
	ρ mix	See next below		Pump suction Pump discharge
ρ mix or α_F inlet or α_F disch	$x_{mixing\ tee}$	$\dot{M}$ water as above $\dot{M}$ steam as above		
	ρ sat liq		°F or P	Lines to mixing tee or pump suct or disch.
	ρ sat vap		°F or P	
	Corrections for heat in or out	From tee to suction	°F, P	"
		Suction to discharge	°F, P	"
		Pump work: $\dot{M}$ (above) H (below)		
		Seal injection spillover $\dot{M}$ & enthalpy	°F, ΔP	Injection inlet Injection outlet
	γ-ray attenuation Phase distribution	(γ densitometer)	ρ suct ρ disch	Pump suction Pump discharge
P_{inlet}	direct		P suct	Pump suction (1) (or (2))
H	ΔP_{pump} ρin, out, or avg	as above	P suct P disch	" " Pump discharge
N	direct		N	Pump shaft
T_{hyd} torque	T_{shaft}	Direct	T	Pump shaft
	$T_{frict.\ \&\ windage}$	See discussion		
	T_{acc}	Shaft acceleration		
	$I_{pump\ \&\ coupling}$	See next page.		

TABLE 7.2

REQUIRED MEASUREMENTS AT EACH LOCATION

LOCATION	MEASUREMENTS
Water line to mixing tee	
Main orifice	Water temp., press., press. drop
Bypass orifice	Same
Steam line to mixing tee	
Main orifice	Steam temp., press., press. drop
Bypass orifice	Same
Pump suction pipe	
Station (1) (See Fig. 3.1)	Press., temp., density (γ-densitometer), velocity (turbine meter), ρV^2 (drag disk)
Station (2)	Pressure
Pump discharge pipe (4)	Same as suction station (1)
Pump suction to discharge	
(1) to (4)	Pressure difference
Pump suction	
(1) to (2)	Pressure difference
Across pipe at (2)	Pressure difference
Pump shaft	Speed, torque
Pump seal injection inlet	Temp., flow press. drop
Pump seal injection outlet	Temp., flow press. drop
High pressure drum	Temp., water height press. difference
Ambient	Barometric pressure
Around test loop	Pressure drops (see text)
Other	Time

20 percent, would be adequate for current LOCA calculations, and that ±10 percent would probably be acceptable even if blowdown peaks again become limiting.

At this point, the primary basis for suggesting required measurement accuracies for the pump test program is to satisfy what has been developed as good working practice for balanced input to CEFLASH-4A calculations with regard to pressure differentials, loss coefficients, flow rates, etc. Also, the accuracy should be sufficient to detect significant performance trends as a function of the key parameters, such as whether head does degrade at certain void fractions, and to permit a systematic quantitative description of such effects in terms compatible with the calculational model. Where good commercial instrumentation provides compatible or only slightly less than desired accuracy, it has been accepted. For some parameters and/or parts of their ranges, the planned instrumentation is more than adequate and advantage of this can be taken to enhance the results.

The required measurement accuracies resulting from the above considerations are listed in Table 7.3. For a few of the parameters, some distinction should be noted between the measured quantities and the derived parameters to be used in calculations. Thus, the density and associated void fraction must be derived from three-beam gamma-ray attenuation measurements using assumed homogeneity or deduced variation from homogeneity of the two-phase mixture as discussed in Section 8.1 below. Hydraulic torque is actually not measured directly but calls for determination of friction and windage torques to be subtracted from the measured shaft torques as discussed in Section 7.2 above.

7.4 Data Acquisition

In order to record the many instrument signals effectively for transient blowdown tests, the data acquisition system must be capable of recording all signals with little lag either continuously or repeatedly in very rapid succession at known times. The errors in this process should of course be low since they must be included in the total measurement errors. It is helpful if the fast system for transient recording can also be used for the steady-state tests, thereby saving time and permitting several readings for each run in order to check on stability of the operating conditions.

TABLE 7.3

REQUIRED MEASUREMENT ACCURACIES

Parameter	Accuracies, Max. % of Value, or Alternate Limits*
HEAD	± 1 psi or 5%, whichever is less, down to ± 0.1 psi
TORQUE	
T shaft	± 2% down to ± 8 ft-lb for $T \geq 400$ and ± 2 ft-lb for $T < 400$
T hyd	± 5 or 6%
PRESS. LEVEL	± 5 psi for levels
VOID FRACTION	± 3% (of value) down to ±.0015, for void fractions 0 to 0.2
Pump suction or discharge	± 2% for void fractions 0.2 to 0.7 ± 1% for void fractions 0.7 to 1.0
SPEED	± 0.6% down to ± 5 rpm
VOL. FLOW	± 2.5% for void fractions 0 to 0.5 then rising linearly to ± 4% at 1.0 void fraction
DENSITY	± 0.5% for void fractions 0 to 0.5 then rising to ± 4% @1.0 void fraction
MASS FLOW	± 2% for flows down to total of 65,000 lb/hr but may need 1 to 1.4% for highest void fractions
TIME (From reference at beginning of transient)	± 0.001 sec. from 0 to 0.5 sec.
	± 0.010 sec. after 0.5 sec.
TEMP. OF FLUID	± 0.5°F

*Accuracy figures are regarded as workable maximums, and any readily available reductions are to be taken advantage of.

The data acquisition system which will be used to satisfy these requirements is basically a rapidly scanning digital voltmeter capable of handling repeated cycles of up to 100 channels at a rate of up to 98 channels per second with very low error. The recorded signals can be quickly stored in permanent form appropriate for the rapid computer processing described in Sections 8 and 9 below. For recording very steep transient signals such as may occur during the first second of a blowdown, the digital scanner may need to be supplemented with an optically recording light beam galvanometer or an FM magnetic tape system. Details of the data acquisition system specifications and mode of operation as well as auxiliary recording equipment are given in the Test Facility Description Report (Reference 3.1).

8. PRESENTATION OF TEST DATA

8.1 Conversion of Raw Data

The data reduction program to be used for the model pump tests incorporates routines that have been developed by KDL for use with a time-sharing computer system. The data reduction program reads the information stored in the instrument conversion constant and instrument data files, converts the instrument millivolt outputs to the proper engineering units, calculates the test results, prints the results in a desired format, and stores the data in a file for access by the data analysis program. A description of the test data reduction is outlined below.

8.1.1 Instrument Conversion Constant Data File. The data reduction program reads the instrument conversion constants for each instrument on the test facility from a permanent file. Five constants are given for each instrument. Four of these are used in the data reduction program to convert the instrument millivolt output to the proper engineering units. The fifth constant is the calibration error obtained from the instrument calibration procedure. This value will be used in an error analysis for determining the error in the calculated pump performance data.

The conversion constant file also contains a section that includes the number of measurements obtained with given type instrument and the data scanner numbers on which the output is recorded. This permits additional instruments to be added as the test progresses and to be easily reduced in the proper sequence.

8.1.2 Manual Data. Data is manually typed into the data scanner and stored on the data tape for each test. This data consists of the test number, time and date of the test, barometric pressure, and comments or indices describing the facility operation pertinent to the data reduction.

8.1.3 Instrument Data File. The data reduction program accesses the stored data from the punched paper tape. Included with the instrument millivolt outputs are a zero shift reading of the data scanner DVM and manual inputs.

8.1.4 Instrument Zero Data File. Periodic zero readings of the instruments are obtained to correct for instrument drift during the test program. These zero readings are stored in a zero file for access by the data reduction program. These zero readings are used with the instrument data readings in the instrument conversion sections outlined below to arrive at values of the measurements.

8.1.5 Data Interpolation. The data scanner records data from each of the instruments sequentially for very short periods of time. A longer interval of time exists between these readings while the other instruments are being read. During a transient test, these sequential readings vary significantly with time. This can produce substantial error when two or more instruments, read at significantly different times, are used together in a calculation for a different time period in the same interval.

This scanning time error is reduced significantly by using an interpolation routine to linearly interpolate the signal of each instrument value at a common point in the time interval. All calculations are made for the same common time in the interval using the interpolated values.

8.1.6 Thermocouple Conversion. All thermocouple EMF readings are converted to degrees F with the conversion routines based on the IPTS-68 and published in the March 1974 Bureau of Standards Handbook on thermocouples.

8.1.7 Resistance Temperature Device (RTD) Conversion. The data reduction program converts the instrument millivolt output to degrees F with an equation of the form,

$$R = C_1 + [C_2D + C_3D^2]C_4,$$

where D is the millivolt output and C_1, C_2, C_3, and C_4 represent the instrument conversion constants.

8.1.8 Pressure Cell Conversion. Pressure cell millivolt outputs are reduced to units of psi using instrument conversion constants obtained from the instrument calibrations. A correction is made to the resulting pressure for the elevation difference between the pressure cell and the test loop

pressure tap. An equation in the data reduction program with the form $P = C_1V + C_2 + C_3D + C_4D^2$ is used to convert the instrument output, where C_1 is the elevation difference, V is the connecting tube fluid specific volume, and C_2, C_3, and C_4 are the instrument conversion constants.

8.1.9 Differential Pressure Cell Conversion. Reduction of the differential pressure cell reading to psid is accomplished with the equation, $DP = C_1V + C_4 (C_2 + C_3D)$. The equation uses instrument calibration constants, C_2 and C_3, a correction for the elevation difference between the two test loop pressure taps, C_1, the connecting tube fluid specific volume, V, and an index which indicates positive (+1) or negative (-1) connection of the differential pressure cell, C_4.

8.1.10 Drag Disk Conversion. Conversion of the drag disk ρV^2 by the data reduction program to fluid velocity head is performed using an equation of the form,

$$\rho V^2 = C_1 + [C_2D + C_3D^2] C_4$$

where D is the instrument millivolt output and C denotes the instrument conversion constants.

8.1.11 Turbine Meter Conversion. The turbine meter millivolt output is converted to velocity by the data reduction program with the equation,

$$V = C_1 + [C_2D + C_3D^2] C_4$$

where D is the instrument millivolt output and C_1 through C_4 denote the instrument conversion constants.

8.1.12 Torquemeter Conversion. The pump torque is measured with a torquemeter which the data reduction program converts to the appropriate engineering units using the instrument output voltage, D, and conversion constants, C_1 through C_4, as

$$TM = C_1 + [C_2D + C_3D^2] C_4.$$

8.1.13 Speedmeter Conversion. A measure of the pump speed is determined by converting the instrument millivolt output using the instrument conversion constants and the appropriate conversion equation,

$$N = C_1 + [C_2 D + C_3 D^2]\ C_4.$$

8.1.14 Fluid Property Calculation. Using the converted instrument output data, the data reduction program calculates the fluid properties in the test loop. Steam table values are obtained using a packaged program derived from the 1967 ASME Steam Tables. The viscosity of the steam and water are determined from subroutines that were used to derive these steam tables.

8.1.15 Test Loop Flow Calculations. The test loop flow rates are measured with standard ASME flange tap flat plate orifice meters and calculated using a subroutine developed from ASME flow orifice calculations. Measured inputs to the flow subroutine include the orifice pressure, the orifice pressure drop, and the fluid temperature at the orifice. Also, inputs for the pipe inside diameter, orifice diameter, and type of fluid are required. Using this procedure with data from orifices located in each flow path, flow rates will be calculated for water and steam flows into the mixing tee and for test pump input discharge flows of seal injection fluid.

8.1.16 Fluid Density Calculations. Average fluid densities in the pump suction and discharge pipes will be calculated from the multibeam densitometer attenuation measurements for both steady-state and transient tests. Each beam will measure an integrated density along its path as

$$\rho = C_0 \ln\left[\frac{C_2 - C_1}{D - C_1}\right]$$

where ρ = integrated fluid density (lb/ft^3)

C_0 = densitometer calibration conversion constant (lb/ft^3)

C_1 = offset voltage (mv)

C_2 = steam only voltage (mv)

D = detector reading (mv)

The integrated density for each beam of the multibeam densitometer will be used in an iterative mode with various assumptions of flow regime to arrive at an average density in the measurement section and a void fraction distribution. The flow regimes that will be considered are:

homogeneous - dispersed
horizontal - stratified
annular (concentric or eccentric steam core)

A second method of determining steady-state average densities, which will enable cross-checks, will be to use the quality calculated at the mixing tee from measured single phase steam and water flow rates and assume homogeneous flow, with corrections for changes in quality between the mixing tee and the pump.

Fluid density during two-phase flow conditions is quite sensitive to quality. The quality in turn is sensitive to heat losses. The quality will be corrected by a heat loss calculation to arrive at the correct condition in the pump suction and discharge pipes. This correction will be calculated from a correlation of the heat loss vs. operating temperature derived from subcooled water calibration at the same temperatures.

The pump outlet pipe quality is also affected by heat gained from the pump work and injection seal water flowing into the fluid. The hydraulic work will be calculated and added to the inlet fluid enthalpy to determine the correct outlet enthalpy. A heat and mass balance will be applied to the injection seal water and working fluid to account for the addition of the seal water. The amount of seal water entering the pump will be calculated by subtracting the external seal discharge flow from the seal input flow.

Also, the density and velocity of the fluid in the test pump suction and discharge pipes can be calculated by using for each pipe a combination drag disk and turbine meter system for transient as well as steady-state tests. The fluid velocity will be directly measured by the velocity meter as outlined in Section 8.1.11. This velocity, combined with the velocity head term measured by the drag disk reading (8.1.10), will give fluid density at that point. These are point measurements that will be correlated to the average densities calculated as above for steady-state operation with both single and two-phase steam water conditions.

8.1.17 Pump Performance. The pump performance will be calculated in terms of pump head and hydraulic torque for various volumetric flows, void fractions, and speeds using data and fluid properties calculated in the preceding sections. The pump head measurement will be corrected for differences in velocity head and elevation going from the pump suction to discharge pipe. The pump torque will be corrected for bearing and seal friction and windage torque.

8.1.18 Error Analysis. The cumulative measurement error for each performance variable will be calculated with the following procedure. Each variable is calculated from a combination of measurements. Each measurement has an error (S_y) determined from its calibration. The probable error of each variable will be calculated using the relationships of probable error for the following operations as outlined in Reference 8.1.

Function	Probable Cumulative Error
$F = (A^L)(B^M)(C^N)....$	$S_F = \pm F \sqrt{\left(\frac{LS_A}{A}\right)^2 + \left(\frac{MS_B}{B}\right)^2 + \left(\frac{NS_C}{C}\right)^2}$
$F = A \pm B \pm C \pm ....$	$S_F = \pm \sqrt{S_A^2 + S_B^2 + S_C^2 + ...}$

8.1.19 Reduced Data Storage File. The reduced data is stored in a temporary data file. The printed data is then checked for acceptability (see Section 9.1). If the data is acceptable, the reduced data is transferred from the temporary to a permanent data file for future data analysis.

8.1.20 Data Printout. The reduced data is printed on data sheets in a desired format using headings stored in a heading file. The output data will be in both English and Metric units. Headings will be English language only. Xerox copies of the data sheet will be included in the final report.

8.2 Parametric Presentation

Processing data from the pump test program will involve transforming the experimentally determined heads, flows, speeds, torques, pressures and void fractions into a workable format that can be used in a calculational model to predict the performance of pumps under single and two-phase flow conditions during postulated NSSS accidents.

When predicting the pump head and torque, it is assumed that any analytical simulation of a system will provide pump speed, flow, and inlet void fraction as independent parameters. Based on these inputs, the calculational model must then be able to produce the corresponding head and torque. Since analogous procedures will be used in computing head and torque, only the calculation of the head will be described.

Equations will be fitted to the converted test data using a regression analysis program. The program selected is "Multiple Linear Regression" from IBM's System/360 Scientific Subroutine Package. Basically, regression analysis uses the method of least squares to determine the "best" functional relationship, of an assumed form, between a dependent variable and given independent variables. The dependent variable, H, will be predicted as a function of the independent variables (Q, N, α_F). Several methods of checking the quality of the fit have been built into the data processing program. Each regression analysis will yield a multiple correlation which provides an overview of the quality of the fit. Multiple correlation can be described mathematically as:

$$\text{Multiple Correlation} = \frac{\Sigma (\hat{Y}_i - \overline{Y})^2}{\Sigma (\hat{Y}_i - \overline{Y})^2}$$

with $\hat{Y}_i$ = value predicted by regression analysis

Y_i = actual test value

$\overline{Y}$ = overall mean of the test values.

If the correlation approaches unity, the overall fit can be assumed to be satisfactory. A residual comparison is also provided which gives an indication of the accuracy of the fit for each data point. A residual can be defined as the difference between what is actually observed and what is predicted by the regression equation. If the curve fit is correct, then the residual error should be small for each test value. The two kinds of numerical checks are necessary since the multiple correlation may indicate that the overall fit is reasonable, yet the residual comparisons would show that one or more data points are in poor agreement with the fitted curve.

Once a curve fit has been obtained which meets the correlation and residual criteria, the equation will be plotted mechanically with an overlay of the experimental data. This will provide the following information:

(a) A visual check for unrealistic inflections.

It will be necessary to look for any unrealistic inflections in the plot of the H vs. Q curves as illustrated in the following figure.

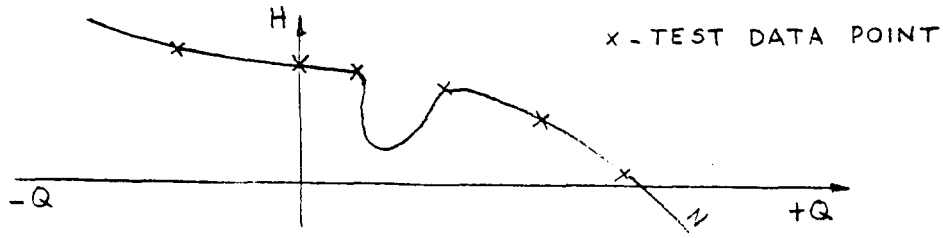

(b) A visual check for undesirable inflections.

Small inflections can be expected in the plot of the H = f (Q) regression equation as shown in Figure A.

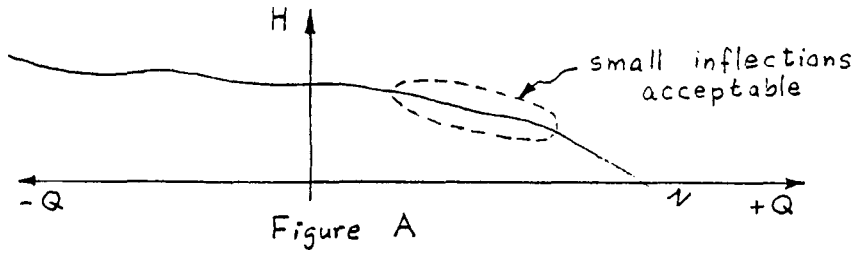

Figure A

The inflections in Figure A will be caused by the exponents associated with the Q terms used in the regression equations.

Large inflections, as shown in Figure B, should be avoided due to the errors they would cause in determining head values at intermediate speeds.

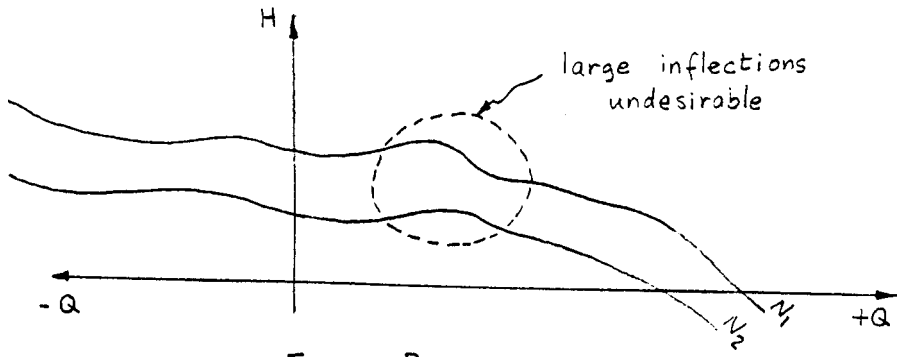

Figure B

If the graphical check is satisfactory, then the regression equation will be considered satisfactory. If not, then another regression model will be assumed for regression analysis. See Figure 8.1 for a flow diagram of the regression analysis.

The number of regression runs and visual checks for each regression equation will determine the time involved to establish a satisfactory expression. The average time involved in determining a regression equation to meet the multiple correlation and residual criteria will be a matter of hours, assuming rapid computer turnaround time. The turnaround time for plots is normally overnight. Therefore, the following day after the converted test data is available, some insight should be achieved for the test values and the associated analysis.

Three possibilities to describe head were considered:

Option 1: A regression equation such that $H = f(Q, N, \alpha_F)$.

Option 2: A regression equation at each void fraction such that $H = f(Q, n)$.

OPTION 3

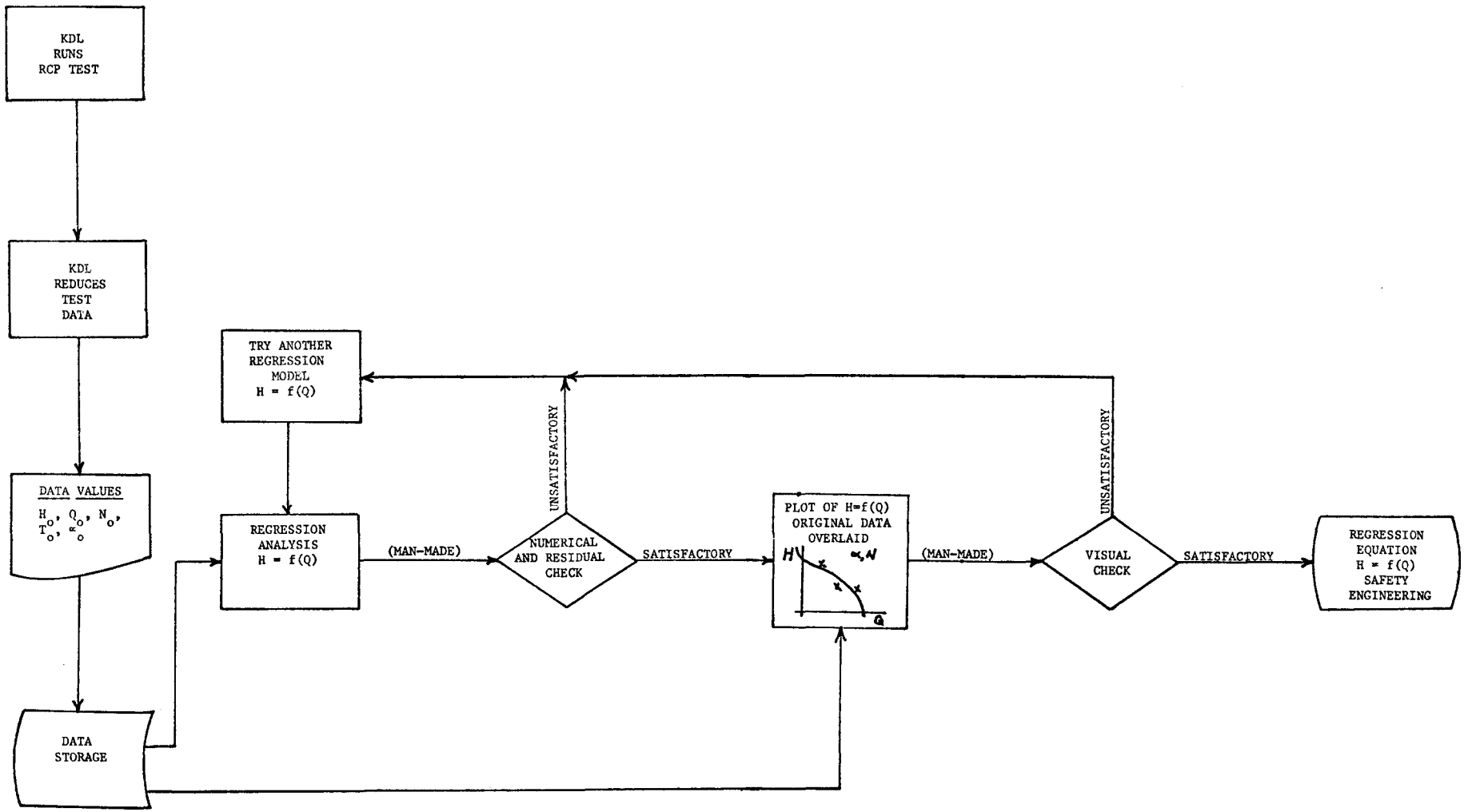

Flow Diagram of the Regression Analysis

FIGURE 8.1

Option 3: A family of regression equations at different speeds for each void fraction such that $H = f(Q)$.

In order to check out these approaches, points from the Byron-Jackson cold water test 4-quadrant curve for the 1/5 model pump (Figure 6.5) were selected to see which method and type of mathematical expression could best fit such representative pump performance "data points." A matrix was set up similar to the one to be applied to a performance map in the test program. Individual points were taken from the positive flow and speed quadrant, positive speed and negative flow quadrant, and negative speed and flow quadrant.

Option 1 was impossible to model due to the fact that the B-J cold water 4-quadrant curves were all taken at zero void fraction. A regression equation was attempted to describe $H = f(Q, N)$ at zero void fraction by using 55 selected points over a wide range of flow and speed. A large variety of functional combinations of flow and speed were tried, but no satisfactory expression could be found. Because Option 2 was unfeasible, it was assumed that Option 1 would also be unfeasible. (More will be said, however, about handling minor deviations in speed and void fraction set points.)

Therefore, a regression analysis was performed to describe head as a function of flow for constant speeds, Option 3. Sets of data ranging from negative to positive flows at constant intervals of speed were inputed into the regression program. Satisfactory regression equations were determined by regression analysis. A workable expression seems to be $H = f(Q, |Q|^{3/2}, Q^2, |Q|^{5/2}, Q^3)$. The two most heavily weighted parameters are Q^2 and Q^3, with Q^2 featuring in agreement with the Affinity Laws and a cubic in Q^3 being representative of the gross shape of the H vs. Q curves. The additional parameters are used to aid in reducing the residual error between the "data points" and predicted head values. In most cases, it has been found that only the Q, Q^2 and Q^3 parameters are necessary to closely describe the pump head. It is felt that higher order expressions should be avoided to help minimize the potential for inflection in the H vs. Q curves.

Figures 8.2 and 8.3 illustrate the satisfactory results for the sample cases of Option 3. Associated with each figure is a list of the regression equations as given in Tables 8.1 and 8.2. On the plots any appreciable

FIGURE 8.2

Sample Case for H = f(Q) at Constant N

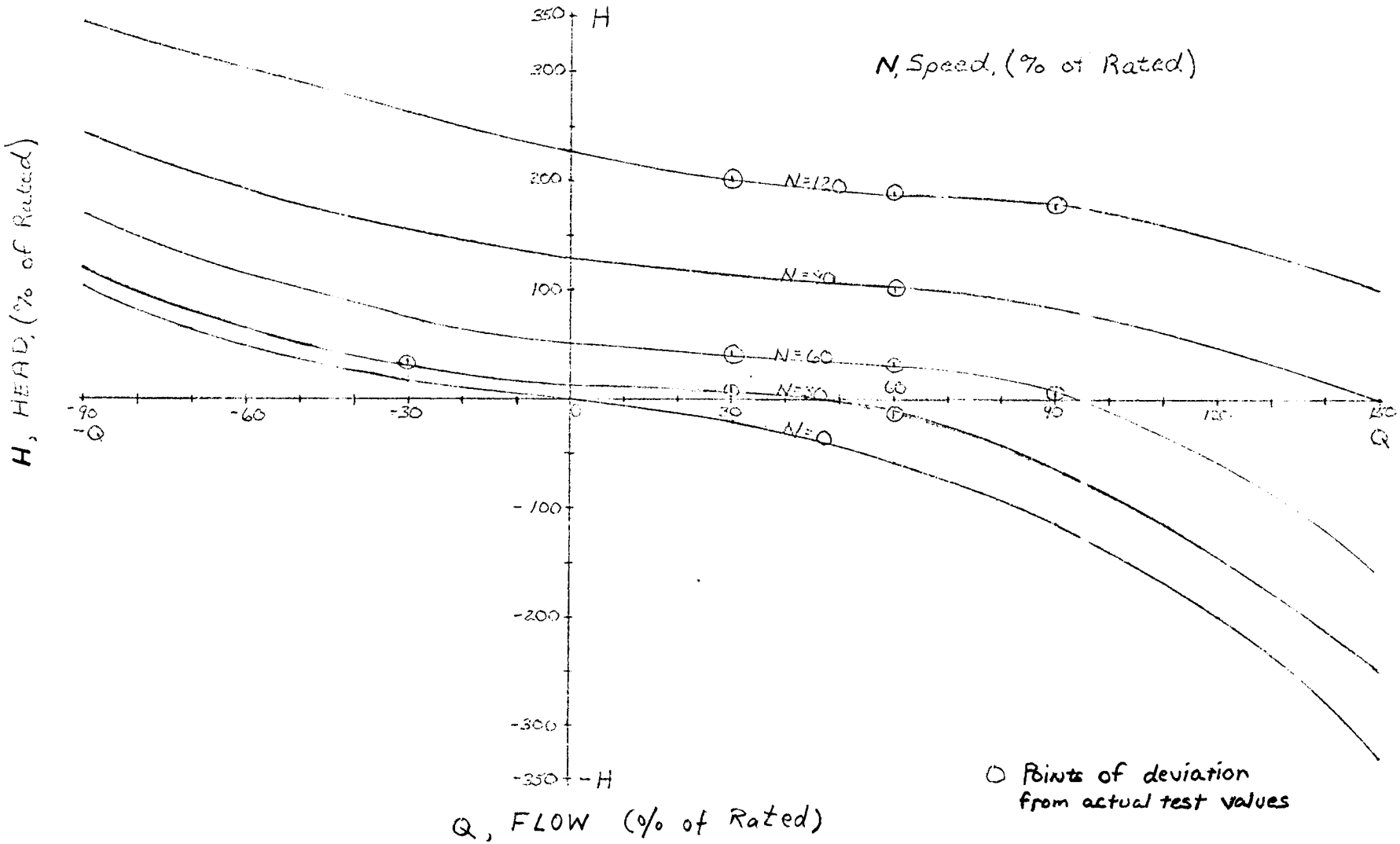

FIGURE 8.3

Sample Case for $T_h = f(Q)$ at Constant N

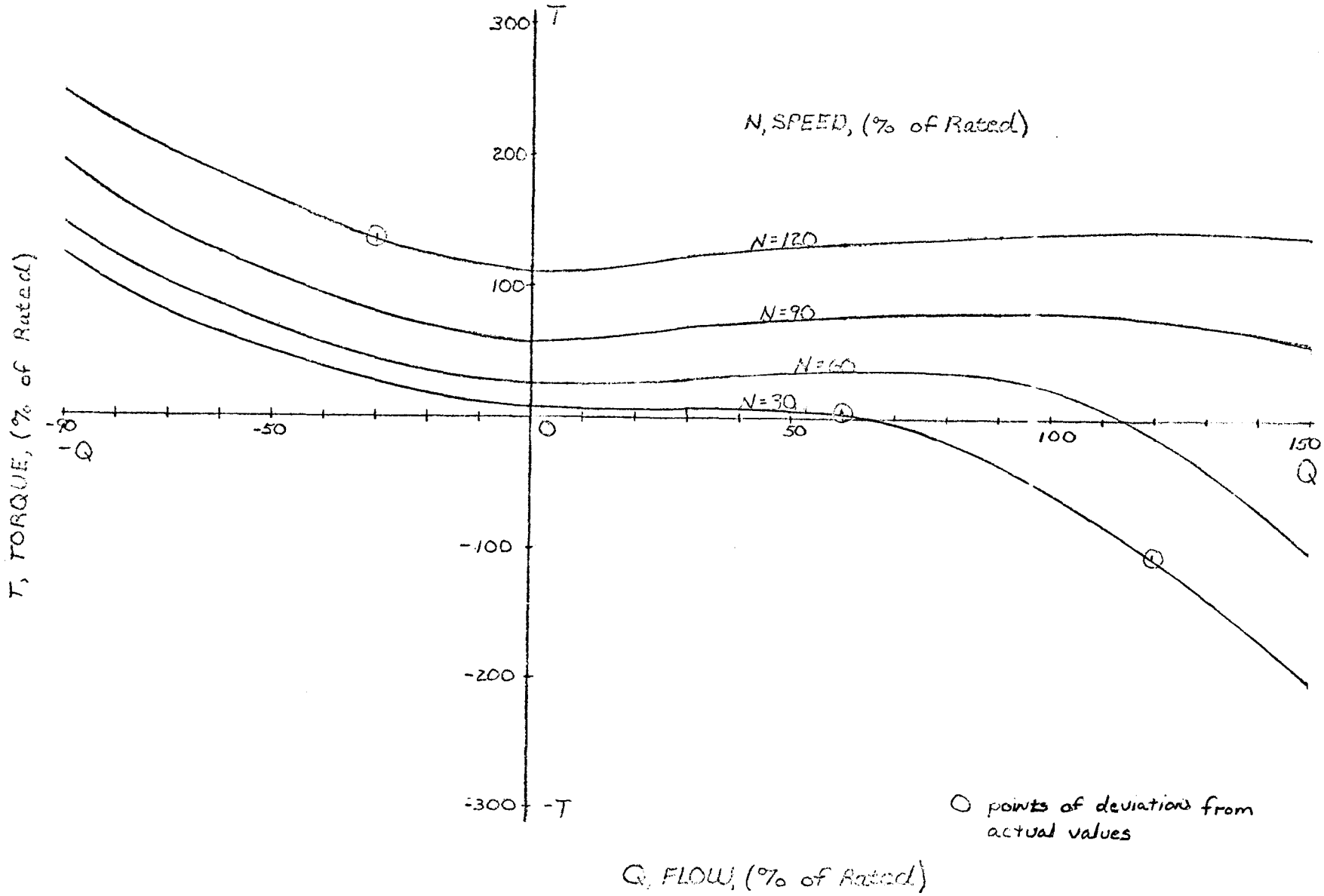

TABLE 8.1

THE REGRESSION EQUATIONS FOR THE SAMPLE CASE FOR H = f(Q) AT CONSTANT N

1. N = 120

$$H = -.99393Q + .01886Q^2 - .00154|Q|^{5/2} + .0000076Q^3$$

Multiple Correlation = .99916

2. N = 90

$$H = -.638Q + .0037Q^2 - .000036Q^3$$

Multiple Correlation = .99950

3. N = 60

$$H = -.4794Q + .1039|Q|^{3/2} - .0062Q^2 - .000056Q^3$$

Multiple Correlation = .99945

4. N = 30

$$H = -.3347Q + .3517|Q|^{3/2} - .0691Q^2 + .0036|Q|^{5/2} - .000086Q^3$$

Multiple Correlation = .99957

5. N = 0

$$H = -.6648Q - .0004Q^2 - .000065Q^3$$

Multiple Correlation = .99987

TABLE 8.2

THE REGRESSION EQUATIONS FOR THE SAMPLE CASE FOR $T = f(Q)$ AT CONSTANT N

1. N = 120

$$T = -.232Q + .2018|Q|^{3/2} - .0255Q^2 + .0015|Q|^{5/2} - .000044Q^3$$

Multiple Correlation = .99871

2. N = 90

$$T = -.1798Q + .2085|Q|^{3/2} - .0282Q^2 + .0017|Q|^{5/2} - .000056Q^3$$

Multiple Correlation = .99960

3. N = 60

$$T = -.1881Q - .0071|Q|^{3/2} + .0199Q^2 - .0012|Q|^{5/2} - .000058Q^3$$

Multiple Correlation = .99982

4. N = 30

$$T = -.2073Q + .2558|Q|^{3/2} - .0443Q^2 + .0023|Q|^{5/2} - .000086Q^3$$

Multiple Correlation = .99950

deviations from actual values are indicated by circled vertical lines representing the magnitudes and directions of the deviations. All of these represent deviations less than 2.5% of the rated head, and toward the ends of these curves the deviations are even smaller. Obviously for this prime-interest single-phase performance range, the fits are close.

Regression analysis will provide H = f(Q) equations at various selected speeds. In order to predict head values at intervening speeds, for which no regression equations are available, an interpolation technique is necessary.

The Lagrange interpolation scheme appears to be adequate. The results of this interpolation scheme used to predict head values at intervening speeds was checked against points from the B.-J. cold water test 4-quadrant curve for the model pump. The comparison indicates that the predicted head values are in good agreement with the B.-J. data. An extrapolation method is presently being developed, in which the trend of the H vs. Q curves as the speed changes will be weighted for determining head values at pump speeds outside the test range.

Associated with Option 3 are two possibilities to describe % H = $f(\alpha_F)$, where % H = $H_{2\text{-phase}}/H_{1\text{-phase}}$. If an expression can be obtained between % H and α_F, it would eliminate the need for expanding H = f(Q) for all intermediate test data sets. The first possibility is a regression analysis to establish a single universal expression for % H = $f(\alpha_F)$ as in Figure C.

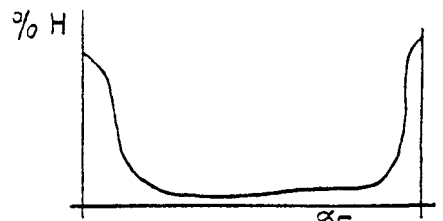

Figure C

However, if this is not feasible and it appears that the depth of the curve, as in Figure D, is governed by the ratio of $\frac{Q/Q_R}{N/N_R}$, i.e., $\frac{\nu}{\alpha_N}$, in which Q_R and N_R are rated conditions, then a family of equations to describe % H = $f(\alpha_F)$ will be developed by regression analysis. See Figure 8.4 for a flow chart of % H = $f(\alpha_F)$ regression analysis.

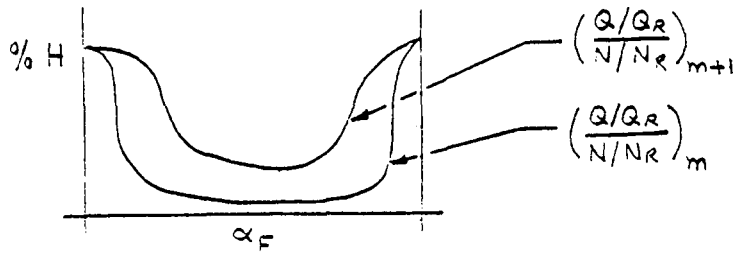

Figure D

An alternate possibility of applying % H as an additive rather than a multiplicative adjustment of head will also be examined.

If the above approaches prove to be unsuccessful, then pump performance will be obtained by using the general form of the regression equations in conjunction with intermediate test points. Presently, three complete sets (55 data points per set) of 4-quadrant data are to be taken at three void fractions. An interpolation between any two of these data sets and the intermediate test points will be performed to obtain intermediate 4-quadrant curves.

In order to save time later in going from the test data to the final curves, the mechanics of data processing, such as the overlay of the test data on the plot of the associated regression equation, interpolation and extrapolation schemes, and transformation of data into 4-quadrant curves to facilitate modeling are being developed now.

FIGURE 8.4

Flow Chart of % H = f(α_F) Regression Analysis

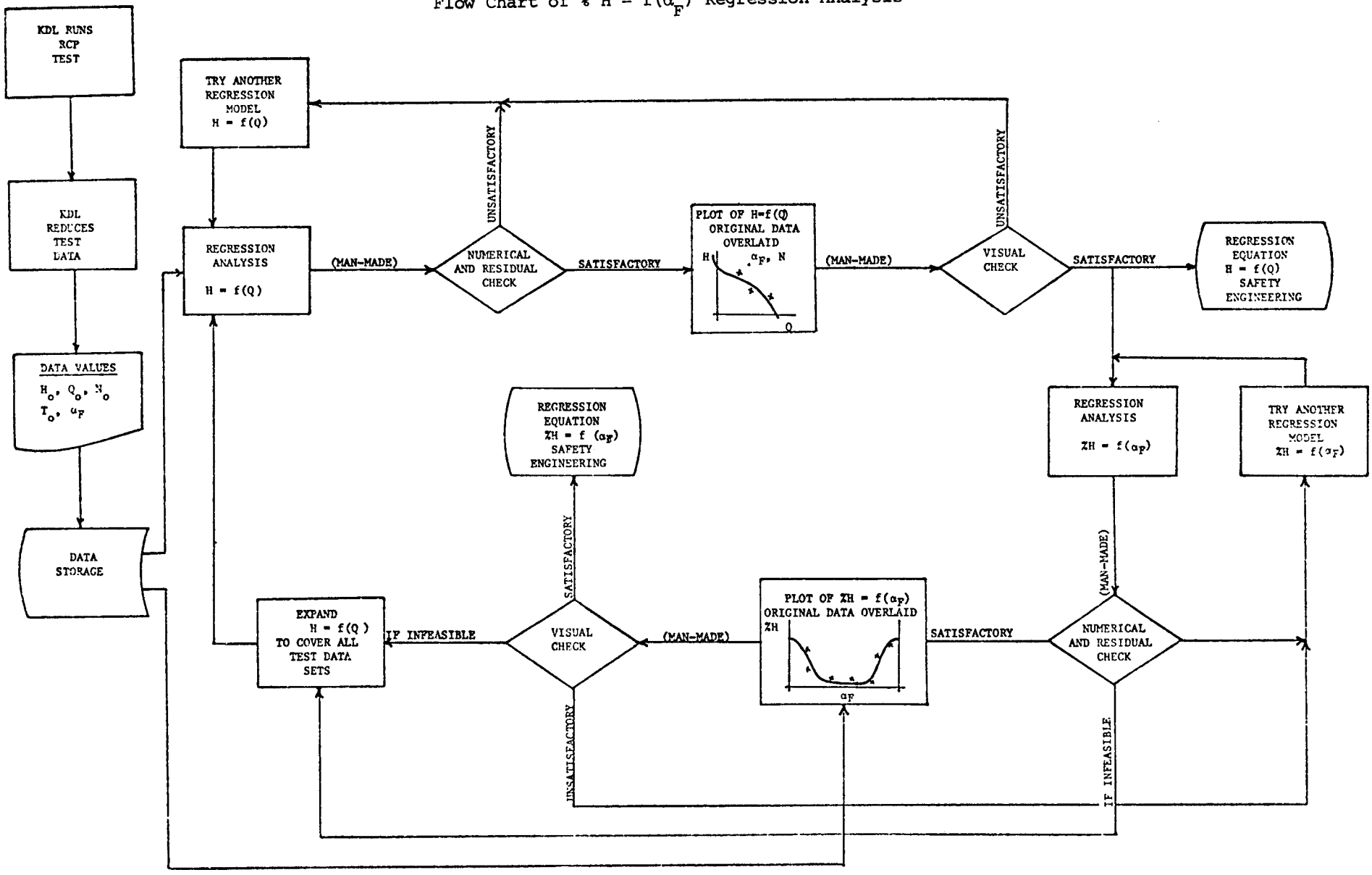

The test data processing scheme as described above would analyze head as a function of flow at constant speed and void fraction. Actually, the test data will have known deviations (beyond measurement errors) in the values of head, flow, speed, and void fraction from the requested set points. These known deviations are a result of keeping the operating time spent in setting a test point to a practical value. For instance, estimated values of set point variation usually attainable within one-half hour are $\pm$10 psi for pressure, $\pm$1°F for temperature and $\pm$5% of value for flow, compared to instrument errors such as $\pm$2.25 psi, $\pm$0.2°F, and $\pm$1.4% of value, respectively.

For the data processing scheme to account for such set point deviations, it becomes necessary to include the known deviations of speed and void fraction as additional parameters in the regression analysis. The dependent variable, H, will then be predicted as a function of Q, ΔN, and $\Delta\alpha_F$. Then by setting ΔN and $\Delta\alpha_F$ equal to zero, an expresssion will result in the form that H = f(Q) at constant nominal set point values of N and α_F. This process accounting for N and α_F deviations will result in equations having two less Q parameters for any given number of data points.

8.3 Generation of Performance Maps

"Four-quadrant" regression equations will be available at the design speed of the pump. Therefore, it will only be necessary to normalize the corresponding head and flow values at the design speed in order to attain the necessary values for the development of a homologous curve. The parameters H (head) and Q (flow) will be normalized by division of the "rated" value of the subject parameter. Additional normalized values for comparison or for extending the range of homologous data can be taken from regression equations at other speeds if the speeds are also normalized to the rated speed. These normalized values will be mechanically plotted in the following manner. The homologous curve includes two sets of four normalized characteristic curve segments. In one set, the normalized head ($h = H/H_R$) divided by the square of the normalized flow ($\nu = Q/Q_R$) is plotted against the normalized speed ($\alpha_N = N/N_R$) divided by the normalized flow, that is, h/ν^2 as a function of α_N/ν. In the second set of four curve segments, the normalized heat divided by the square of the normalized speed is plotted versus the normalized flow divided by the normalized speed, that is, h/α_N^2 as a function of ν/α_N. The set of curves to which a data point belongs is determined by the relative

values of α_N and ν. An ordinate-axis parameter with an absolute value of less than one (α_N/ν or ν/α_N) is used. See Figure 5.1 for an example of a homologous head coordinate system and sample curves, and Figure 5.2 for corresponding torque coordinates and curves.

9. EVALUATION OF TEST DATA

9.1 Data Quality Evaluation

The following criteria will be used in order to determine whether the steady-state test data obtained at a particular test point is acceptable and will, therefore, be transferred to the Permanent Data File, accessible for use in the data analysis process.

(a) The errors calculated as part of the data reduction process will have to be within the error specified by the Test Request.

(b) The drift between three consecutive readings, measured in 60 second intervals will have to be 1% per minute or less.

(c) Redundant readings will be required to agree within the error band of the redundant instruments.

Steady-state test data, taken at the rate of three scans per minute, is converted to engineering units using the data reduction routines discussed in Section 8.1. A maximum of 20 minutes is needed for the data to be obtained, converted to engineering units, and accepted.

The data will be manually scanned to verify its conformity to the desired conditions and its acceptability with regard to expected results. If a discrepancy is noted, the test point may be rerun.

9.2 Adequacy of Parametric Coverage

In the course of (1) preparing various parametric presentations of the pump performance data as described in Sections 8.2 and 8.3, (2) consolidating the data into a system of equations or tables for input to the calculational model, and (3) comparing similarity criteria and applying similarity laws for scaling as discussed above, it should become apparent how well the variations in pump performance can be described and correlated in terms of the various parameters used and their interrelationships. It could be found, for example, that whatever two-phase head degradation occurs correlates better with a nonlinear rather than a linear average void fraction through the pump, and

this could call for modifying the correlation parameter to be used. Also, it could be found that information regarding some additional parameters is needed to explain test results and could be used for better calculated predictions. For example, if choking is found to play a significant role in some parts of the operating range, parameters involved in indicating the onset of choking and the effective choked flow area could become additional required information from the tests. The feasibility and plans for adding more parameters to the pump data and performance description would have to be assessed as any need arises.

9.3 Comparison of Predicted and Measured Transient Behavior

The pump calculational model described in Section 5.2 is the one currently used to calculate pump performance in dynamic transient flow situations occurring during NSSS LOCA's. This calculation model basically assumes quasi-equilibrium and uses a steady-state formulation with no time derivative terms except for $d\omega/dt$ (i.e., angular acceleration), which is set up as a dependent variable applied for calculating speed changes. Also, the input performance data for the calculational model is generally taken from steady-state pump tests.

The question which naturally arises and is to be answered in the pending pump model tests is whether the pump performance (pump head and hydraulic torque) which results from operation at certain conditions (pump speed, volume flow rate, pressure level, density and void fraction) is independent of whether these operating conditions are in steady-state or occur in the course of a rapid transient. Accordingly, the transient predictions to be evaluated and the blowdown tests to generate the transients need not be a matter of trying to duplicate whole time-histories of NSSS LOCA blowdowns, nor even successfully predicting all aspects of test system blowdowns. Whether the dynamic pressure loss characteristics of some elbow or other component in the test system piping can be successfully predicted is really not very important except for trying to forecast what kind of blowdown will generate appropriate pump operating conditions. What is most significant in checking the test results is to see whether the steady-state data as incorporated into and used by the calculational model predicts the same performance as measured during a transient test for a given set of operating conditions even when those conditions are varying rapidly in the transient

test. Whether there are any differences between predicted and measured transient performance depends on whether any significant nonequilibrium lags occur as a result of such factors as fluid inertia and time delays in energy transfer. Analyses by others in the field, (e.g., Reference 5.1), suggest that except during extreme transients (more rapid than the main saturated decompression portion of blowdowns) the fluid inertia in the pump itself is of little effect and a more likely source of nonequilibrium is lag in vaporization or condensation, and this was the basis of using $d\alpha_F/dt$ as a criterion for severity of a transient.

Thus, the primary method of comparing predicted and measured transient behavior will be to (1) generate from steady-state test data a set of input data to the pump calculational model covering a suitable range of operating conditions, (2) run a transient test which passes through operating conditions of interest, (3) list from the transient measurements one or more sets of operating conditions of interest which occurred at various points in time during the blowdown, (4) determine for the operating conditions at each selected point in time what pump performance is predicted by the calculational model, and (5) compare this with the pump performance indicated by the transient measurements for the same time. The part of the operating range in which a particular comparison falls may have been covered directly by steady-state tests in the same range, or the steady-state input may have been derived by scaling from other operating conditions through the use of flow similarity relationships such as the homologous ratios which have been discussed above. Comparisons made involving directly measured steady-state input will provide the simplest checks for any transient effects. Comparisons using scaled data will check transient effects on scaling factors also, and can be further compared with scaling effectiveness between pairs of steady-state points.

It is desirable to have as many as possible of the operating conditions in the test system blowdowns undergoing the same kinds of changes as typically occur in LOCA blowdowns at least momentarily, and so many of the test system blowdowns will be precalculated to guide the selection of test cases and anticipate pump performance calculation questions to be checked. This will be done using the CEFLASH-4A dynamic thermal-hydraulic program as discussed before.

If significant differences are found between the predicted and measured transient pump performance, the data will be analyzed to see whether the differences correlate with the severity of the transients as indicated by $d\alpha_F/dt$ or other rates of change of conditions. Additional tests, either steady-state, transient, or both, may be run as a part of the discretionary reserve tests to try to (1) get a variety of transient rates, (2) reduce the amount of interpolating or extrapolating (similarity scaling) required, and (3) try to separate out the effects of such variables as void fraction and flow velocities as mentioned in Section 9.2. The additional information from these tests would be fed back into the calculational model for further comparisons.

REFERENCES

3.1 CE/EPRI Two Phase Pump Performance Program (RP301-1), Pump Test Facility Description Report, H.P. Habermacher, Kreisinger Development Laboratory, C-E, 1975.

5.1 Single and Two-Phase Performance Characteristics of the MOD-1 Semiscale Pump Under Steady State and Transient Fluid Conditions, D.J. Olson, ANC, October 1974, (ANCR-1165, VC-78d).

5.2 The Flow of Complex Mixtures in Pipes, G.W. Govier and K. Aziz, Van Nostrand Reinhold Co., New York, 1972.

5.3 A Flow Pattern Map for Gas-Liquid Flow in Horizontal Pipes, J.M. Mandhane, G.A. Gregory, and K. Aziz, International Journal of Multi-Phase Flow, Vol. I, No. 4, October 30, 1974.

5.4 Best Estimate Pump Head and Torque Models from Semiscale Pump Data, J.H. Ramsthaler, DMR-7-74 & FWC-3-74, ANC, April 30, 1974.

6.1 Blowdown Behavior of CE/EPRI/KWU Pump Test Facility, W.G. Kennedy and G. Menzel, PE-75-060, June 17, 1975.

8.1 Precision dc Measurements and Standards, D.S. Luppold, Addison Wesley, 1969, p.9.

Not Cited Report on Pump Two-Phase Flow Test Facility Requirements (Draft), R.A. Livingston and N.A. Edelbeck, ANC, June 1974.

APPENDIX A

LIST OF REPORTS PREPARED AS A PART C-E/EPRI TWO-PHASE PUMP PROJECT DOCUMENTATION

The reports listed below may be obtained through the EPRI Library.

Report No/Type	Title/Author(s)	Principal Content
Quarterly	Quarterly Technical Progress Report No. 1, January 1 - March 31, 1975	Project background, objectives, and structure are described. Preliminary designs of test systems are given.